INFORMATION TO USERS

This manuscript has been reproduced from the microfilm master. UMI films the text directly from the original or copy submitted. Thus, some thesis and dissertation copies are in typewriter face, while others may be from any type of computer printer.

The quality of this reproduction is dependent upon the quality of the copy submitted. Broken or indistinct print, colored or poor quality illustrations and photographs, print bleedthrough, substandard margins, and improper alignment can adversely affect reproduction.

In the unlikely event that the author did not send UMI a complete manuscript and there are missing pages, these will be noted. Also, if unauthorized copyright material had to be removed, a note will indicate the deletion.

Oversize materials (e.g., maps, drawings, charts) are reproduced by sectioning the original, beginning at the upper left-hand corner and continuing from left to right in equal sections with small overlaps. Each original is also photographed in one exposure and is included in reduced form at the back of the book.

Photographs included in the original manuscript have been reproduced xerographically in this copy. Higher quality 6" x 9" black and white photographic prints are available for any photographs or illustrations appearing in this copy for an additional charge. Contact UMI directly to order.

U·M·I

University Microfilms International
A Bell & Howell Information Company
300 North Zeeb Road, Ann Arbor, MI 48106-1346 USA
313/761-4700 800/521-0600

Order Number 9207135

Petrologic-geochemical studies of chondritic meteorites: Implications from new types of chondrites

Weisberg, Michael Kevin, Ph.D.

City University of New York, 1991

U·M·I
300 N. Zeeb Rd.
Ann Arbor, MI 48106

A

PETROLOGIC-GEOCHEMICAL STUDIES OF CHONDRITIC METEORITES: IMPLICATIONS FROM NEW TYPES OF CHONDRITES

by

MICHAEL K. WEISBERG

A dissertation submitted to the Graduate Faculty in Earth and Environmental Sciences in partial fulfillment of the requirements for the degree of Doctor of Philosophy, The City University of New York.

1991

This manuscript has been read and accepted for the Graduate Faculty in Earth and Environmental Sciences in satisfaction of the dissertation requirements for the degree of Doctor of Philosophy.

Sep. 25. 1991
Date

Chair of Examining Committee
Prof. Cherukupalli E. Nehru

Sept 27 1991
Date

Executive Officer
Prof. Frederick Shaw

Dr. Martin Prinz

Dr. Roger H. Hewins

Dr. Surendra K. Saxena

Dr. David H. Speidel
Supervisory Committee

The City University of New York

ABSTRACT

PETROLOGIC-GEOCHEMICAL STUDIES OF CHONDRITIC METEORITES:
IMPLICATIONS FROM NEW TYPES OF CHONDRITES

by

Michael K. Weisberg

Advisor: Professor Cherukupalli E. Nehru

Study of several unclassified meteorites has led to characterization of two new chondrite groups and two unique chondrites, and implications for their origins.

The CR2 chondrites represent a new chondrite group having a unique set of petrologic, chemical and isotopic characteristics. These meteorites are breccias and differences in their bulk chemical compositions (i.e., volatile lithophiles) may be explained by differences in their matrix/chondrule ratios. These chondrites experienced parent body aqueous alteration prior to their final lithification.

ALH85085 has several characteristics which set it apart from any known chondritic group. Its chondrules are smaller (25-75 μm), the majority are cryptocrystalline, and all are volatile (Na, K, S) depleted. FeNi metal is more abundant (40.9 wt.%) and sulfide abundance is low (1.1%). The bulk composition of ALH85085 is lower in Na/Si and S/Si and higher in Ni/Si, Fe/Si and Mg/Si than in other chondritic groups. Ca/Si, Al/Si and Mg/Si ratios are closest to those of CR chondrites.

Bencubbin is an unclassified meteorite breccia consisting mainly of host silicate (~40 vol.%) and host metal (~60%) components, and rare (<1%) ordinary chondrite clasts

and a dark xenolith. Two scenarios are offered for the origin of Bencubbin. One is that Bencubbin components are chondritic and were produced in the solar nebula. Later brecciation, reaggregation and minor melting of the chondritic material resulted in it becoming a monomict chondritic breccia. The alternative scenario is that the Bencubbin components formed as a result of major impact melting on a chondritic parent body. Petrologic, chemical and isotopic data are more consistent with Bencubbin being a brecciated chondrite.

Carlisle Lakes, ALH85151 and Y75302 represent a new grouplet which I call the Carlisle Lakes-type chondrites. They have the highest $\Delta^{17}O$ values (up to 2.91) measured. They are olivine-rich (>70 vol.%), essentially metal-free, and most olivine is FeO-rich, equilibrated at Fa_{38}. Some olivine and pyroxene in chondrules and fragments are zoned and their zoning profiles suggest formation by nebular gas-solid exchange reactions accompanied by condensation of new FeO-rich olivine, utilizing existing olivine surfaces as nucleation sites.

Acknowledgements

I am grateful to co-advisors Dr. Martin Prinz and Dr. Cherkupalli E. Nehru for helpful discussions and reviews of this thesis and for collaborating on several earlier projects related to the thesis topic. In addition, I am thankful for the encouragement they have given me to continue in the field of meteoritics. Critical reviews of this thesis by members of the supervisory committee (Dr. David H. Speidel and Dr. Surendra K. Saxena) has led to its substantial improvement. Supervisory committee member Dr. Roger H. Hewins has reviewed much of my work and provided helpful discussions throughout my career as a graduate student. I am also grateful to Dr. Robert N. Clayton and Toshiko K. Mayeda for collaborating with me on several projects, parts of which are included in this thesis. Numerous members of the meteoritic community have also played an important role in reviewing my work at different stages, discussing data, and being overall supportive of my work. Most of all I am indebted to my wife Carolyn for her warm support and patience.

Portions of the text, photographs and diagrams have been substantially reproduced with permission from some of my earlier published papers [(1) Earth and Planetary Science Letters 91, Michael K. Weisberg, Martin Prinz, Chekupalli E. Nehru, "Petrology of ALH85085: a chondrite with unique characteristics", 1988, Elsevier Science Publications; (2) Meteoritics 25, Michael K. Weisberg, Martin Prinz, and Chekupalli E. Nehru, "The Bencubbin chondrite breccia and its relationship to CR chondrites and the ALH85085 chondrite", 1990, The Meteoritical Society; (3) Geochimica et Cosmochimica Acta, in press, Michael K. Weisberg, Martin Prinz, Hideyasu Kojima, Keizo Yanai, Robert N. Clayton and Toshiko K. Mayeda, "The Carlisle Lakes-type chondrites: A new grouplet with high $\Delta^{17}O$ and evidence for nebular oxidation", 1991, Pergamon Press].

TABLE OF CONTENTS

LIST OF TABLES

LIST OF FIGURES

1. INTRODUCTION

1.1 Background

New types of meteorites present a unique opportunity to study previously unsampled regions of the early solar system. Those derived from undifferentiated parent bodies are especially important because they preserve clues which expand our knowledge of the spectrum of the primitive materials from which the asteroids and other solar system bodies formed. Thus, it is important to determine which meteorites have characteristics developed in the early nebula and to determine their relationship to other chondritic samples.

Chondrites are important meteorite groups because they are among the oldest and most primitive materials available in the solar system. They did not undergo planetary differentiation and some exhibit only minor alteration and metamorphism. The components of chondrites include millimeter-sized spheres (chondrules), refractory-rich inclusions, mineral and lithic fragments, FeNi metal, sulfides, and a fine-grained opaque matrix which surrounds the other components and binds the chondrite. Since these components are products of solar nebula processes, the study of chondrites allows constraints to be placed on the conditions of those processes which were active prior to and during planetary formation.

Chondrites are classified into nine major groups on the basis of bulk chemical compositional differences, based largely on work by Wiik (1956), Van Schmus and Wood (1967), Van Schmus (1969), Wasson (1974) and Kallemeyn and Wasson (1981) . These groups are the H, L, and LL ordinary chondrites, the EH and EL enstatite chondrites and the CI, CM, CO and CV carbonaceous chondrites. In addition to bulk chemical data, there are distinct petrologic differences between the nine groups. For example, mean chondrule size, chondrule/matrix ratio, abundance of FeNi metal and sulfide, and oxidation state of the mafic silicates are all parameters which have been used to distinguish between members

of the nine groups. Each chondrite group formed at a specific location (and/or time) in the nebula and they accreted into separate parent bodies.

In addition to chemical groupings, chondrites are also divided into six petrologic types based on degree of aqueous alteration and equilibration/recrystallization (Van Schmus and Wood, 1967). Type 1 and 2 chondrites contain hydrous silicates and types 3 to 6 are anhydrous; the numerical progression from 3 to 6 represents increasing degrees of equilibration/recrystallization. The numerical progression from type 3 to 1 represents increasing degree of aqueous alteration. The ordinary chondrites are all types 3 to 6, e.g. L3, L4, L5, L6. All the CI chondrites are type 1 (CI1). The CM2, CO3, and CV3 chondrites are type 2 and 3 and are very important because they are the least altered and thus better preserve the record of their original environment of formation in the solar nebula.

Oxygen isotopes play a major role in classifying the nine chondritic groups, and in understanding inter- and intragroup relationships. Since chondrites are undifferentiated their oxygen isotopic compositions do not plot on a mass fractionation line (i.e. slope=0.52) on an oxygen three-isotope diagram, but fall instead on a mixing line defined mainly by their chondrule and matrix components, which are representative of the oxygen isotopic reservoirs from which they formed and the ambient solar gas with which they exchanged oxygen (Clayton, 1981).

Some chondrites defy classification and do not belong to any of the nine chondritic groups. Are these chondrites simply anomalous members of the nine groups or do they represent rare samples of other chondritic groups? There is reason to believe that these ungrouped chondrites do represent new types of chondrites and are thus extremely important. New types of chondrites provide the opportunity to better establish the nature of the spectrum of primitive materials recording nebular and parent body (asteroidal) processes. They allow the study of previously unsampled regions of the early nebula and demonstrate the biased nature of the existing chondrite record.

A major source of the important new ungrouped chondrites are the Antarctic meteorite collections. Each year both Japanese and American expeditions to the Antarctic recover hundreds of new meteorite samples. This abundance of specimens has greatly increased the sampling of chondritic meteorites. This is a petrological and geochemical investigation of new types of chondrites and includes a systematic and detailed study of the poorly characterized CR (Renazzo-type) chondrites, the unique ALH85085 chondrite, the Bencubbin meteorite, and the Carlisle Lakes-type chondrites.

1.2 Purpose of This Study

This is a study of several new types of chondrites which include: (1) CR chondrites-a group of seven meteorites with similar petrologic characteristics which have been tentatively called CR (Renazzo-type) chondrites, but most of their petrologic and chemical characteristics have not previously been studied, (2) Allan Hills 85085 (ALH85085)-a unique chondrite which may have a genetic relationship to the CR chondrites, but has grossly different petrographic characteristics, (3) Bencubbin-an FeNi metal-silicate assemblage which may also be related to the CR chondrites, and (4) Carlisle Lakes-type chondrites-a group of three meteorites which may be related to ordinary chondrites, but are more oxidized (Binns and Pooley, 1979; Yanai et al., 1985).

The goals of this study are to: (1) characterize these ungrouped chondrites, (2) establish if they represent new chondrite groups and therefore represent new, previously unsampled, asteroids, and (3) determine which of their characteristics can be relegated to primitive nebular processes and which are the result of processes active on their parent-body asteroids. Some of the specific questions which will be addressed in this study include: (1) Is there a relationship between the CR chondrites, ALH85085 and Bencubbin? (2) Can the unique characteristics of ALH85085 be explained by primary nebular processes or are they the result of impact processes on a chondritic parent body, as suggested by

Wasson (1988)? (3) Can the unusual characteristics of Bencubbin be explained by nebular processes or are they also the result of parent-body impact processes, as suggested by Kallemeyn et al. (1978)? (4) What is the relationship of the Carlisle Lakes-type chondrites to the ordinary chondrites and is their oxidation state the result of primitive nebular processes or is it the result of oxidation during metamorphism on its parent-body, as suggested by Rubin and Kallemeyn (1989)? In this work I will present petrologic and geochemical evidence to show that many of the properties of these new chondrite types are not the result of secondary impact and metamorphic parent body processes, but are the result of primary nebular processes.

1.3 The Ungrouped Chondrites

1.3.1 CR2 Chondrites

The CR2 (Renazzo-type) group was tentatively designated by McSween (1977a), based on petrography, in order to distinguish the Renazzo and Al Rais chondrites from the CV3 group. Kallemeyn and Wasson (1982) showed that Renazzo and Al Rais have similar refractory lithophile and siderophile elements, but volatile elements are lower in Renazzo. Based on these data they suggested that Renazzo and Al Rais are not members of the same group, but may belong to the same "clan". Recently, four antarctic chondrites (Mac Alpine Hills (MAC) 87320, Elephant Moraine (EET) 87770, Yamato (Y) 790112, and Y793495) have been called Renazzo-like (CR2) chondrites (Mason, 1989a, b, Yanai and Kojima, 1987) bringing the number of members in the CR group to six and a seventh CR chondrite has been found in Algeria (A. Bischoff, pers. comm., 1991). However, the CR chondrites have never been established as a major chondrite group. Their properties are generally recognized by meteorite-petrologists, but have never been clearly outlined in detail.

Recovery data for all known CR chondrites are presented in Table 3.1.1. Preliminary studies of the four antarctic meteorites, and Renazzo and Al Rais have shown

them to have similar petrologic characteristics (Weisberg et al., 1989). Their oxygen isotopic compositions constitute a unique mixing line on an oxygen 3-isotope diagram (Clayton and Mayeda, 1989 and Weisberg et al., 1989).

The CR2 chondrites are important for several reasons. Their FeNi metal may record a primitive nebular condensation event (Weisberg et al., 1988a). Renazzo has a ^{15}N-rich component which may also be a result of primitive nebular processes (Kung and Clayton, 1978; Robert and Epstein, 1982; Prombo and Clayton, 1985). Chondrules in the CR chondrites exhibit multi-layered rimming which has important implications for chondrule-forming processes (Prinz et al., 1985). Matrices in the CR chondrites have petrologic and oxygen isotopic similarities to the primitive CI chondrites (Kallemeyn and Wasson, 1982; Fredriksson et al., 1981; Clayton and Mayeda, 1977). The CR chondrites may be related to other important primitive meteorites, i.e., Allan Hills (ALH) 85085 and Bencubbin (Weisberg et al., 1988a).

The CR chondrites have been studied in order to establish the characteristics of this chondrite group and understand the nebular as well as parent-body processes that have acted to shape this group. One important goal of meteorite research is to untangle the complex histories of chondrites and distinguish between primary nebular processes and parent-body processes and study of the CR chondrites may shed light on this problem. To these ends, (1) modal abundances of the various components (chondrules, matrix, inclusions, etc.) in the CR chondrites have been determined, (2) the mineral phases in most components have been analyzed, (3) phase relationships have been studied, (4) bulk chemical compositions of the the various components have been determined, and (5) CR chondrules and matrix were separated for oxygen isotopic analysis.

1.3.2 ALH85085

There are other ungrouped chondrites that appear to be related to the CR chondrites. These include the ALH85085 chondrite and the Bencubbin metal-silicate breccia.

ALH85085 has been described as having unique characteristics (Mason, 1987; Weisberg et al., 1988a; Grossman et al., 1988; Scott, 1988). It contains components similar to other chondrites (chondrules, inclusions, metal, matrix), but the abundances and sizes of these components differ from those of the nine chondrite groups. For example, its chondrules are very small (25-75μm), as are its other components. Most chondrules are cryptocrystalline in texture, whereas in most chondrites these are one of the least abundant types (Gooding and Keil, 1981). Lithic fragments (which may be broken chondrules) are abundant making up ~70 vol.%. It contains more metal than any other chondritic meteorite, but sulfide is very sparse. Matrix is absent, but material compositionally and texturally identical to opaque matrix occurs as clasts. All these features clearly make ALH85085 a unique chondrite.

Nevertheless, ALH85085 has many features which indicate a relationship to the CR chondrites. The FeNi metal is very similar to that in CR chondrites, which has a unique Co vs. Ni trend (Weisberg et al., 1988a). The whole rock oxygen isotopic composition is the same as that of the CR chondrites (Clayton and Mayeda, 1989). In addition, ALH85085 has anomalously high ^{15}N, with a $\delta^{15}N$ up to 1497‰, making it the most ^{15}N enriched meteorite ever measured (Grady and Pillinger, 1989, 1990). The CR chondrites also have unusually high ^{15}N with a $\delta^{15}N$ of ~200‰ (Kung and Clayton, 1978; Robert and Epstein, 1982). Most meteorites have $\delta^{15}N$ values which range from -90 to +50‰.

To understand the unique set of characteristics of the ALH85085 chondrite and its relationship to the CR chondrites, (1) textural characteristics, (2) modal abundances, (3) mineral compositions, and (4) bulk chemical compositions of matrix and chondrules of ALH85085 have been determined.

1.3.3 Bencubbin

Another ungrouped meteorite which appears to be related to the CR chondrites is Bencubbin. Bencubbin is a metal-silicate breccia which consists of chondritic silicate clasts in what Simpson and Murray (1932) refer to as a "skeleton" of FeNi metal. This metallic skeleton is made up of rounded to angular, and in some cases, polycrystalline FeNi clasts (Newsom and Drake, 1979). The breccia is cemented together by a "matrix" consisting of silicate material and metal droplets suggestive of spontaneous fusion (Ramdohr, 1973; Newsom and Drake, 1979). The Weatherford meteorite is similar.

The silicate portion of Bencubbin has been described as "achondritic" (Lovering, 1962; McCall, 1968) and identical material in Weatherford has been called "aubritic" (Mason and Nelen, 1962). Aubrites are a group of enstatite-rich achondrites. However, Ramdohr (1973) noted that the Bencubbin silicates texturally resemble chondrules, and it has more recently become clear that they are compositionally chondritic (Kallemeyn et al., 1978; Hutchison, 1986). Weisberg et al. (1987) carried out a preliminary investigation of these silicates and showed that they texturally resemble barred olivine (BO) chondrules.

FeNi metal in Bencubbin is also very similar to that in CR chondrites, with the same unique Co vs. Ni trend, but the range in compositions in Bencubbin is more restricted (Newson and Drake, 1979; Weisberg et al., 1988). The whole rock oxygen isotopic composition also plots with the CR chondrites on an oxygen three-isotope diagram (Clayton and Mayeda, 1977). Finally, Bencubbin also has anomalously high ^{15}N with $\delta^{15}N$ values up to ~1000‰, similar to CR chondrites and ALH85085 (Prombo and Clayton, 1985; Franchi et al., 1986; Keeling et al., 1987).

Thus, CR chondrites, ALH85085, and the Bencubbin-related meteorites represent a suite of highly primitive chondrites. A petrologic study of this suite and oxygen isotopic analysis on whole rocks, on separated chondrules, and on matrix have been performed in order to better characterize these meteorites and understand the nature of the relationship

between Bencubbin, ALH85085 and CR chondrites and the nature of the processes these meteorites record.

1.3.4 Carlisle Lakes-type chondrites

Chondrites range from highly reduced (e.g. EH) to highly oxidized (CI), and their oxidation states are the result of a complex combination of their nebular and parent-body histories. (See Rubin et al. (1987) for a review of oxidation states of chondrites.) The equilibrated H, L, and LL ordinary chondrites are closely related, but have different oxidation states. H chondrites are the most reduced and LL are the most oxidized of the known ordinary chondrite groups. Their oxidation states are reflected in their mineral and bulk chemical compositions. More reduced meteorites have lower concentrations of FeO in their silicates and higher Fe^0/total Fe ratios. For example, olivine compositions are $Fa_{20, 25 \text{ and } 28}$ and Fe^0/total Fe ratios are 0.38, 0.66, and 0.88, in equilibrated H, L, and LL chondrites, respectively. Unequilibrated ordinary chondrites are aggregates of components of varying oxidation states, but most have bulk chemical properties that reflect a general kinship with one of the three equilibrated groups.

One method used in trying to understand oxidation processes in chondrites has been the study of compositional zoning in Fe-Mg silicates in type 3 chondrites. Zoning may be the result of crystallization processes during chondrule formation, thermal events on a chondrite parent body, reactions with a nebular gas, or some combination of these processes. All of these processes took place in the early solar system and it is important to distinguish between the effects of each in chondritic meteorites.

The Carlisle Lakes, ALH85151, and Y75302 chondrites have been studied because these meteorites may be related to the ordinary chondrites, but are considerably more oxidized than the LL chondrites. ALH85151 was preliminarily classified as a C4 chondrite by Mason (1987) based on its high abundance of Fe-rich olivine. Carlisle Lakes, a similar

meteorite, was described as a highly oxidized ordinary chondrite by Binns and Pooley (1979). The third chondrite, Y75302, was also described as a highly oxidized ordinary chondrite (Yanai et al., 1985) and is also related (Rubin and Kallemeyn, 1988). Based on bulk chemical compositional data, Rubin and Kallemeyn (1989) suggested that both ALH85151 and Carlisle Lakes are members of the same meteorite group, but cannot be classified as ordinary, carbonaceous, or enstatite chondrites, instead they were considered to be members of a new chondrite group with affinities to the ordinary chondrites. The oxygen isotopic compositions of ALH85151 and Carlisle Lakes, presented in a preliminary study (Weisberg et al., 1989), showed that these meteorites are similar and occupy a unique position on an oxygen 3-isotope diagram, having the highest known $\Delta^{17}O$ values.

These meteorites will be referred to as the the Carlisle Lakes-type chondrites. Petrologic data, especially on mineralogical zoning patterns, and oxygen isotopic analyses of the whole chondrites and some of the chondrules are presented in order to better understand the petrogenesis of these chondrites and their relationship to other chondrites. Detailed zoning profiles of the mafic silicates were measured in order to determine the environment(s) in which their oxidation states were established.

2. ANALYTICAL TECHNIQUES

Polished thin sections (PTS) and hand samples of most of the non-Antarctic meteorites were supplied by the American Museum of Natural History. A PTS and small fragment of CL001 is currently on loan from the Western Australian Museum. Two PTS of CR chondrites (Y790112,92-2 and Y793954,92-3) were loaned from the National Institute of Polar Research (NIPR), Japan. Two PTS of ALH85151 were loaned from National Aeronautics and Space Administration (NASA), Johnson Space Center. PTS of ALH85085, EET87770 and MAC87320 were also supplied by NASA. Small chips of Renazzo and Al Rais were supplied by the American Museum of Natural History (AMNH) and NASA and NIPR supplied samples of the Antarctic meteorites for oxygen isotopic analysis.

Chondrules and matrix were separated from samples of Renazzo, Al Rais, ALH85151 and Carlisle Lakes. The procedure for dislodging chondrules involves the use of fine dental tools and a diamond-tipped drill to scrape away surrounding matrix. Once the chondrules are dislodged they were sliced with a diamond impregnated saw blade into two halves. One half was cemented to a glass slide and polished for reflected light and backscattered electron microscopy and electron microprobe analysis. The other half was used for oxygen isotope analysis.

All PTS and polished chondrules were studied with a petrographic microscope in both plain and polarized transmitted light and reflected light. Photomicrographs of all samples were taken to use as maps for electron microprobe work. A thin coat of carbon was then deposited on each polished surface so that silicates and other non-metallic minerals would conduct electrons and could be analyzed with the electron microprobe.

The electron microprobe used was an ARL-SEMQ. It contains nine fully focusing crystal spectrometers and a fully automated stage. Six of the nine spectrometers are fixed

to analyze common elements: Si, Al, Fe, Mg, Ca, Ti. The other spectrometers can be adjusted to analyze additional elements.

In this analytical technique (Wavelength Dispersive Spectrometry) electrons are focused on a sample causing it to emit X-rays. Each element in the sample emits X-rays which are characteristic of that element. The X-rays are dispersed by a crystal (with a suitable d value) arranged in the correct position to satisfy Bragg's equation. The X-rays are diffracted by the crystal to X-ray detectors/counters and the intensity of the X-rays is proportional to the quantity of the element in the sample.

As in other analytical techniques, standards are used. Before each mineral is analyzed X-rays are collected from a series of natural and synthetic standards of known composition as a basis for comparison. Appropriate standards were chosen based on their similarity to the minerals being analyzed. Operating conditions used varied between accelerating voltages of 15 to 25kV and sample currents of 10 to 20 nA, depending on the excitation level and volatility of the elements being determined. A table of the standards used for all mineral analyses and operating conditions are presented in Table 2.1. The diameter of the electron beam for mineral analysis was ~1-2 μm and and counting times of 20 seconds on peak positions and 10 seconds on backgrounds were used. For some elements, background measurements were made using standards. For others, they were measured by offsetting to both the low and high sides of the peak. All analyses were corrected using alpha factors generated by using MAGIC IV (Colby, 1968). The resulting analyses are given in weight percent of oxides.

In addition to mineral analysis, the electron microprobe was used to determine bulk chemical compositions using a defocused beam. In this method both standards and unknowns are analyzed with a beam which is 50μm in diameter. Equally spaced spots are analyzed to cover the area of interest. Each point is corrected using the alpha factors determined by Colby (1968) and all points are then averaged to give a bulk chemical composition.

Table 2.1. List of standards used for peak and backgrounds in electron microprobe analyses of mineral phases and bulk compositions.

	Olivine/Pyroxene		Feldspar		Phyllosilicates		Ca-carbonate		FeNi Metal		Bulk Comp.	
	Peak	Bkgd	Peak	Bkgd	Peak	Bkgd	Peak	Bkgd	Peak	Bkgd	Peak	Bkgd
Si	DIOPS	CORUN	AMPHI	CORUN	KAKHB	CORUN	QUARZ	CACLT	QUARZ	IRON	A209	CORUN
Ti	CORNW	DIOPS	A209	QUARZ	"	QUARZ	•		•		CORNV	QUARZ
Al	A209	"	AMELI	"	"	"	•		•		A209	"
Cr	CORNV	±200	•		CORNV	"	•		•		CORNV	"
Fe	FAYAL	DIOPS	A209	"	KAKHB	"	SIDER	CACLT	IRON	NICKL	FAYAL	"
Mn	CORNW	±125	•		"	"	"	"	•		CORNW	"
Mg	HYJON	QUARZ	A209	QUARZ	"	"	DOLOM	"	•		OL-SC	"
Ca	DIOPS	"	PLAG	"	"	"	CALCT	QUARZ	•		A209	"
Na	A209	±250	AMELI	±300	"	"	•		•		AMELI	"
K	•		MCLIN	±150	"	"	•		•		MCLIN	"
Ba	•		BENIT	±150	•		•		•		•	
Sr	•		•		•		SIDER	CACLT	•		•	
P	•		•		•		•		FENIP	IRON	APTIT	"
S	•		•		•		•		TROIL	"	TROIL	IRON
Ni	•		•		•		•		FENIP	"	FENIP	"
Co	•		•		•		•		COBLT	"	•	
Sample Current (nA)	20		15		15		5		5		20	
Accelerating Voltage (Kv)	20		15		15		15		15		20	

A209-Augite	CORNW-Corning W-Glass	FENIP- Schreibersite	OL-SC-San Carlos Olivine
AMELI- Albite	CORUN-Corundum	HYJON-Johnstown Hyperstene	PLAG-Lake C0. Plagioclase
APTIT-Apatite	CR2O3- Synthetic Cr_2O_3	IRON-Pure Fe-Metal	QUARZ-Quartz Glass
BENIT-Benitoite	DIOIPS-Diopside Glass	KAKHB-Kakanui Hornblende	SIDER-Siderite
CALCT-Calcite	DOLOM-Dolomite	MCLIN-Microcline	STRUNT-Sr
COBLT-Synthetic CoS	FAYAL-Rockport Fayalite	NICKL-Pure Ni-Metal	TROIL-Troilite
CORNV-Corning V-Glass			

Analyses of all standards are on file at the Department of Mineral Sciences, American Museum of Natural History.
• Element not analyzed for the given phases.
± values denote wavelength units offset from the peak used to make background measurements for a given element.

Finally, the automated stage of the electron microprobe was used to perform modal analysis. In this method, the user selects points to outline the area of interest and selects the number of points to be analyzed in the chosen area. The computer then generates a grid of equally spaced points. Each point is analyzed for 2 seconds. Based on the analysis the computer determines the phase. Each of the points is then checked for phase overlaps or holes in the thin section.

The electron microprobe is equipped with a scanning electron microscope. In addition, a Zeiss digital scanning electron microscope (SEM) with a backscattered electron (BSE) detector was used. Backscattered electron imaging is a highly valuable method for studying zoning patterns in minerals. This is because the amount of backscattering of electrons is proportional to atomic number. Therefore backscattered electron images display contrast in atomic number.

Finally, oxygen isotope analysis were obtained via collaboration with Dr. Robert N. Clayton at the University of Chicago. In this method oxygen is extracted from samples by reaction with bromine pentafluoride. The oxygen is then measured as O_2 by mass spectroscopy. Both $^{18}O/^{16}O$ and $^{17}O/^{16}O$, relative to SMOW (Standard Mean Ocean Water) as a standard, were measured. The data are presented as $\delta^{17}O$ and $\delta^{18}O$ where:

$$\delta^{17}O = \frac{17O/16O_{sample}}{17O/16O_{SMOW}} - 1 \times 1000$$

and

$$\delta^{18}O = \frac{18O/16O_{sample}}{18O/16O_{SMOW}} - 1 \times 1000$$

Gas samples are then converted to CO_2 by reaction with graphite and reanalyzed for $\delta^{18}O$. This method of analysis is also described in Clayton and Mayeda (1963, 1983). The oxygen isotope data are generally plotted on an 3-isotope diagram ($\delta^{17}O$ vs. $\delta^{18}O$). Some

data are also presented as $\Delta^{17}O$, where

$$\Delta^{17}O = \delta^{17}O - (0.52 \times \delta^{18}O)$$

and this value is the position of a sample with respect to the terrestrial mass fractionation line on an oxygen 3-isotope diagram.

3. RESULTS

3.1 CR Chondrites

The seven known CR chondrites are listed in Table 3.1.1 with their recovery data. The following includes work carried out on all samples except El Djouf, which is a very recent find from Algeria. Renazzo and Al Rais are the only falls.

Table 3.1.1. Recovery data of the CR chondrites.

Meteorite	Locality	Date of Fall	Weight Recovered (g)		Reference
Al Rais	Saudi Arabia	12/10/1957	160.0		1
Renazzo	Italy	1/15/1824	10,000.0		1
MAC87320	Antarctica	find	16.2		2
Y790112	"	"	24.0		3
Y793495	"	"	45.0		3
EET87770	"	"	38.6		4
(Paired with:)					
EET87711			5.7		
EET87747			38.2	149.9	
EET87812			11.9		
EET87846			8.1		
EET87847			32.9		
EET87850			14.5		
El Djouf	Algeria	find	1250.0		5

1-British Museum Catalog of Meteorites, fourth edition (1985)
2-Antarctic Meteorite Newsletter 12 (1) (1989)
3-Photographic Catalog of Antarctic Meteorites (NIPR) (1987)
4-Antarctic Meteorite Newsletter 12 (3) (1989)
5-A. Bischoff, Personal Communication (1991)

3.1.1 Abundances of Components in CR Chondrites

The CR chondrites are aggregations of chondrules of all textural types, irregular-shaped objects (fragments), refractory-rich inclusions (Calcium-Aluminum-rich inclusions (CAI) and amoeboid olivine aggregates (AOA), FeNi metal, and sulfides, all surrounded

by a fine-grained, black, opaque matrix. Black opaque inclusions with discrete boundaries (dark inclusions (DI)) also occur and these are texturally and mineralogically similar to the matrix and may be consolidated aggregates of matrix. Many of the smaller CAI and AOA are concentrated in the DI, as are microchondrules.

Abundances of the various components vary widely among the CR chondrites (Table 3.1.2) and are reflected in marked textural differences (Fig. 3.1.1 a-f). Chondrules range from 38 vol.% in Al Rais and up to 63% in EET87770, matrix is as high as 50% in Y793495, and matrix+DI in Al Rais=70%. Thus the ratios of matrix/chondrules range from 0.6 to 1.8. Matrix values in Table 3.1.2 include DI because of the textural and compositional similarities of these components, and the assumption that DI are consolidated matrix material. Most chondrites have matrix/chondrule ratios that are characteristic of their group. Ordinary chondrites have relatively low ratios of about 0.2. Matrix/chondrule ratios in CV3 chondrites range from 0.5 to 1.2 (McSween, 1977a); those reported in CM chondrites are much wider, ranging from 3.5 to 17% (McSween, 1979), and ratios in CO3 chondrites have a much more narrow range from 0.5 to 0.7 (McSween, 1977b). From these data it can also be concluded that matrix abundances in some CR chondrites are generally higher than those in CV and CO chondrites, but lower than in CM chondrites, as shown in Fig. 3.1.2.

CR chondrites contain relatively few refractory-rich inclusions (CAI+AOA), from 0.1 to 3%. In comparison, CV chondrites contain 2 to 13% (McSween, 1977a), CM have 1 to 13% (McSween, 1979), and CO have 10 to 18% (McSween, 1977b). It should be noted that some of the thin sections studied covered very small areas and they may not be representative of the whole chondrite. Each of the components in CR chondrites are examined in detail below.

(a)

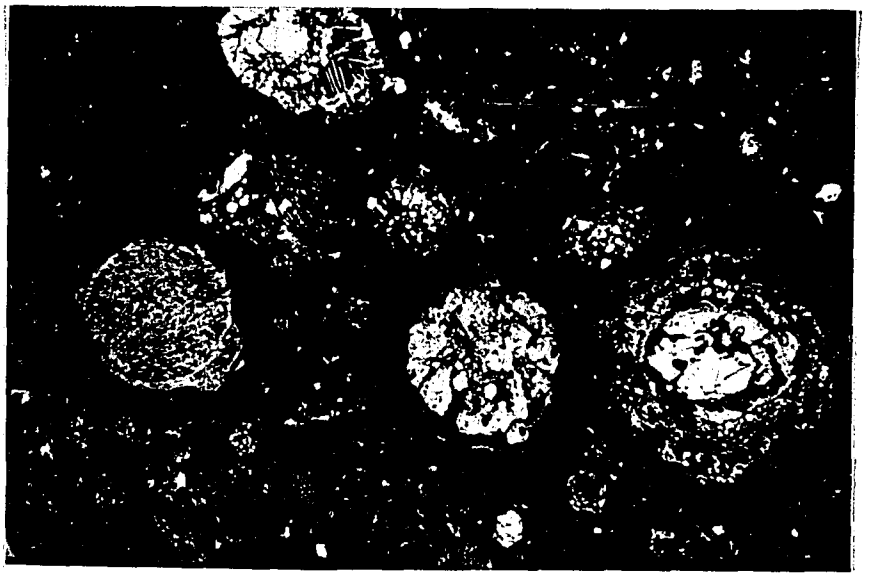

(b)

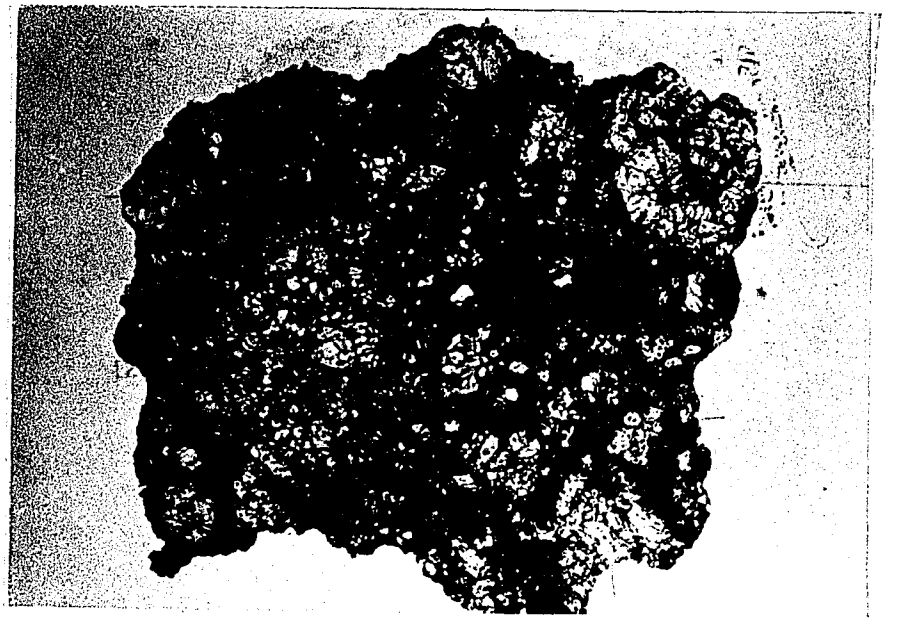

Fig. 3.1.1. Photomicrographs of six CR chondrites (a) Al Rais, (b) Y793495, (c) Renazzo, (d) MAC87320, (e) Y790112, (f) EET87770, showing their components (chondrules, matrix, etc.) and the variations in the matrix/chondrule ratios of the members of the CR group (Field of view = 0.6 cm). Al Rais (a) has the highest matrix/chondrule ratio (1.8) and EET87770 the lowest (0.6).

(c)

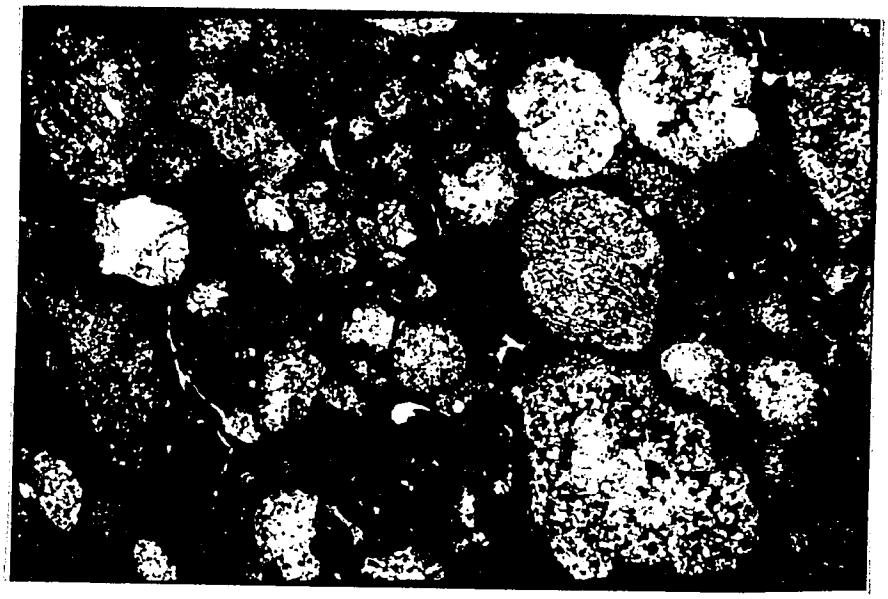

(d)

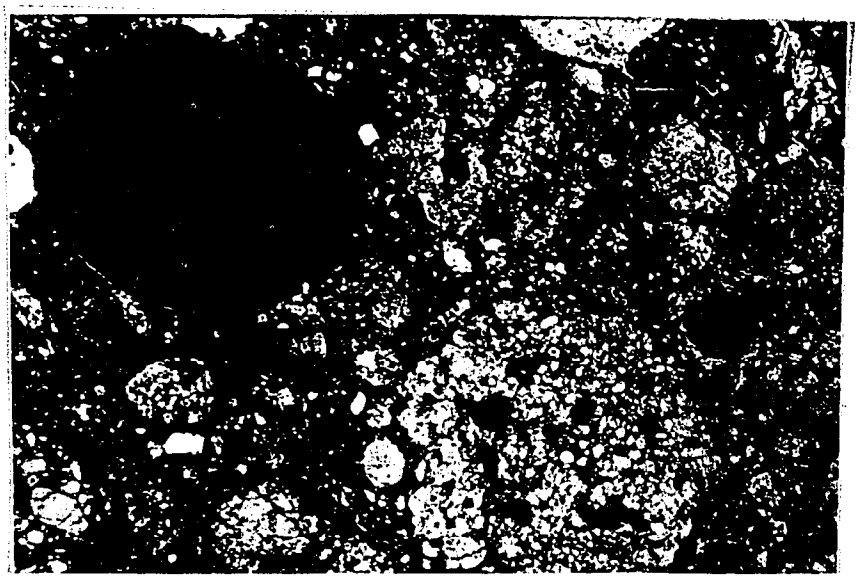

(e)

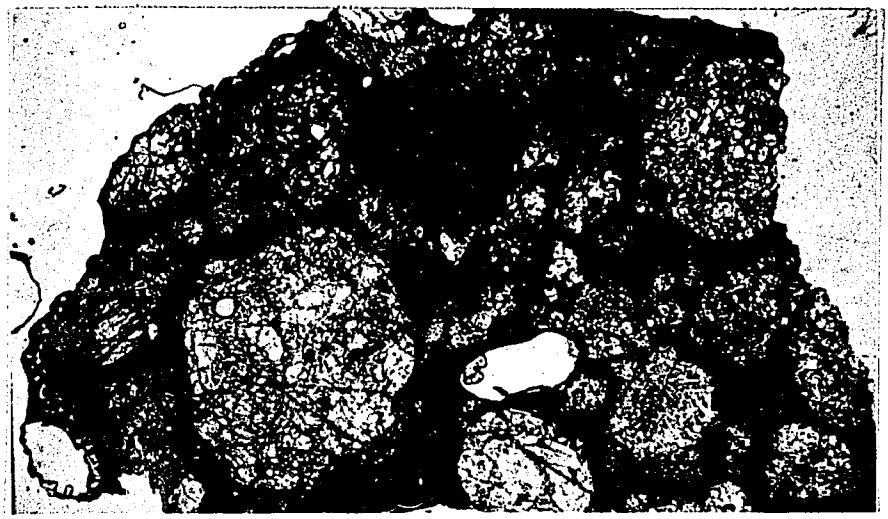

(f)

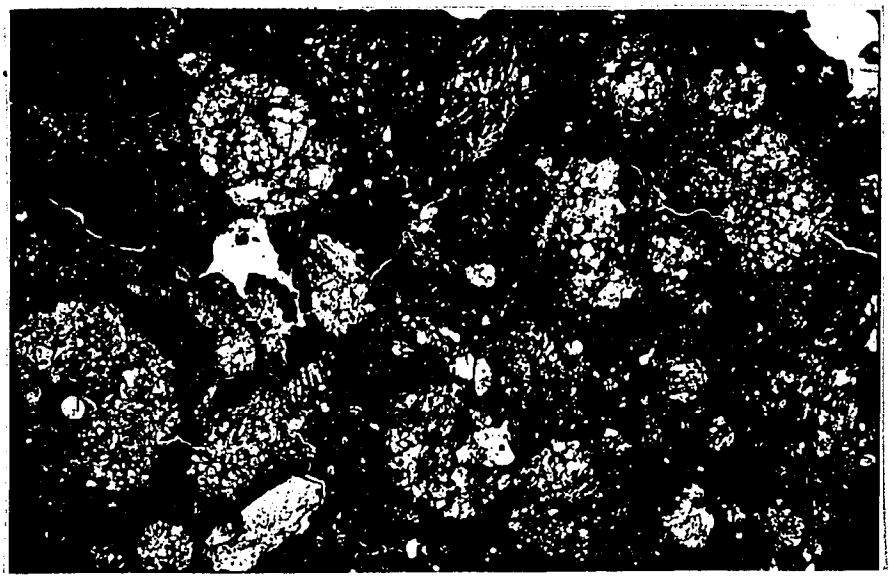

Table 3.1.2. Abundances (vol.%) of components in the CR chondrites.

	Renazzo	Renazzo[1]	Renazzo[2]	Al Rais	Al Rais[1]	Al Rais[2]	EET87	MAC87	Y790112	Y793495
Chond./Frag.	54.0	61.9	60	38.0	39.0	37	63.1	60.1	62.2	49.9
Refractory Inc.	1.0	2.6		2.0	2.5		0.7	0.1	0.2	0.3
Matrix*	37.5	36.6	40	44.7	58.7	63	34.4	38.2	29.7	49.8
Dark Inc.	7.5			25.8			1.8	1.6	7.9	
(Matrix+ Dark Inc.)/Chond.	0.83	0.59	0.67	1.85	1.50	1.70	0.57	0.66	0.60	1.00
Silicates#	91.9			95.2			89.8	92.1	94.0	91.3
Sulfides	0.7			1.1			2.7	1.6	1.2	1.0
FeNi	7.4			3.7			7.5	6.3	4.8	7.7

Chond.-chondrule, Frag.-fragment, Refractory Inclusions-(Calcium-Aluminum-rich inclusions and amoeboid olivine aggregates).
1-Data from McSween (1977).
2-Estimated by applying the lever rule to the oxygen isotope data in Fig. 3.1.10.
* Includes metal and sulfide not associated with chondrules.
#Mainly silicates, but includes carbonates, oxides and all other phases.

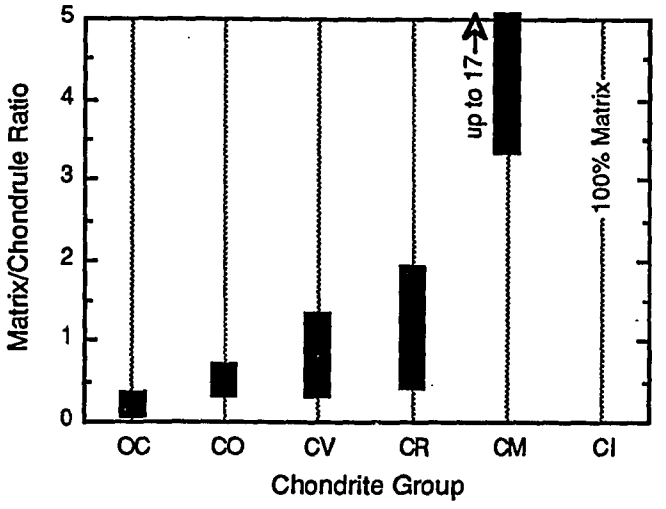

Fig. 3.1.2. Plot of chondrule group vs. their range of matrix/chondrule ratios. CR chondrites have matrix abundances closest to those of the CV chondrites, but generally greater than in O, CO and many CV and less than in CM and CI chondrites.

3.1.2 Chondrules

Chondrules in CR chondrites can be classified as either porphyritic olivine (PO), porphyritic pyroxene (PP), porphyritic olivine-pyroxene (POP), cryptocrystalline (C), radial pyroxene (RP) or barred olivine (BO), using the modal-textural classification of Gooding and Keil (1981). BO, RP and C types are exceptionally rare. Many can also be characterized as type I or type II using the textural-chemical classification of McSween (1977a). Chondrule shapes range from spherical to subspherical and some have broken surfaces. Sizes of chondrules range from 0.2 to 3.0 mm in maximum diameter and the average is 1mm, making them most similar in size to CV chondrules (Simon and Haggerty,

Table 3.1.3. Representative analyses of olivines in the cores and rims of chondrules in CR chondrites.

Chondrule	AR 4168-2		AR 4168-6		R 588-63		Y79-2	
	core	rim	core	rim	core	rim	core	rim
SiO_2	39.3	40.2	38.6	40.8	40.3	40.2	42.0	41.6
Cr_2O_3	0.59	0.56	0.12	0.64	0.20	0.89	0.34	0.42
FeO	2.34	3.1	0.40	1.79	1.29	1.71	1.23	1.48
MnO	0.39	0.24	0.10	0.24	0.07	0.32	0.03	0.09
MgO	56.8	55.9	61.0	56.2	56.7	55.9	55.1	55.3
CaO	0.18	0.16	0.60	0.20	0.32	0.21	0.34	0.16
Total	99.62	100.16	100.82	99.87	98.88	99.23	99.18	99.11
%Fa	2.3	3.0	0.4	1.8	1.3	1.7	1.2	1.5

AR-Al Rais, R-Renazzo, Y79-Y790112

1980). Most chondrules are Type I, having olivine compositions of Fo_{90-99}. Type II chondrules are present, but rare, making up less than 1% of the chondrule population.

Many chondrules in CR chondrites are concentrically layered having olivine and/or pyroxene-rich cores surrounded by finer grained olivine-, pyroxene-, phyllosilicate-, carbonate-, or sulfide-rich shells (Fig. 3.1.3a). However, the boundaries are not always sharp between the cores and rims or between the layers within the rims. Chondrule cores are mostly type I, having phenocrysts of Mg-rich olivine ($Fa_{0.5-10}$) (Table 3.1.3) and pyroxene ($Wo_{0.5-1.0}$, $Fs_{0.5-2.0}$) (Table 3.1.4) surrounded by a feldspathic or green to brown phyllosilicate (chlorite- or serpentine-rich) mesostasis (Fig. 3.1.3c). In the PO and POP chondrules, pyroxene (mainly clinoenstatite) is concentrated on the margins of the cores, tangential to the curved chondrule surface and they contain poikilitic olivine. Tiny crystals of Ca-pyroxene occur in the mesostasis and on surfaces of low-Ca pyroxene.

Table 3.1.4. Representative analyses of pyroxenes in the chondrules of CR chondrites.

Chondrule	AR 4168-2		R 588-50	
	Low-Ca	Hi-Ca	Low-Ca	Hi-Ca
SiO2	57.7	51.5	57.6	51.0
TiO2	0.26	1.26	0.13	0.76
Al2O3	1.28	5.7	0.89	5.4
Cr2O3	0.64	0.96	0.80	1.73
FeO	0.68	0.35	1.31	1.12
MnO	0.10	0.15	0.13	0.32
MgO	38.9	23.1	38.4	23.9
CaO	0.57	16.5	0.45	15.0
Na2O	0.02	0.03	0.02	0.04
Total	100.16	99.61	99.75	99.30
Wo	1.0	33.7	0.8	30.5
Fs	1.0	0.6	1.9	1.8

AR-Al Rais, R-Renazzo.

The phyllosilicate mesostases in some chondrules are green in color and compositionally are chlorites, but may be mixtures on the submicrometer scale of two or more types of phyllosilicates and/or relicts of anhydrous silicates that survived the alteration event. They are aluminous (~15 wt.% Al_2O_3), vary in FeO (20-30%) and MgO (10-20%) and contain 10-12% H_2O (Table 3.1.5). While many chondrule mesostases are chlorites, others are serpentine-rich and a few chondrules have retained their original, relatively unaltered feldspathic glassy mesostasis. The phyllosilicate mesostases appear to be replacement products of the feldspathic mesostases typically found in anhydrous chondrules; olivine and pyroxene contributed Fe and Mg and FeNi metal and sulfides contributed Fe.

(a)

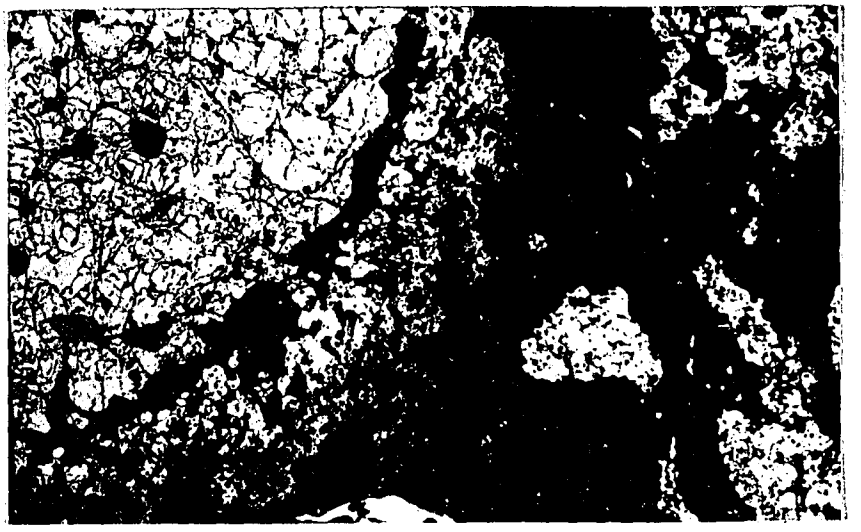

(b)

Fig. 3.1.3 Photomicrographs of chondrules in CR chondrites. (a) R-63 is a large (3mm) multilayered chondrule from Renazzo containing an olivine-rich core with spheres of FeNi metal (opaque phase) (field of view=1.1mm). The core is surrounded by a discontinuous layer of FeNi metal, followed by a layer of fine-grained olivine and pyroxene; it is lastly rimmed by a serpentine-rich layer. The enlargement of the rim (b) shows relicts of pyroxene that survived the serpentinization event. (c) AR-7 is a pair of chondrules from Al Rais (field of view=1.1mm) which have a chlorite-rich mesostasis in the core and the chondrules are bridged by chlorite similar in composition to that in the core. Serpentine-rich brown microspherules occur on the chondrule margin and in the chondrule interior. (d) Y790-7 is a broken chondrule from Y790112 (field of view=1.1mm) which is rimmed by Ca-carbonate, as also shown in the Ca X-ray map (e). Note that the Ca-carbonate rim occurs only on the original curved surface of the chondrule and not on the broken one. (f) Backscattered electron image of magnetite framboids in the matrix of Y790112.

(c)

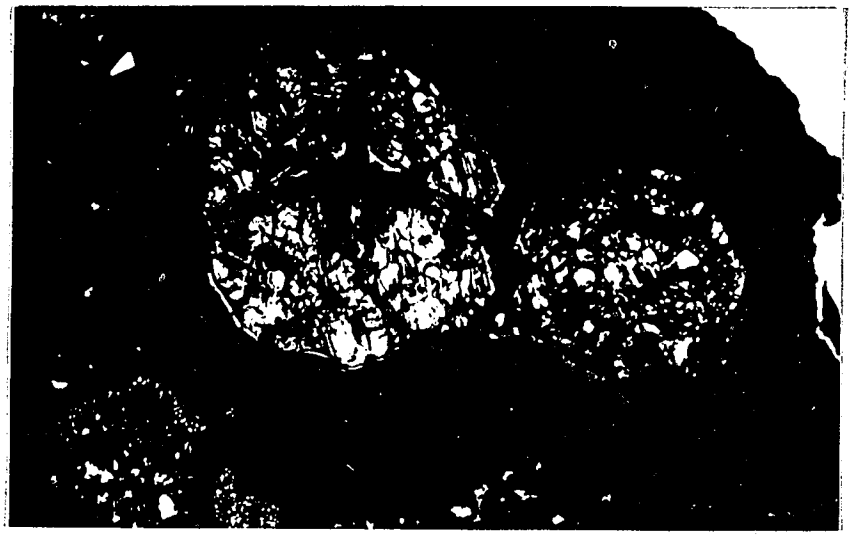

(d)

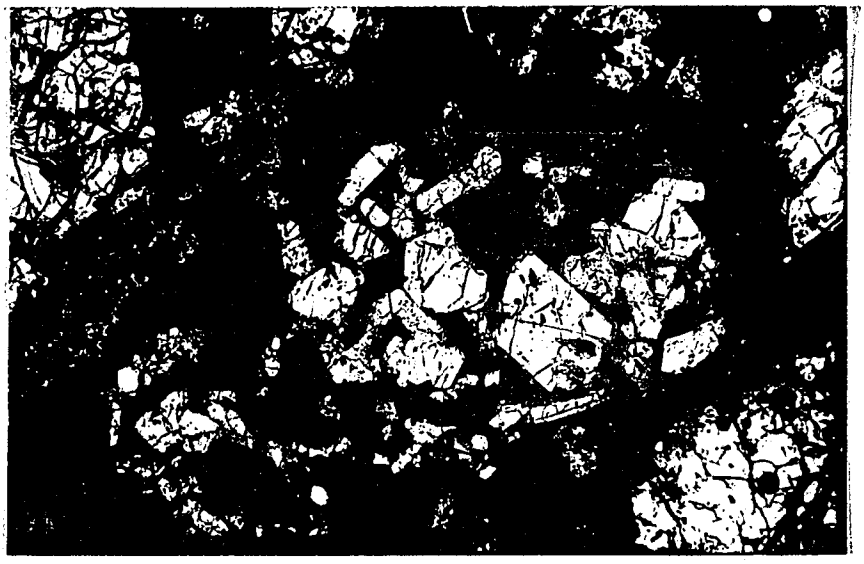

(e)

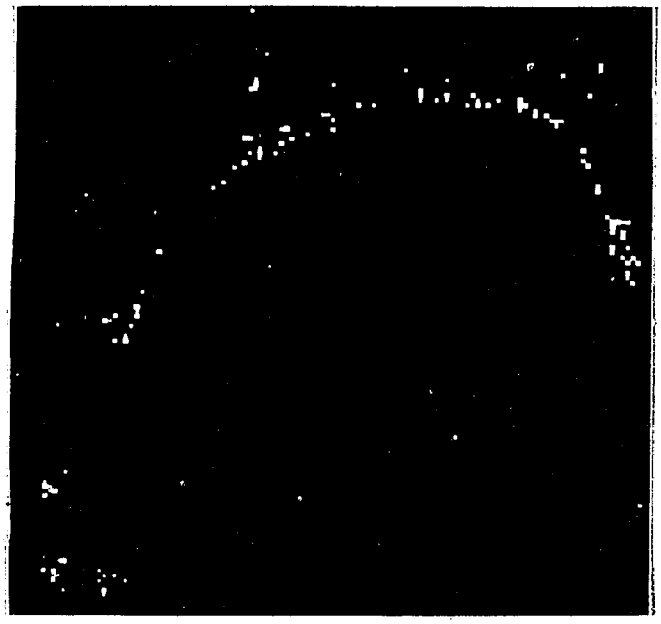

(f)

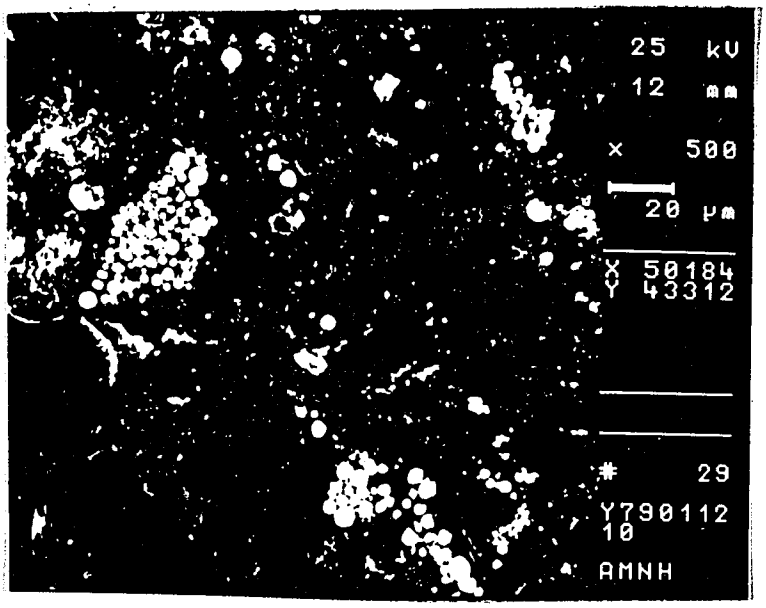

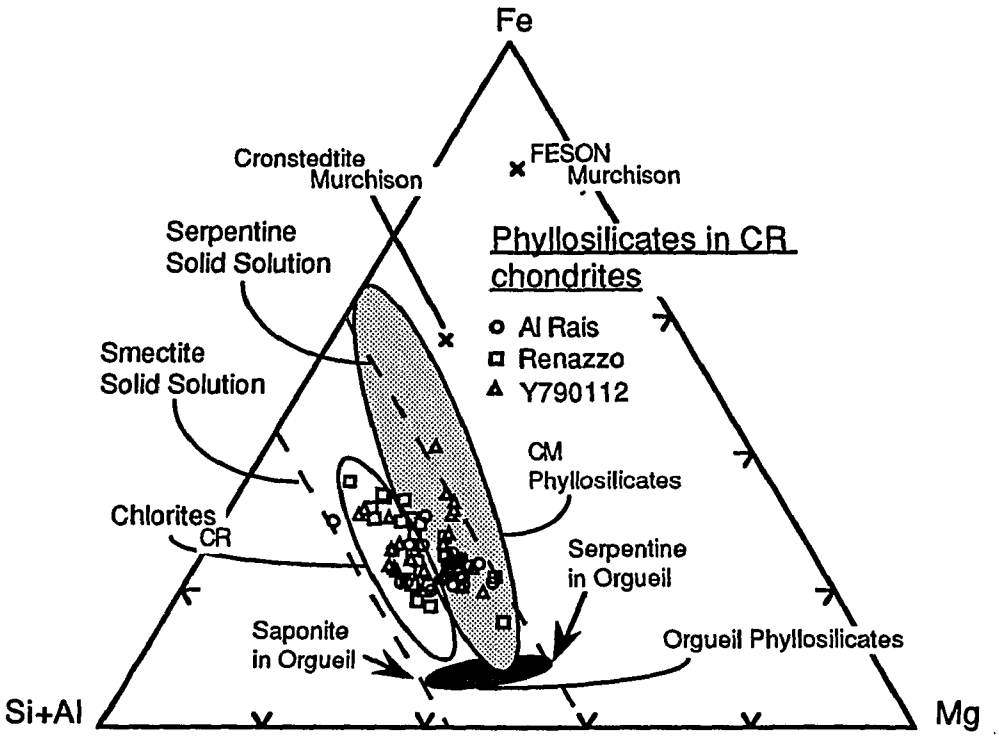

Fig. 3.1.4. Compositions of phyllosilicates in CR chondrites plotted on an Fe-(Si+A)-Mg ternary diagram shown in comparison to phyllosilicates in CI (solid loop) and CM (light-shaded loop) chondrites, and ideal serpentine and smectite solid solution tie lines. Chlorites in the CR chondrites are enclosed by a loop, the other points are serpentines (mixed with saponite).

Rims of chondrules vary in thickness, numbers of layers, and composition. Olivine and pyroxene layers in rims are generally finer grained and in many cases the olivine is richer in FeO than olivine in the cores; in some cases rim olivine contains more Cr_2O_3 (Table 3.1.3). The FeNi metal layers of chondrule rims (Fig. 3.1.3a) are also

Table 3.1.5. Representative analyses of phyllosilicates in the CR chondrules.

	Cores (Chlorites)			Rims (Serpentines/smectites)			Spheres (Serp/smect)		
	R-8	AR-40	Y79-20	R-53	AR-40	Y79-22	R-300	AR-6	Y-20
SiO_2	29.1	30.4	27.9	41.9	37.5	34.6	35.8	35.7	39.5
TiO_2	0.30	0.21	0.07	0.07	0.08	0.09	0.10	0.09	0.07
Al_2O_3	15.1	15.1	15.5	2.30	2.86	2.89	2.15	4.2	2.08
Cr_2O_3	0.23	0.15	bd	0.17	0.30	0.33	3.0	na	0.31
FeO	32.7	20.9	25.9	22.1	22.4	33.8	28.8	27.1	25.0
MnO	0.36	0.41	0.14	0.26	bd	0.19	0.27	0.17	0.11
MgO	11.5	21.1	18.3	18.2	20.6	17.4	13.6	17.9	21.5
CaO	0.76	1.07	0.22	0.10	0.27	0.33	0.12	0.17	0.14
Na_2O	0.31	0.23	0.15	0.31	bd	0.35	0.09	0.17	0.11
K_2O	0.06	0.07	0.08	0.12	bd	0.13	0.06	0.15	0.18
Total	90.4	89.6	88.3	85.5	84.0	90.1	85.0	86.1	89.0
H_2O*	9.6	10.4	11.7	14.6	16.0	9.9	15.0	13.9	11.0

na-not analyzed.
bd-below detection.
*Calculated by difference.

compositionally different from the FeNi in the cores, having lower Ni and Co (described in section 3.1.5). Most chondrule rims have a layer of phyllosilicate (serpentine-rich) and some have a carbonate-rich rim (Fig. 3.1.3c,d) while others have phyllosilicate-rich layers followed by a carbonate-rich shell. Many chondrules have an outermost sulfide-rich layer which is compositionally and texturally similar to matrix.

The phyllosilicate-rich shells are typically brown in color and compositionally appear to be mixtures of Fe-rich serpentine and smectite group minerals (saponite) and/or chlorite minerals. The serpentines typically contain 35-42% SiO_2, 2-3% Al_2O_3, 22-34% FeO, and 17-21 % MgO (Table 3.1.5). Brown phyllosilicate microspherules also occur on chondrule margins (Fig. 3.1.3c), in chondrule cores and unassociated in the matrix, and also within the phyllosilicate-rich chondrule rims. These microspherules are compositionally similar to the serpentine-rich rims on chondrules and may also be mixtures of serpentine and smectite minerals. Although the compositions of phyllosilicate rims and microspherules overlap, some brown microspherules have high Cr_2O_3, up to 3.0% (Table 3.1.5).

The serpentine in CR chondrites is most similar to that described in the Nogoya CM2 chondrite (Bunch and Chang, 1980). However, in general, the serpentines in CR chondrites are more restricted in composition than those in CM chondrites (Bunch and Chang, 1980), and are more magnesian than those in CI or CV chondrites (Bunch and Chang, 1980; Tomeoka and Buseck, 1988; Keller and Buseck, 1990; Tomeoka and Buseck, 1990) (Fig. 3.1.4).

In some cases, rims of phyllosilicates surround broken chondrules, including their broken angular surfaces, suggesting that this hydrous layer formed after chondrule breakage. In another case, a broken chondrule has a carbonate rim, but it is present only on the original curved chondrule surface (Fig. 3.1.3d,e). This suggests that either this chondrule originally contained a rim of material that was susceptible to Ca-carbonate

Table 3.1.6. Representative Ca-Carbonates in CR Chondrites

CaO	55.5	53.8	52.7	48.2
FeO	0.31	0.73	1.11	7.3
MnO	bd	1.96	bd	0.33
MgO	bd	1.66	3.1	1.66

bd-below detection

formation or the Ca-carbonate rim formed prior to chondrule breakage and therefore prior to lithification of the host chondrite. It should also be noted that among chondrules and inclusions in the same chondrite, the degree of aqueous alteration varies, supporting the latter scenario.

3.1.3 Matrix

Matrix in CR chondrites is black and opaque, as in highly unequilibrated chondrites, and constitutes up to 60 vol.% (Al Rais) of the meteorite. It consists of anhydrous and hydrous silicates that are too small to analyze with a 1-2μm electron beam. However, high resolution transmission electron microscope (HRTEM) investigations of Renazzo matrix indicate that it contains serpentine, saponite, and olivine (M. Zolensky, pers. comm., 1991). Ca-carbonates, blades of sulfides and magnetite framboids and platelets are also abundant in CR matrices (Fig. 3.1.3f). Sulfide and magnetite morphologies are similar to those described in CI chondrites. In some cases, magnetite framboids occur in clusters containing spheres of different sizes. However, framboids do not occur in all CR chondrites. None were observed in Renazzo, and instead, the magnetites are larger and irregular in shape.

Table 3.1.7. Bulk compositions (wt.%) of Dark Inclusions and matrices in CR chondrites.

	Darkl Inclusions								Matrix*	
	Renazzo	(sd)	Al Rais	(sd)	M87320	(sd)	Y790112	(sd)	Renazzo	Al Rais
SiO_2	31.0	(1.56)	26.5	(1.18)	26.8	(1.62)	30.3	(.97)	31.4	26.5
TiO_2	0.08	(.02)	0.07	(<.01)	0.08	(<.01)	0.09	(.02)	0.07	0.06
Al_2O_3	1.74	(.22)	2.49	(.15)	2.26	(.10)	2.58	(.71)	2.66	2.13
Cr_2O_3	0.29	(.03)	0.34	(.11)	0.43	(.07)	0.32	(.03)	0.35	0.32
FeO	25.5	(1.99)	25.7	(3.20)	28.4	(2.05)	28.8	(3.38)	24.3	22.2
MnO	0.23	(.05)	0.25	(.01)	0.36	(.02)	0.26	(.06)	0.33	0.17
MgO	17.5	(1.27)	15.5	(.84)	17.9	(1.30)	16.0	(.67)	15.8	15.2
CaO	2.01	(1.50)	1.68	(.52)	1.10	(.20)	1.54	(.47)	0.87	1.33
Na_2O	0.90	(.19)	0.71	(.08)	0.36	(.20)	0.57	(.10)	1.16	0.98
K_2O	0.15	(.04)	0.29	(.06)	0.30	(.06)	0.25	(.04)	na	na
S	2.71	(.72)	2.57	(.50)	2.96	(.13)	2.77	(.47)	3.18	2.98
Ni	0.76	(.11)	0.95	(.17)	1.12	(.32)	1.04	(.27)	1.16	1.69
Total	83.14		77.28		82.15		84.69		81.54	73.69
No. Inc.	4		4		3		4			

sd-standard deviation.
na-not analyzed.
*McSween and Richardson (1977).

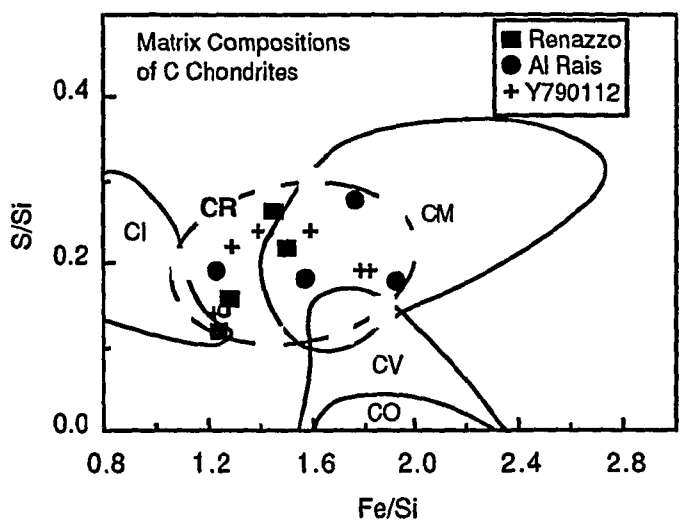

Fig. 3.1.5. Bulk compositions of Dark Inclusions (DI) in CR chondrites compared with matrices in other carbonaceous chondrites, on a S/Si vs. Fe/Si plot. Cr matrix and DI mainly plot in between and overlap with CI and CM matrices.

The Ca-carbonates in CR matrices range from nearly pure to having up to 7.3% FeO, 3.1% MgO and 1.9% MnO (Table 3.1.6); FeO may be overestimated due to intergrowths of magnetite with the carbonate that are too fine to be resolved with a 1-2μm electron beam. Texturally, the Ca-carbonates are irregular in shape, similar to those in CI chondrites, but some are twinned like those typically found in the CM chondrites (Johnson and Prinz, 1991).

Dark inclusions (DI) contain petrographic features and bulk compositions similar to those in CR matrices (Table 3.1.7) and are considered to be the same material concentrated into sharply bound lumps. Some DI contain high abundances of microchondrules (chondrules having diameters less than 500 μm) and micro-refractory-rich inclusions. These components are also found throughout the matrix. Fig. 3.1.5 is a plot of bulk S/Si vs. Fe/Si in matrices from CI, CM, CO, and CV chondrites, as compiled by Zolensky (1989). Zolensky (1989) suggested that these ratios are useful in distinguishing matrices from each of the chondrite groups. On this diagram (Fig. 3.1.5) several DI from four CR chondrites are plotted. With respect to these ratios, CR matrices plot in a unique position on this diagram, in between and overlapping with the CI and CM fields.

3.1.4 Refractory-Rich Inclusions

Most existing knowledge of refractory-rich inclusions comes from studies of Allende because of the abundance of this CV3 chondrite and the larger sizes and greater abundances of its inclusions. Much less information is known about these inclusions in other chondrite groups. A total of 22 inclusions were studied in CR chondrites: Renazzo (8 inclusions), Al Rais (5), EET 87770 (4), MAC87320 (1), and Y793495 (4). None were found in Y790112, but this may be due to sampling. The types of inclusions that were found include compact type A (CTA), fluffy type A (FTA), spinel-pyroxene aggregate (sp-pyx agg), Ca-Al-rich

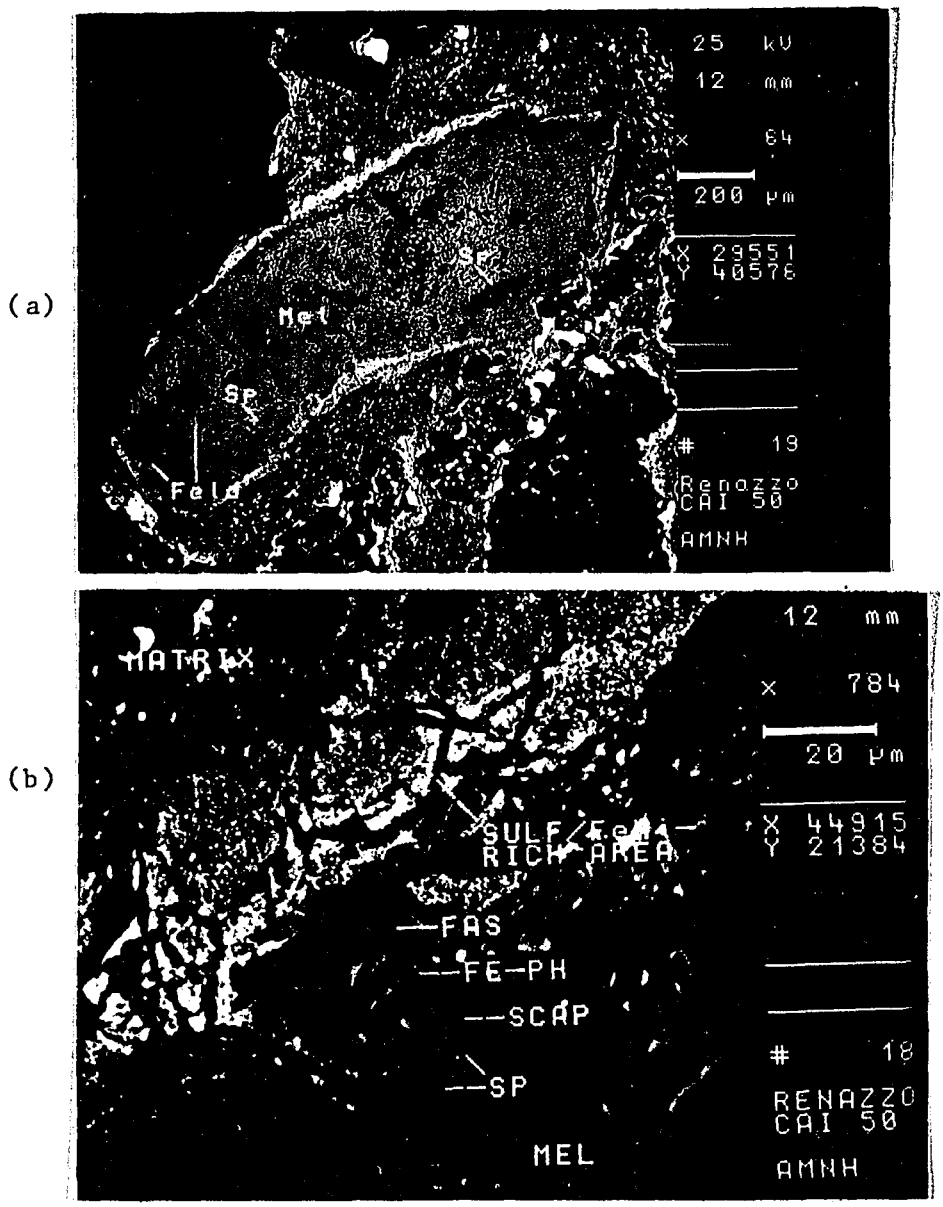

Fig. 3.1.6. Backscattered electron images of refractory-rich inclusions in CR chondrites. R-50 is a melilite (MEL) -rich compact type A inclusion from Renazzo (a) surrounded by a Wark-Lovering rim sequence The rim consists of spinel (SP), scapolite (SCAP), Fe-rich Phyllosilicate (FE-PH), and a sulfide/FeNi metal-rich layer (b). R151 is a spinel-pyroxene aggregate (c). R310 is a spinel-pyroxene aggregate having spinel nodules of different sizes (d). M87-18 is a fluffy type A inclusion from MAC87320. It consists of nodules having cores of melilite, surrounded by anorthite and rimmed by diopside (e) . Fine inclusions of spinel occur in the melilite. R131 is a Ca-Al-rich chondrule consisting of anorthite, low-Ca pyroxene, fassaite, and olivine (f). Y793-6 is an amoeboid olivine aggregate in Y793495, consisting of a refractory-rich nodule (spinel+fassaite) surrounded by an aggregate of olivine (g).

(c)

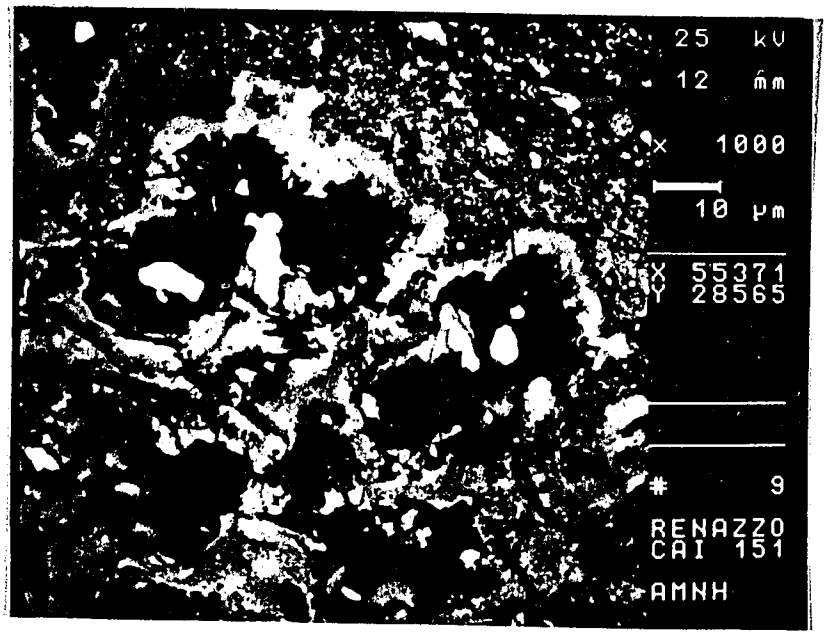
25 kV
12 mm
X 1000
10 µm
X 55371
Y 28565
9
RENAZZO
CAI 151
AMNH

(d)

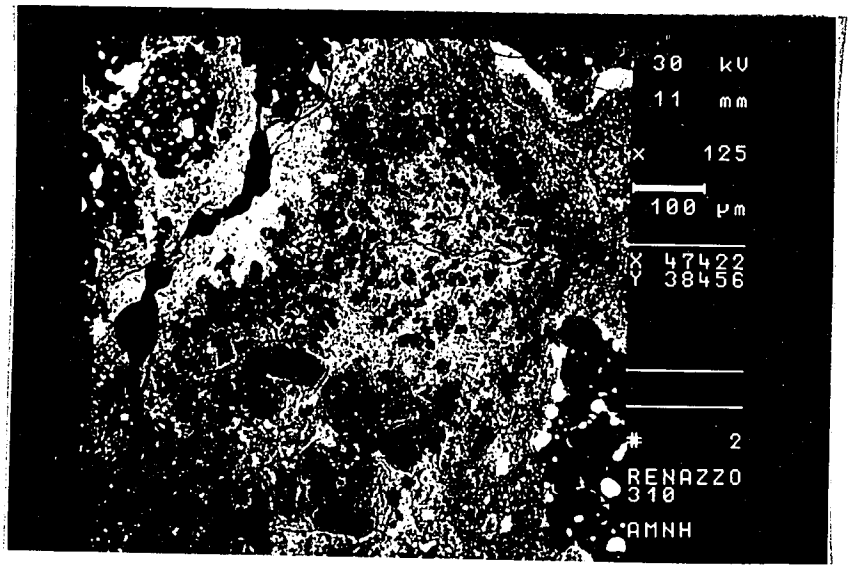
30 kV
11 mm
X 125
100 µm
X 47422
Y 38456
2
RENAZZO
310
AMNH

(e)

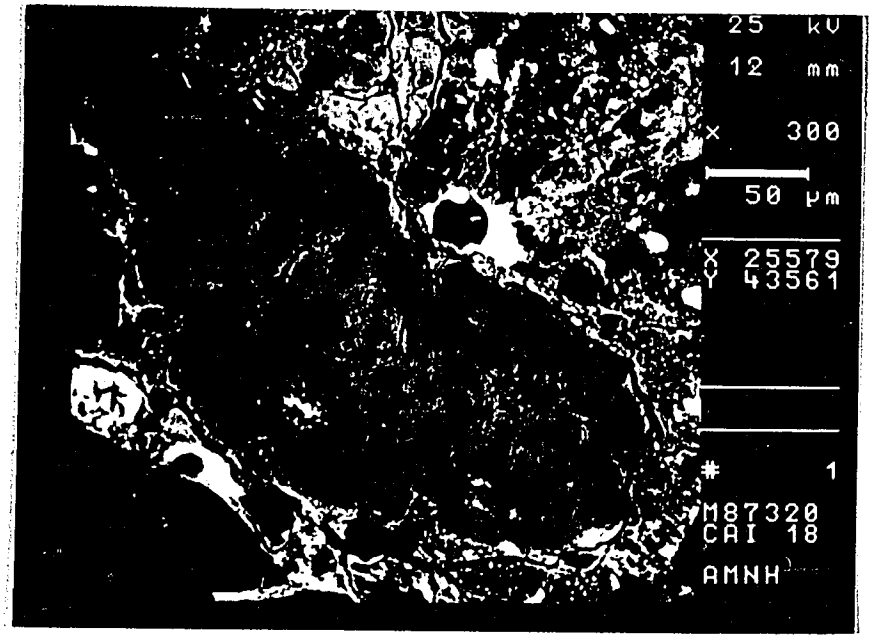
25 kV
12 mm
x 300
50 µm
X 25579
Y 43561
1
M87320
CAI 18
AMNH

(f)

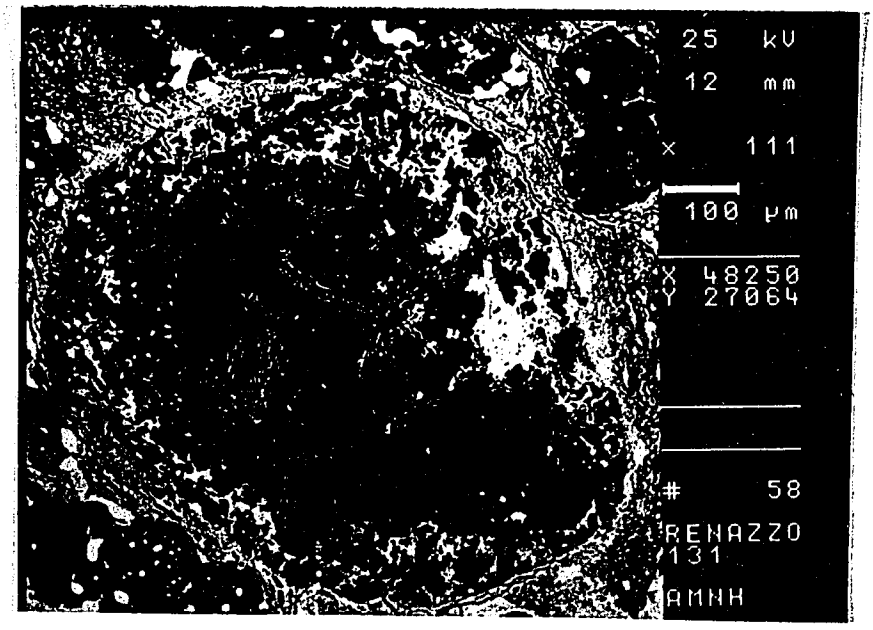
25 kV
12 mm
x 111
100 µm
X 48250
Y 27064
58
RENAZZO
#131
AMNH

(g)

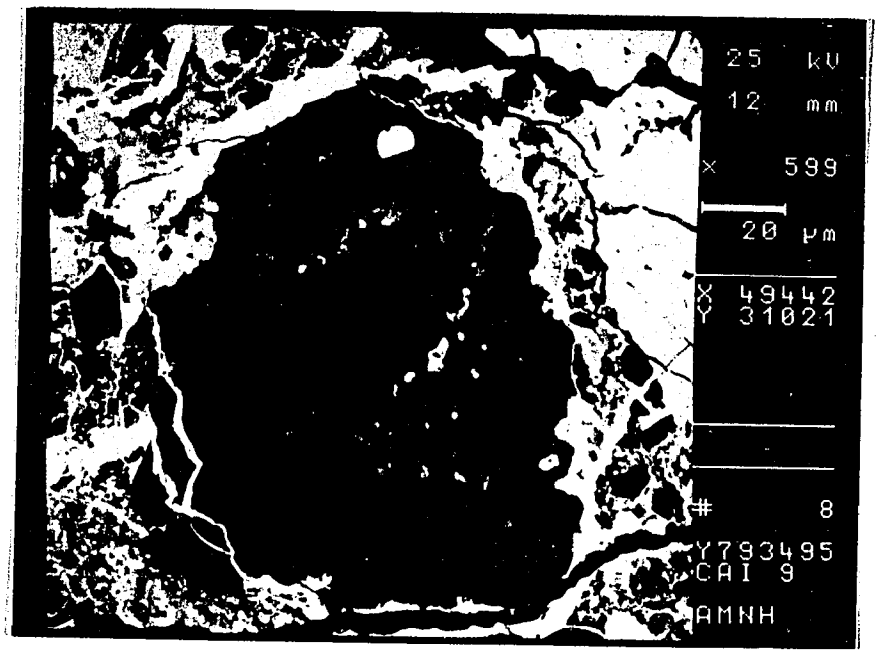

Table 3.1.8. Representative spinels from Sp-Pyx Aggregates and Fluffy Type A Inclusions

	CR (Renazzo)			CM (Murchison)		CV (Allende)
TiO_2	0.07	0.20	0.13	0.27	nd	0.6-0.32
Al_2O_3	69.6	71.1	70.8	68.6	71.9	61.9-71.2
Cr_2O_3	0.27	0.12	0.13	na	na	0.15-0.21
V_2O_3	0.65	nd	0.26	0.23	nd	0.60-4.9
FeO	0.44	0.06	0.21	0.04	nd	0.06-20.7
MgO	27.6	28.1	27.9	27.1	28.4	12.0-28.7
CaO	0.10	nd	nd	0.59	nd	0.33-1.2
Total	98.70	99.58	99.43	97.56	100.29	98.89-102.27

nd below detection
na not analyzed

chondrules (CAC), and amoeboid olivine aggregates (AOA). The 22 inclusions are described in detail below.

R-50 from Renazzo is a melilite-rich CTA inclusion (Fig. 3.1.8a) similar to those described in Allende (Grossman, 1975). It is an elongate inclusion (1.5x0.5 mm) consisting of 88% coarse melilite ($Ak_{\sim 25}$) with fine spinel (8%) and perovskite (1%) inclusions, and 3% anorthitic feldspar (Fig. 3.1.8a). The inclusion is surrounded by a Wark-Lovering rim sequence (Wark and Lovering, 1977) of spinel and perovskite, followed by feldspar, followed by fassaitic pyroxene, and surrounded by clastic Fe-rich material which resembles chondrite matrix (Fig. 3.1.6b).

Five inclusions (R-151, -310, -311, -315, -316) that were studied are sp-pyx aggregates similar to those in Murchison (CM2) (MacPherson et al., 1983). These are aggregates of spinel nodules with minor perovskite inclusions Fig. 3.1.6c). Each nodule is rimmed by a band of diopsidic and/or fassaitic pyroxene. [Fassaite is defined as a pyroxene solid solution of diopside, Ca-Tschermak's molecule ($CaAl_2SiO_6$) and Ti-Tschermak's

molecule ($CaTi^{4+}Al_2O_6$).] Some have spinel rimmed by melilite and can be considered spinel-melilite aggregates. The aggregates are irregular in shape, and vary in size and length/width ratios. R151 is narrow (1000x150 μm) and partly indented by a chondrule. Most, however, have length/width ratios of 1-2 and are up to 800 μm, making them similar in size to Murchison aggregates (MacPherson et al., 1983). Individual nodules within the aggregates range in size from 1-200 μm. In most aggregates, nodules are approximately uniform in size, except for R310 which contains an area of numerous 1μm-sized nodules, and another portion of 200μm-sized nodules Fig. 3.1.6c-d). The spinel is essentially $MgAl_2O_4$, but some contain FeO (up to 0.44%) and V_2O_3 (up to 0.65%) (Table 3.1.8), similar to spinel in Murchison sp-pyx aggregates (MacPherson et al., 1983). Some of the melilite-bearing nodules contain nearly pure gehlenite. In between the nodules is fine grained Fe-rich matrix-like material which, in some cases, contains abundant calcite.

MacPherson et al. (1983) pointed out that the sequence spinel rimmed by diopside is inconsistent with crystallization of sp-pyx nodules from spinel-rich melt droplets, and suggested that this type of inclusion formed by direct condensation in the solar nebula. Sp-pyx aggregates in CR2 chondrites contain melilite associated with the spinel and thermodynamic calculations predict that melilite will condense from a gas of solar composition in the same high temperature range as spinel, supporting the condensation model. The sp-pyx aggregates were probably once loosely bound aggregates of nodules which were floating freely in the solar nebula, as proposed for fluffy type A inclusions in Allende (MacPherson and Grossman, 1984). Voids between the aggregates were probably later filled by a lower temperature component, probably Fe-rich matrix-like material. It is of interest that sp-pyx aggregates have previously been found only in CM2 chondrites (MacPherson and Grossman, 1984). Now they are shown to occur in another group of C2 chondrites- the CR2 group.

One melilite-rich FTA inclusion (M87-18) was found in MAC87320. It is 300x150 μm, has a concentric structure with a core of melilite surrounded by anorthite, and is rimmed by diopside (Fig. 3.1.6e). Spinel occurs as inclusions in the melilite. Adjacent melilite-spinel-anorthite nodules share diopside rims. Texturally, this inclusion is similar to some of the fluffy type A inclusions described in Allende (MacPherson and Grossman, 1984). The concentric sequence of minerals is consistent with the predicted order of condensation from a solar gas in the temperature range ~1600-1400K.

R-131 is nearly spherical and is a CAC. Its bulk composition is similar to fassaite-poor type C chondrules (Wark, 1987). It consists of 55% anorthitic plag, 26% low-Ca pyroxene, 14% fassaitic pyroxene, 2% olivine and 2% spinel (Fig. 3.1.6f). The spinel contains 0.35% V_2O_3 similar to that in sp-pyx aggregates, but contains 1.3% Cr_2O_3. The plag appears to have been recrystallized, having a granular texture with "ghosts" of lath-like crystals. Olivine and pyroxene occur on the edges of the CAC and as inclusions in its anorthite-rich core. The spherical shape suggests it may have crystallized from a molten droplet. Additionally, the mineral relationships are consistent with the order of crystallization determined from phase equilibria (Stolper, 1982).

Fourteen AOA were found. One is from Renazzo (R-100), five from Al Rais (AR-51, -101, -102, -121, -122), four from EET87770 (E87-1,-2, -3, -4) and four from Y793495 (Y79-1, -6, -7, -8). These are fine-grained aggregates of olivine. Some aggregates are large (up to 1.5 mm) and consist of variable proportions of olivine rimming cores of fassaitic pyroxene with spinel inclusions, and plag (Fig. 3.1.6g). The Renazzo and Al Rais aggregates contain calcite and their phase relationships are less clear, suggesting that they have experienced greater degrees of aqueous alteration than inclusions in the other CR chondrites. R100 contains a nodule similar to nodules in the sp-pyx aggregates described above.

Table 3.1.9. Representative analyses of olivines from AOA in CR2 chondrites.

	Al Rais		Y793495	
	Blue	Red	Blue	Red
SiO_2	41.6	41.6	42.2	42.3
Cr_2O_3	0.25	0.41	0.14	0.29
FeO	0.18	0.22	0.48	0.52
MnO	0.10	0.43	nd	0.33
MgO	57.2	56.4	56.0	56.3
CaO	0.09	0.05	0.12	0.10
Total	99.42	99.11	98.94	99.84
Fo	99.8	99.8	99.5	99.5

nd below detection

The most striking feature of AOAs in CR2 chondrites is the occurrence of two types of olivine. One type has a blue cathodoluminesence and the other fluoresces red; both types are highly magnesian ($Fo_{99.5-99.8}$). Red olivine contains more MnO and Cr_2O_3 than blue olivine (Table 3.1.9, Fig. 3.1.7). Surprisingly, MnO abundances in some of the red olivine equals or surpasses FeO. Similar high MnO/FeO ratios were reported in interplanetary dust particles (IDP) (Klock et al., 1989) and their compositions are attributed to nebular condensation processes.

The irregular shapes and aggregational appearance of the AOA suggest that they did not crystallize from a melt. In addition, the occurrence of fassaitic pyroxene with spinel inclusions and sp-pyx nodules in the aggregates, suggests that they are related to refractory-rich inclusions believed to be products of nebular condensation. A possible scenario that will be explored is that early condensates (fassaite-spinel nodules) floated freely in the nebula, and then at ~1450K forsterite condensed and aggregated onto these nodules. The aggregates remained in contact with the nebular gas until Mn_2SiO_4 condensed in solid solution with forsterite at ~1,100°K (Klock et al., 1989; Larimer, 1967; Wai and Wasson, 1977). High

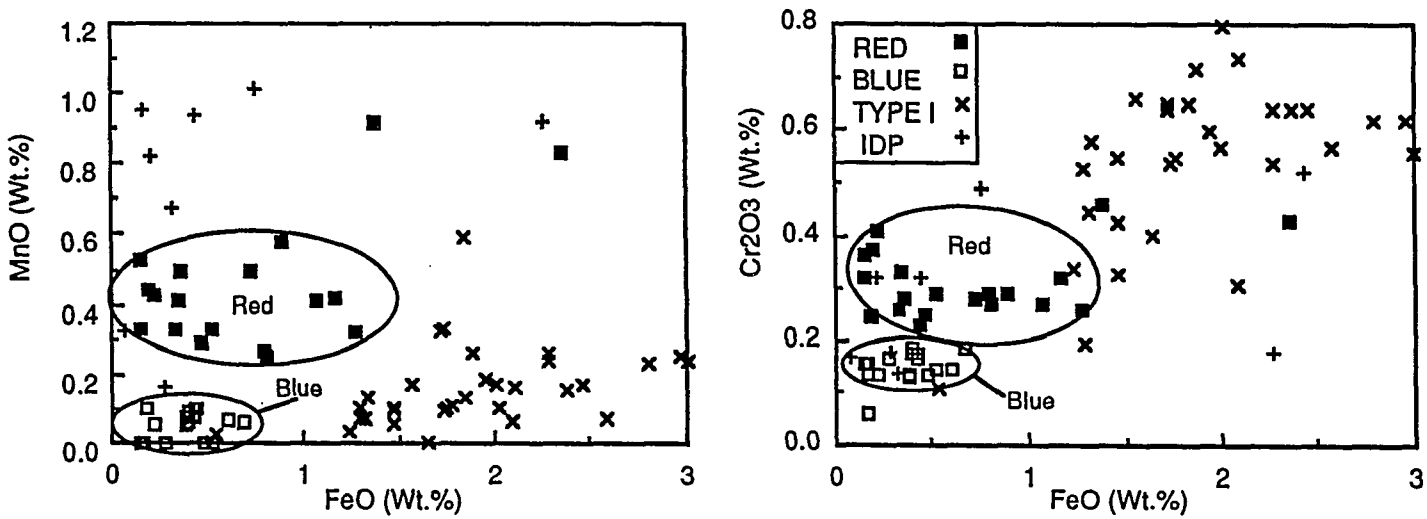

Fig. 3.1.7. FeO vs. MnO and Cr2O3 in olivine from amoeboid olivine aggregates in CR chondrites, compared with typical type I CR chondrule olivine and LIME (Low Iron Mn Enriched) olivine from IDP (Interplanetary Dust Particles). IDP data are from Klock et al. (1989).

MnO/FeO ratios in olivine may result because the fayalite molecule does not form until much lower temperatures. Mn_2SiO_4 forms earlier than Fe_2SiO_4 because Mn is not stable as a metal in the solar nebula and thus condenses in solid solution in olivine. Fe, however, condenses as a metal and does not react to form fayalitic olivine until ~500K.

3.1.5 Metal

The FeNi metal in CR chondrites is concentrated mainly in the chondrules. It occurs as spheres in chondrules and as rims on layered chondrules. Rare metallic chondrules also are found and some of these are rimmed by anhydrous and hydrous silicates like the silicate chondrules. FeNi metal was analyzed in three CR chondrites and it is compositionally similar in all three, having 4-14 wt.% Ni, 0.1-0.6% Co, 0.01-1.2% Cr, and 0.05-1.1% P. As discussed above, Ni and Co is generally higher in the FeNi in the chondrule cores than in the rims (Table 3.1.10, Fig. 3.1.8a). In addition, FeNi in all CR chondrites has a positive Ni-Co trend which overlaps with that of a calculated condensation path using the calculations of Grossman and Olsen (1984) and data from Cameron (1985) (Fig. 3.1.8). However, plots of Ni vs. Cr and P do not show clear trends. For Ni vs. Cr the data fall below the condensation curve, but appear to loosely follow the condensation trend (Fig. 3.1.8b). For Ni vs. P, again, there is much scatter in the data, but many datum points cluster about the condensation curve (Fig. 3.1.8c). Some of these trends may be the result of chromite and phosphate exsolution found in Renazzo metal (Zanda et al., 1991).

As shown in Fig. 3.2.4, the FeNi in the unique ALH85085 chondrite and the Bencubbin meteorite is compositionally similar to CR metal. Thus, the FeNi in these unique meteorites may have formed under similar conditions and processes as the FeNi in the CR chondrites.

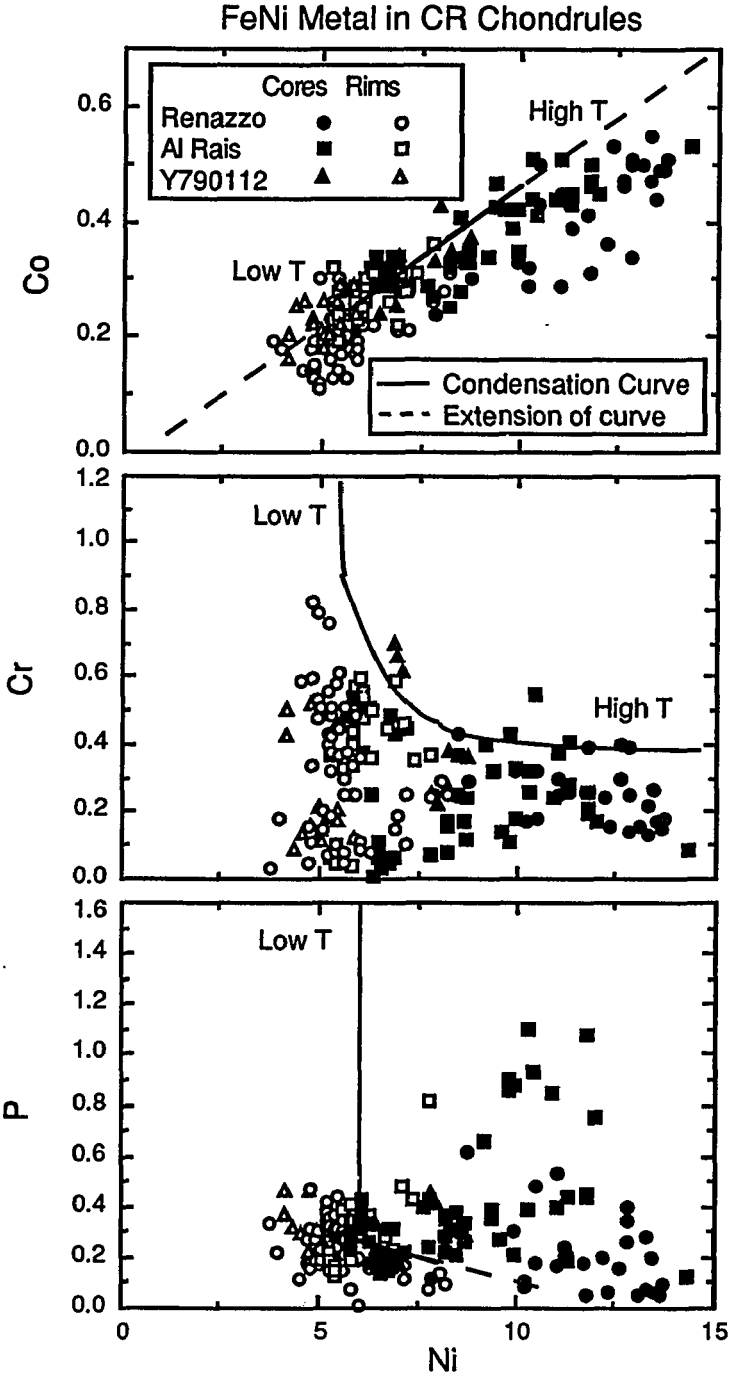

Fig. 3.1.8. Plots of (in weight %) Ni vs. Co (a), Cr (b), and P (c) for FeNi metal in chondrule cores and rims in CR chondrites. Also shown is the calculated equilibrium condensation path of FeNi condensing from a solar gas, as according to Grossman and Olsen (1972). Ni and Co in the CR chondrites overlap with the condensation trend, but their values extend beyond the upper and lower limits of metal predicted to condense from the nebula. Cr and P do not follow the condensation trend.

Table 3.1.10. Compositional ranges of metallic FeNi grains in CR chondrules.

	Renazzo		Al Rais		Y790112	
	Cores	Rims	Cores	Rims	Cores	Rims
Ni	5.8-13.7	3.8-8.2	5.8-14.3	5.3-7.8	5.6-8.8	4.2-5.9
Co	0.21-0.55	0.11-0.31	0.23-0.53	0.19-0.36	0.24-0.43	0.16-0.29
Cr	0.13-0.43	0.01-0.87	0.01-1.20	0.04-0.60	0.08-0.70	0.09-0.52
P	0.05-0.62	0.01-0.47	0.13-1.10	0.13-0.82	0.17-0.45	0.17-0.46
No. Grains	31	56	49	25	11	16

3.1.6 Bulk Chemical Compositions

Bulk chemical compositions of Renazzo and Al Rais whole chondrites are shown in Table 3.1.11. They appear to be similar with the minor exception that Al Rais contains more H_2O (8.5%) than Renazzo (5.7%). This may be result of a higher matrix/chondrule ratio and a greater degree of aqueous alteration observed in Al Rais.

Kallemeyn and Wasson (1978) reported INAA bulk chemical compositional data for Renazzo and Al Rais and also showed that they are generally similar, but that Renazzo is depleted in volatiles relative to Al Rais. As a result, they suggested that they should not be grouped together. However, the lower volatile abundance in Renazzo may reflect its lower abundance of matrix, since volatiles are mainly concentrated in the matrix (Table 3.1.7 and 3.1.11).

Table 3.1.11. Bulk chemical compositions of Renazzo and Al Rais.

	Renazzo[1]	Al Rais[1]	Renazzo[2]	Al Rais[2]
SiO_2	33.83	30.29	42.83	45.0
TiO_2	0.186	0.08	0.23	0.11
Al_2O_3	2.36	1.97	2.99	2.93
Cr_2O_3	0.56	0.57	0.71	0.84
FeO	15.35	10.0	19.43	14.86
MnO	0.24	0.23	0.30	0.34
MgO	23.76	21.20	30.1	31.50
CaO	1.78	2.00	2.25	2.97
Na_2O	0.55	0.62	0.70	0.92
K2O	0.042	0.033	0.05	0.04
P_2O_5	0.28	0.27	0.35	0.40
V_2O_5	0.048	0.030	0.06	0.04
C	1.44	2.49		
N	0.06	0.19		
H_2O^*	5.67	8.49		
FeNi	12.07	10.92		
FeS	3.59	7.29		
Σ	101.816	96.67		
FFM			0.45	0.38

1-Renazzo data from Mason and Wiik (1962), Al Rais data from Mason and Wiik (1962). Total Fe in silicates and oxides reported as FeO; FeNi calculated based on an average Fe:Ni ratio of 7.94.

2-Recalculated to 100% silicate and oxide components, total Fe in these components reported as FeO.

FFM-Fe/(Fe+Mg)

* Reported as total H_2O and is assumed to be H_2O+

3.1.7 Oxygen Isotopic Compositions

Oxygen isotopic compositions of six CR whole chondrites, as well as chondrules and matrix from Renazzo and Al Rais are presented in Table 3.1.12 and Fig. 3.1.9 and 3.1.10. In comparison to other chondrite groups, the CR chondrites occupy their own region on the oxygen 3-isotope diagram and form a unique mixing line having a slope of 0.79 (Fig. 3.1.9). Matrices from Renazzo and Al Rais plot near the intersection of the CR mixing line and the terrestrial mass fractionation line. Relative to the CI chondrites, they are displaced southwest, along the terrestrial fractionation line.

Chondrules and matrices from Renazzo and Al Rais plot on the CR mixing line and those from Renazzo are displaced toward lighter oxygen relative to those in Al Rais (Fig. 3.1.10). Differences in the oxygen isotopic compositions of their components contribute to the relative positions of their whole rock compositions, as does the large abundance of matrix in Al Rais. This shift in the Al Rais components, toward heavier oxygen, may be related to its greater degree of aqueous alteration. Thus, a liquid component having heavier oxygen, may have mixed with these components and pulled their oxygen compositions in a northeast direction on the CR mixing line. For CM chondrites, Clayton and Mayeda (1984) suggested a water component having relatively heavy oxygen ($\delta^{17}O$=30.3, $\delta^{18}O$=20.2).

Table 3.1.12. Oxygen isotopic compositions of CR chondrites, chondrules and matrix.

	$\delta^{18}O$	$\delta^{17}O$
Whole Chondrite		
Renazzo	6.25	2.29
Al Rais	10.94	4.68
EET 87770	2.76	0.22
MAC87320	1.79	-0.87
Y790112	2.39	-0.39
Y793495	1.39	-0.91
Chondrules		
Renazzo		
Re-1	4.60	1.25
Re-2	3.21	-0.24
Re-3	2.33	-0.71
Al Rais		
AR-1	4.72	1.56
AR-2	4.11	0.49
AR-4	4.73	0.82
AR-5	5.38	1.88
AR-9	4.68	0.87
AR-10	4.59	1.01
Matrix		
Renazzo		
MX1	10.44	5.01
MX2	9.90	5.41
Al Rais		
MX1	10.77	5.09
AR-3*	13.26	6.68

* Matrix lump
Data from Clayton and Mayeda (1989) and Weisberg et al. (1989).

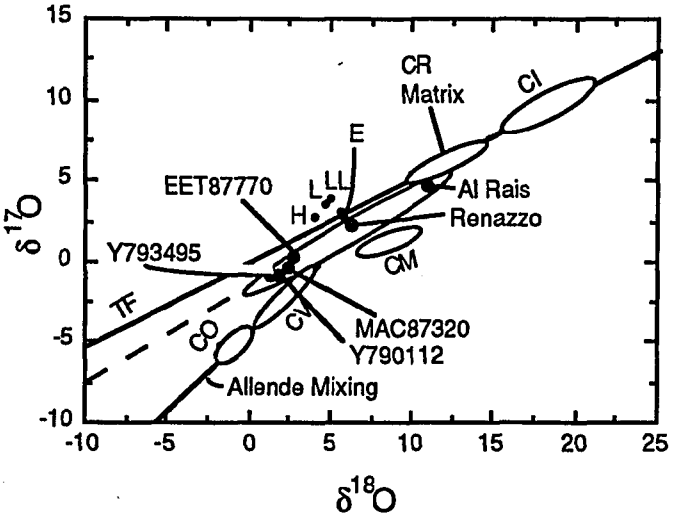

Fig. 3.1.9. Oxygen 3-isotope diagram showing whole chondrite and matrix compositions of the CR chondrites in relation to other chondrite groups (H, L, LL, E, CI, CO, CV, CM) and the terrestrial mass fractionation line (TF). CR chondrites occupy their own region on this diagram and form a mixing line having a slope of 0.79.

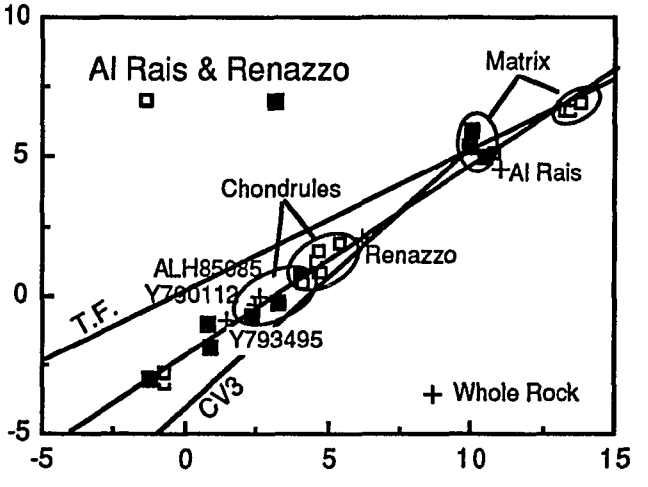

Fig. 3.1.10. Enlarged oxygen 3-isotope diagram showing whole chondrite, chondrules and matrix compositions of the CR chondrites. Note that components in Renazzo are displaced toward lighter oxygen relative to those in Al Rais.

3.2 The ALH85085 Chondrite

ALH85085 consists of components similar to those in other chondrites. These include chondrules, lithic and mineral fragments, opaque matrix, refractory-rich inclusions, sulfides, and metal. However, the abundances and some of the characteristics of these components differ from those previously reported for established chondritic groups. Fig. 3.2.1a is a photomicrograph showing the general texture. A description of its components follows.

3.2.1 Modal abundances

Whole-chondrite modal data are presented in Table 3.2.1. The FeNi metal is present at 40.9 wt.% (22 vol.%), a concentration greater than that in any known chondrite, except for the Bencubbin metal-silicate assemblage. Sulfide, on the other hand, is very low, at 1.1 wt.%. The only other chondritic group with sparse sulfides are the CR chondrites (Table 3.2.1). The feldspathic component of ALH85085 also appears to be less abundant than in most chondrites, but this is probably due to the fine grain size and cryptocrystalline character of most chondrules which makes it difficult to discern feldspar modally. The Al_2O_3 content of the chondrite (Table 3.2.2) indicates a typical feldspathic component. The high abundance of low-Ca pyroxene warrants comparison with enstatite chondrites but the olivine/pyroxene ratio is much greater than in EH3 chondrites (Table 3.2.1).

Other trace phases present, not included in Table 3.2.1, are hibonite, Mg-Al spinel, osbornite (TiN), and pentlandite. Also, present in minor amounts are magnetite, phosphate, and possibly phyllosilicates. These latter phases are mainly located in the lumps of opaque matrix.

Table 3.2.1

Modal abundances (wt.%) in the ALH85085,9 chondrite compared with those in E, H and CR chondrites and the Bencubbin meteorite

	ALH85085	EH3 (Parsa)	EH4,5 (avg.)	H	CR (Renazzo)	Bencubbin
Silicates						
Olivine	26.0	5.2		48.4		43.1
Pyroxene	69.1 [a]	83.5 [b]	100.0 [b]	38.2	100.0	45.5
Feldspar/glass	4.8	8.9		13.4		11.4
Silica	–	2.4		–		–
Phyllosilicate	–	–		–		–
Olivine/pyroxene	0.38	0.06	0.0	1.26		0.95
Non-silicates						
Sulfide	1.1	16.0 [c]	11.9 [c]	5.3	0.6	–
FeNi	40.9	16.7	22.6	18.6	17.3	78.9 [d]
Phosphide	–	0.6	0.6	–	–	–
Reference	this study	[6]	[2]	[7]	this study	[8,9]

Silicates recalculated to 100% (metal-sulfide-free).

[a] Includes non-stoichiometric enstatitic materials.

[b] Essentially all low-Ca pyroxene.

[c] Includes troilite, daubreelite, niningerite, oldhamite.

[d] Includes minor sulfide.

–: not detected.

Fig. 3.2.1. Photomicrographs of ALH85085,9 and ,5 showing: (a) general texture (field of view=1.1mm); note the high abundance of FeNi and the 75 μm chondrule in the lower center; (b) an osbornite-Mg-Al spinel-clast (clast field=25 μm); dark grayish phase is Mg-Al spinel, reflective phase is osbornite and light grayish area is Ti-Al- and Zr-bearing phase(s); (c) isolated framboidal magnetite (field=55 μm); similar to those in the matrix lumps and CI chondrites; (d) a magnetite grain (field=240 μm); this grain is much larger than those in matrix lumps and is rimmed by sulfide; (e) a matrix lump (field=240 μm); note the sulfides (white) and magnetites (gray) in the clast.

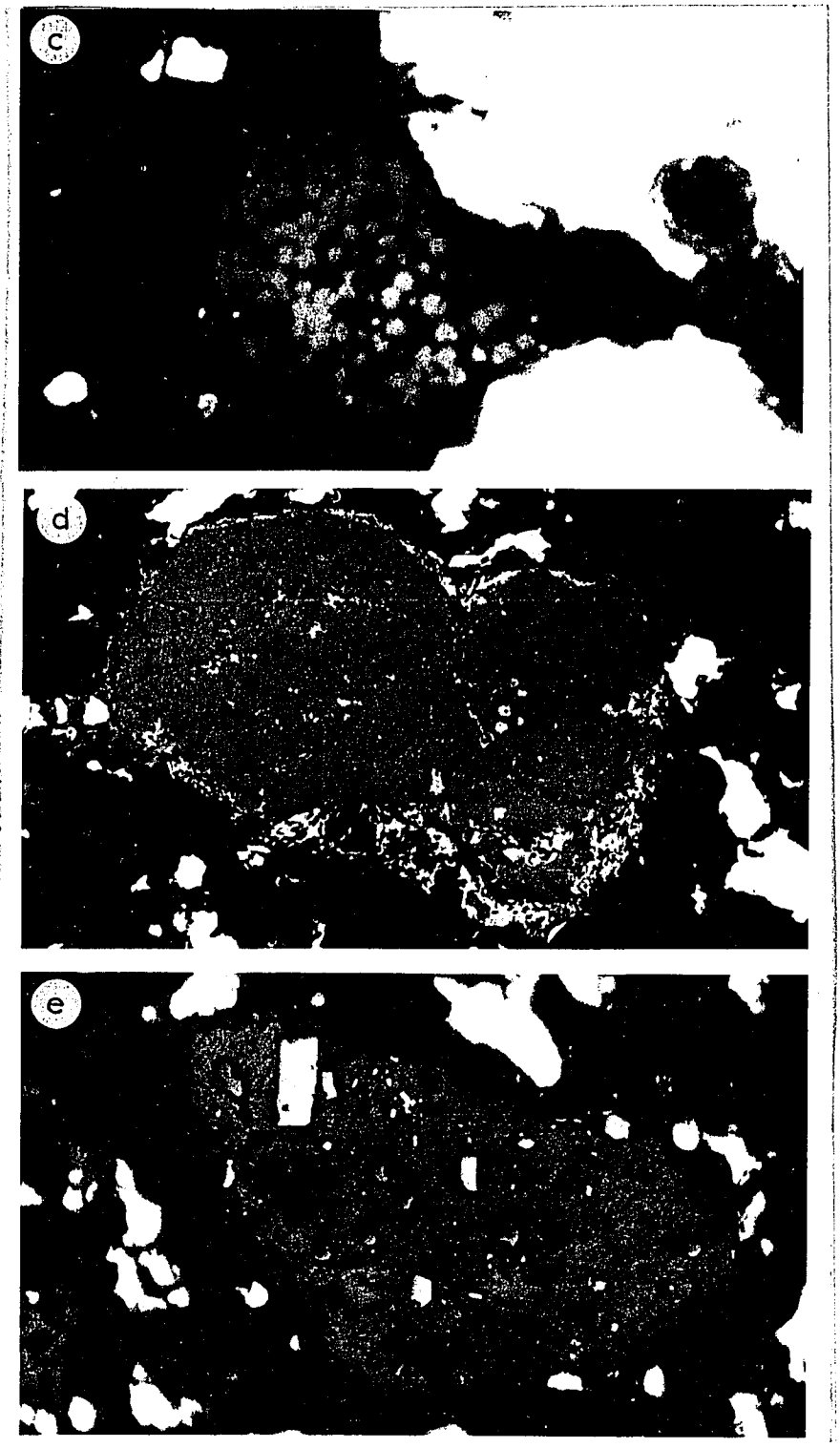
c
d
e

Table 3.2.2

Compositions (wt.%) of the ALH85085 chondrite, and its matrix lumps and chondrules obtained by broad-beam electron microprobe analysis

	Whole rock	Matrix lumps	Chondrules				
			C	BO	PO	POP	GP
SiO_2	48.9	40.6	55.4	48.1	46.7	47.2	55.6
TiO_2	0.2	0.1	0.1	0.4	0.4	0.1	0.1
Al_2O_3	3.6	2.2	1.1	11.9	12.0	5.9	3.0
Cr_2O_3	0.8	0.6	0.7	0.4	0.5	0.6	0.8
FeO	4.0	25.8	0.5	2.1	1.8	3.4	3.7
MnO	0.4	0.3	0.2	0.03	0.03	0.2	0.4
MgO	38.8	27.5	40.8	30.3	30.0	39.2	34.6
CaO	2.6	1.0	1.2	7.6	7.5	3.2	1.6
Na_2O	0.4	1.2	–	0.04	0.1	0.2	0.2
K_2O	0.08	0.2	–	–	–	0.2	0.7
P_2O_5	0.2	0.3	0.04	–	–	0.02	0.07
	100.0	99.8	100.0	100.9	99.0	100.1	100.8
FeS	1.1	9.2	–	–	–	–	0.1
FeNi	40.9	tr.	–	–	–	–	6.3
FeNiS	0.01	3.9	–	–	–	–	–
Number of analyses		9	12	2	1	1	1

Silicate portions are recalculated (metal-sulfide-free) to 100%.
C = cryptocrystalline; BO = barred olivine; PO = porphyritic olivine; POP = porphyritic olivine-pyroxene; GP = granular pyroxene.
–: less than 0.01%.

3.2.2 Chondrules

Chondrules make up 5-10vol.% of ALH85085 and are unique in several respects. They are typically smaller than in other chondrites, most ranging from 25 to 75 μm in apparent diameter, and are similar in size to those in the microchondrule-bearing clast in the

Piancaldoli LL3 chondrite (Rubin et al., 1982), which are 0.2-0.6 μm in apparent diameter. Few chondrules were found to be as large as 250 μm. Most chondrules are cryptocrystalline, whereas in most chondrites these are one of the least abundant type (Gooding and Keil, 1981). Barred, porphyritic, and granular chondrules are also present, but are rare in comparison to cryptocrystalline ones.

The majority of cryptocrystalline chondrules all have similar bulk compositions, which approximate low-Ca pyroxene with a minor feldspathic component (Table 3.2.2) and are depleted in volatiles (Na, K and S). Porphyritic and barred olivine chondrules contain olivine and abundant feldspathic glass with or without low-Ca pyroxene. These chondrules have higher FeO, Al2O3 and CaO, and lower SiO2 and MgO, than the cryptocrystalline varieties (Table 3.2.2). Their Al2O3 contents commonly exceeds 10%, making them Al-rich chondrules according to the criteria of Bischoff and Keil (1984). The granular chondrules appear to contain less feldspathic component as indicated by lower Al2O3.

The chondrule feldspathic glass is generally clear, nearly isotropic, and highly calcic (anorthitic) as indicated by the bulk compositions in Table 3.2.2. Chondrule pyroxene is essentially all of the low-Ca variety, and highly magnesian, Wo_{1-3}, En_{95-99} (Fig. 3.2.2); olivine is $Fo_{90-99.5}$.

3.2.3 Fragments

The majority of the lithic fragments, about 70% of the meteorite, are similar in texture and composition to the cryptocrystalline chondrules. Other lithic fragments have barred olivine and porphyritic textures and appear to be broken chondrules. These chondrule fragments are similar in size to the whole spherical chondrules, indicating that they were derived from a larger chondrule population which was broken up.

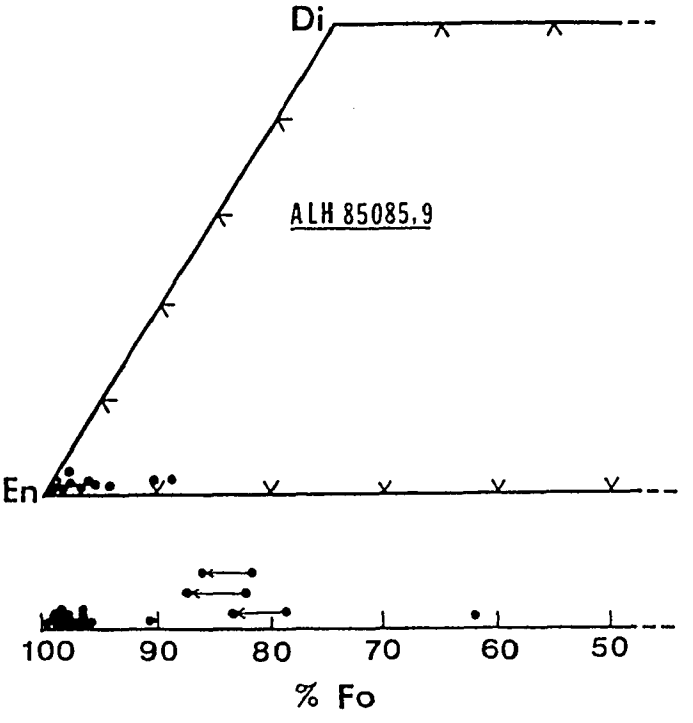

Fig. 3.2.2. Portion of the pyroxene quadrilateral and olivine plane showing compositions of the mafic silicates in ALH85085. The end members are Di (diopside), En (enstatite), Fo (forsterite), and Fa (fayalite). Points with arrows indicate large isolated olivine grains with reverse zoning. Most chondrule compositions are magnesian, and some mineral fragments are Fe-rich.

Small fragments of CAIs have also been found. They are melilite-rich and contain spinel, hibonite, and perovskite (Grossman et al., 1988). One fragment found in ALH85085,5 is composed of osbornite (TiN), Mg-Al Spinel, diopside, and Ti-, Al-, and Zr-bearing phase(s) (Fig. 3.2.1b). The Ti-, Al-, Zr-bearing phases are too small to resolve with an electron microbeam. The assemblage appears to be related to the CAIs, and this is the first occurrence of osbornite with this type of assemblage.

Mineral fragments include olivine, low-Ca pyroxene, magnetite, osbornite, and hibonite. Olivine occurs as angular fragments which are dispersed throughout the thin sections. These are generally 10-20 μm in size and smaller, but rarely as large as 200 μm. Olivine fragments range from Fo_{62} to Fo_{99} and the larger grains generally contain more FeO than the smaller ones. Some of the large olivine grains are reversely zoned, ranging from Fo_{82} in the center to Fo_{88} on the edge (Fig. 3.2.2) suggesting that they experienced reduction after initial formation.

Isolated magnetite fragments usually occur as spheroids 10-20 μm in size, and as framboids (Fig. 3.2.1c) similar to those found in CI chondrites (Kerridge et al., 1979), CR matrix (Fredriksson et al., 1981) and in ALH85085 matrix lumps described below. In addition, an unusually large (190μm) magnetite grain was observed (Fig. 3.2.1d). It contains inclusions of troilite, and is surrounded by a halo of troilite. This grain is much larger than, and differs in shape from any magnetite observed in the matrix lumps. One 25μm osbornite fragment, and a 5μm hibonite grain were also found.

3.2.4 Matrix lumps (DI)

Matrix material between chondrules and fragments is extremely sparse and difficult to characterize. However, opaque matrix-like material occurs throughout the sample as lumps with sharp boundaries (Fig. 3.2.1e). They range in size up to 300 μm, and consist of troilite and magnetite surrounded by a fine-grained mixture of silicate, oxide, sulfide and minor FeNi metal.

Troilite is relatively large up to 25 μm long, and contains up to 2% Ni; this may be a fine mixture of troilite and pentlandite. Magnetite grains range up to 20 μm. The large magnetites are typically irregularly shaped grains. In some matrix lumps, magnetite occurs as spheroids and framboids similar to those in CI chondrites (Kerridge et al., 1979) and CR matrix (Fredriksson et al., 1981). Platelets of magnetite are also present (Grossman et al., 1988).

Magnetite and troilite are the only phases optically identifiable in the matrix lumps. All others are submicrometer-sized and only partially resolvable with a 1-2 μm electron beam. These fine grained phases almost certainly include Ca-phosphate, FeS, pentlandite and low- and high-Ni metal. A Ti-rich phases is probably osbornite. Fe-rich olivine, low-Ca pyroxene and a feldspathic component may be present if the matrix is anhydrous.

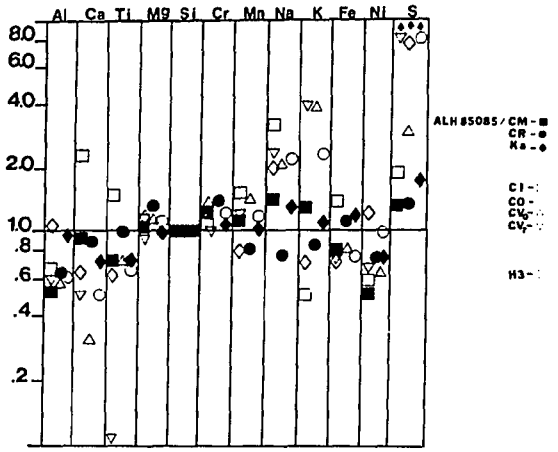

Fig. 3.2.3. Si-normalized major elemental abundances in ALH85085 matrix lumps, normalized to abundances in average matrices of other carbonaceous and ordinary chondrite groups and Kakangari (Ka). CV_O and CV_r are the oxidized and reduced CV groups, respectively. Data for C chondrites from (McSween and Richardson, 1977) and H3 datum from (Huss et al., 1981). ALH85085 matrix is most similar to CR and CM matrices.

Broad beam determination of bulk matrix lumps always results in low totals, which may be due to the porous nature of the material, or hydrous phases may be present. If the latter is true, then serpentine and phyllosilicates are present in the matrix lumps.

Nine matrix lumps analyzed by the broad-beam electron probe technique have essentially identical compositions, and the average bulk matrix lump is presented in Table 3.2.2. As in most chondrites, the opaque matrix is much more FeO-rich than the chondrules. In addition, the matrix lumps are enriched in volatile elements (Na_2O, K_2O and S) relative to the chondrules and most other components in ALH85085 (Table 3.2.2).

As a means of comparison, Si-normalized elemental abundances in matrix lumps have been normalized to those of average matrices from other chondrite groups (Fig. 3.2.3). Normalized to average CM and CR chondrites, the data generally plot close to 1.0, indicating similarity in the bulk compositions of these matrices. In most cases, matrices in other chondrite groups are more depleted in volatiles (Na, K, S) and richer in refractory elements (Ca, Ti, and less so for Al).

3.2.5 Metal and sulfide

FeNi metal is evenly distributed throughout the meteorite (Fig. 3.2.1a), is generally irregular in shape, and sometimes wraps around chondrules and fragments (Grossman et

al., 1988). Metal grains range in size up to 300μm and appear to be in parallel alignment (Fig. 3.2.1a). Compositions vary from grain to grain, and even individual grains exhibit heterogeneity. In general, Ni ranges from 4.5 to 10.9 wt.%, Co from 0.1 to 0.4%, Cr and P from below detection (<0.01%) to 0.5% (Table 3.2.3). Several grains were found to have Ni contents up to 23%, and are probably kamacite finely mixed with taenite. Scott (1988) noted that grains with Ni concentrations greater than 8% are composed of plessite (kamacite-taenite intergrowths) and that the larger of these are concentrically zoned with kamacite rims and plessite cores.

Three grains of kamacite were found to contain Si in amounts of 3.3, 4.8 and 7.5% Si, respectively, (Table 3.2.3). The grain with 3.3% Si contains P as high as 1.0%. The Si contents of 4.8% and 7.5% are higher than those found in any enstatite chondrite. Aside from these rare grains, Si is essentially absent from FeNi metal.

Ni vs. Co for FeNi in ALH85085 is shown in Fig. 3.2.4, and compared with metal in ordinary chondrites (Affiatalab and Wasson, 1980), the Bencubbin meteorite, and CR chondrites. FeNi in ALH85085 differs from that in unequilibrated and equilibrated ordinary chondrites, and also differs from metal in other chondrite groups not shown in Fig. 3.2.4. However, Ni vs. Co in CR chondrite metal has a similar trend, as does the metal in Bencubbin. Small differences in the slopes of their trends may be due to analytical error in Co determination or to minor variations in their histories.

Sulfides are rare and unevenly distributed; ALH85085,5 contains more sulfide than ALH85085,9. Grain sizes are generally small, ranging up to 25μm. Troilite is the main sulfide, and in some cases it contains up to 2% Ni and 1% Cr. In terms of size and composition it is identical to the sulfide in matrix lumps. Less commonly, pentlandite

Table 3.2.3

Compositional averages and ranges of the Si-free and Si-bearing FeNi-metal in the ALH85085 chondrite compared with CR and E chondrites and Bencubbin

	Si-free metal			Si-bearing metal						
	ALH85085	CR	Bencubbin	ALH85085			EH3 (Parsa)	EH4, 5	EL6	Bencubbin
Fe	88.0–95.9	84.9–94.4		88.2	88.1	83.4	93.6–97.7 (95.8)	88.1–94.3 (89.8)	88.4–94.3 (91.5)	
Ni	4.5–25.0 [a]	5.2–14.0	5.3–7.5	7.7	6.0	7.3	2.0–4.0 (2.4)	2.3–8.5 (6.4)	5.2–8.4 (6.4)	5.8
Co	0.11–0.40	0.14–0.54	0.25–0.35	0.31	0.27	0.26	0.31–0.43 (0.40)	0.40–0.79 (0.54)	0.32–0.52 (0.48)	0.35
Cr	b.d.–0.50	0.07–0.89	0.07–0.33	b.d.	b.d.	0.96	b.d.	n.a.	n.a.	0.10
P	b.d.–0.48	0.06–0.63	0.16–0.35	0.92	0.22	0.07	b.d.	0.03–0.70 (0.23)	0.03–0.21 (0.12)	0.50
Si	b.d.	b.d.	b.d.	3.3	4.8	7.5	1.5–3.0 (2.3)	2.3–3.8 (3.8)	1.0–2.1 (1.3)	2.3
Number of grains	38	167	37	1	1	1	8	200	310	3
Reference	this study	this study	[19]		this study		[6]	[2]	[2]	[19]

[a] Most Ni values are less than 11%.

b.d.: below detection; n.a.: not analyzed.

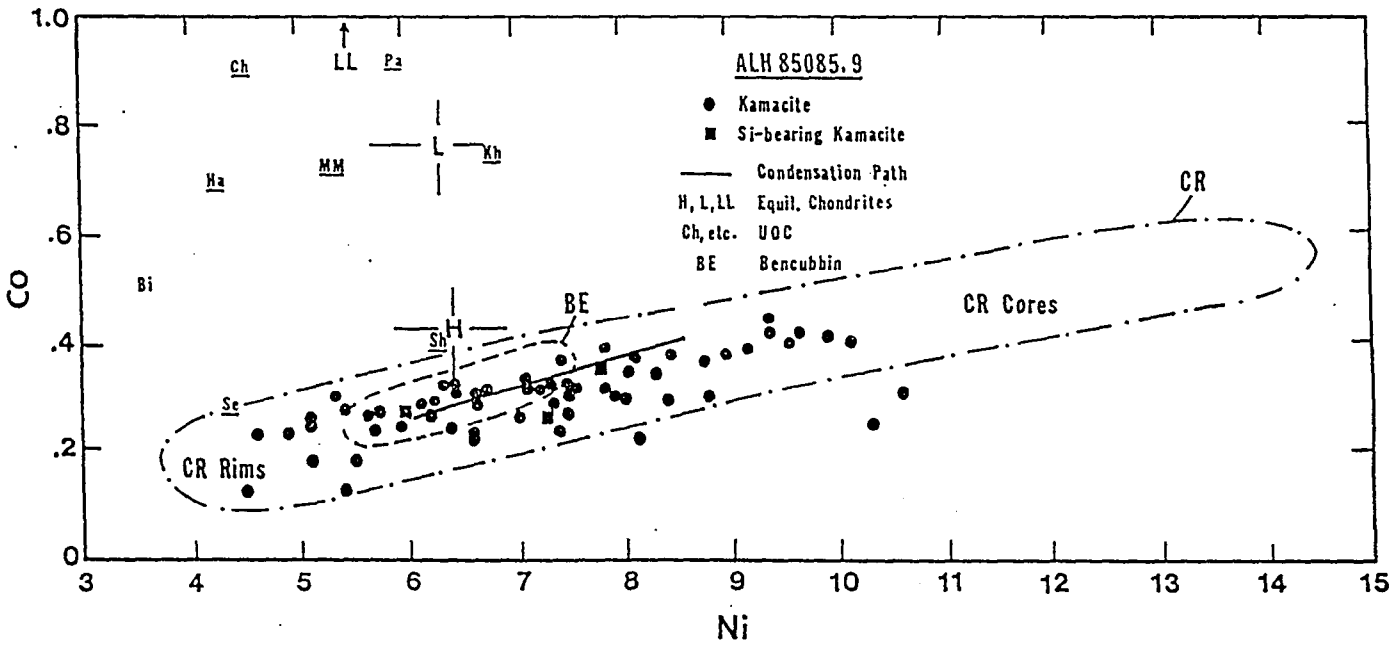

Fig. 3.2.4. Plot of Ni vs. Co for FeNi metal in the ALH85085 chondrite. Also shown are data for CR chondritic metal from Fig. 4(large dashed loop), Bencubbin (BE, small dashed loop) (Newsom and Drake, 1979), equilibrated O chondrites (H, L, LL) and uequilibrated O chondrites (Ch=Chainpur, MM=Mezo Madaras, Pa=Parnallee, Kh=Khohar, Ha=Hallingeberg, Bi=Bishunpur, Se=Semarkona, Sh=Sharps) from (Afiattalab and Wasson, 1980). The solid line is the calculated condensation path from (Grossman and Olsen, 1974). The ALH85085 trend is similar only to that of the CR chondrites and Bencubbin.

occurs with troilite. Scott (1988) reported troilite with 6% Cr, and suggested that this contains exsolved submicron daubreelite.

3.2.6 Bulk composition

An approximate bulk composition of the whole-rock chondrite is presented in Table 3.2.2. Elemental ratios Mg/Si, Al/Si and Ca/Si are presented in Fig. 3.2.5. Al/Si increases from enstatite (E) to ordinary (O) to carbonaceous (C) chondrites, with EL chondrites having the lowest values and CV_{re} (reduced CV) chondrites having the highest. The Al/Si ratio in ALH85085 plots between CR and CM-CO chondrites. Ca/Si correlates well with Al/Si in chondritic groups (as shown in Fig. 3.2.5), and Ca/Si in ALH85085 plots close to the CR chondrite for this ratio. Mg/Si ratios also increase from E to O to C chondrites. Their ratio in ALH85085 is somewhat greater than in any other chondrite group, but fairly close to the CR chondrite group also. The X/Si ratios, especially Mg/Si, may be slightly overestimated due to inaccuracy in using alpha factors for correcting broad beam microprobe analysis of heterogeneous samples.

Na/Si and S/Si ratios in ALH85085 are much lower than in most other chondrite groups and Ni/Si and Fe/Si are much higher (Table 3.2.4). This reflects the low volatile contents and great abundance of FeNi metal in this meteorite. Cr/Si levels in ALH85085 are closest to those in C chondrites.

Table 3.2.4

Elemental abundances (normalized to Si) in the ALH85085 chondrite compared with the averages of other chondritic groups

	ALH 85085	H	L	LL	EH	EL	CI	CM2	CO3	CV3 (reduced)	CV3 (oxidized)	CR	Kakan-gari
Na	0.012	0.037	0.035	0.035	0.041	0.033	0.098	0.031	0.025	0.012	0.020	0.026	0.045
Mg	1.023	0.824	0.812	0.831	0.647	0.719	0.890	0.904	0.911	0.937	0.938	0.906	0.861
Al	0.083	0.071	0.066	0.062	0.055	0.099	0.090	0.090	0.091	0.115	0.106	0.079	0.070
S	0.051	0.121	0.133	0.130	0.347	0.172	0.529	0.263	0.136	0.103	0.157	0.083	0.328
K	0.004	0.005	0.006	0.009	0.006	0.006	0.010	0.004	0.004	0.002	0.002	0.002	0.003
Ca	0.077	0.074	0.073	0.076	0.061	0.045	0.101	0.102	0.100	0.117	0.121	0.080	0.069
Ti	0.005	0.003	0.005	0.006	0.004	0.001	0.005	0.004	0.005	0.006	0.006	0.007	0.004
Cr	0.026	0.017	0.018	0.012	0.014	0.011	0.019	0.022	0.022	0.023	0.022	0.024	0.008
Mn	0.013	0.011	0.011	0.013	0.011	0.004	0.017	0.012	0.010	0.009	0.009	0.012	0.014
Fe	2.190	1.626	1.161	1.120	1.964	1.296	1.716	1.644	1.588	1.454	1.512	1.577	1.331
Ni	0.164	0.096	0.060	0.052	0.106	0.080	0.091	0.097	0.090	0.083	0.086	0.085	0.075
Refer-ence	this study	[7]	[7]	[7]	[2]	[2]	[17]	[17]	[17]	[17]	[17]	this study	[17]

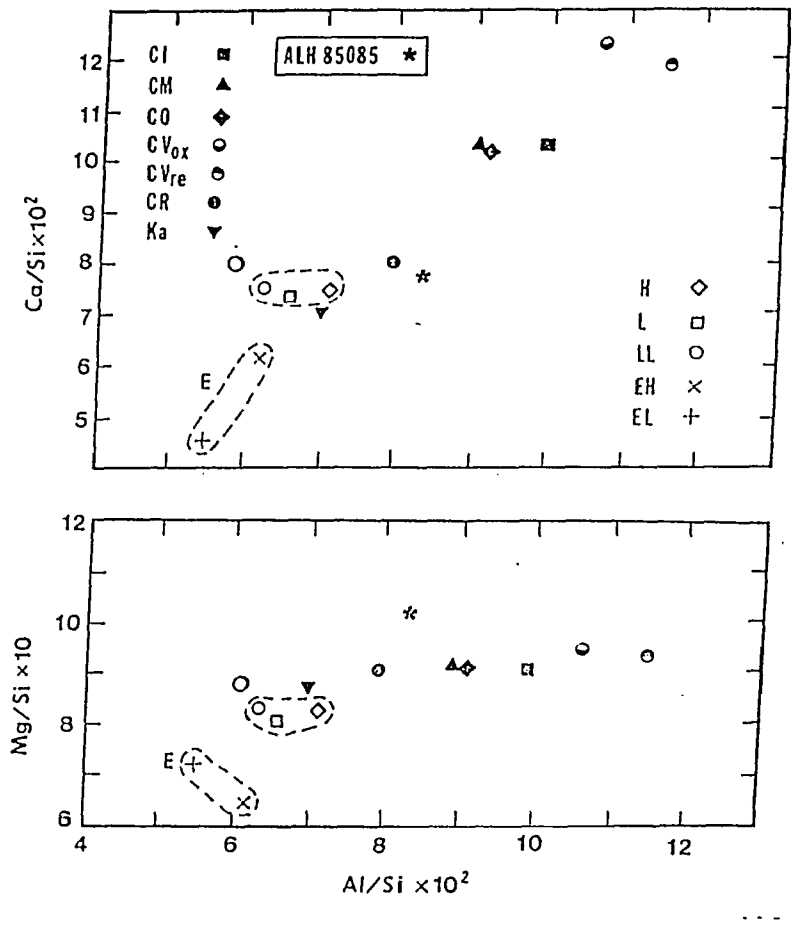

Figure 3.2.5. Plots of Al/Si vs. Mg/Si and Ca/Si for the ALH85085 chondrite, compared with C, O and E chondrite groups (Keil, 1968; Mason, 1963; McSween and Richardson; 1977) and Kakangari (Ka). CV_{ox} are oxidized, and CV_{re} are reduced, CV groups. ALH85085 does not plot with any chondrite group, but is closest to CR chondrites.

3.3 Bencubbin

In this paper the term "host silicate" is used to describe the major silicate portion of Bencubbin; this is the term used previously by Kallemeyn et al. (1978). These are the same silicates referred to as "achondritic" (Lovering, 1962; McCall, 1968), and which Newsom and Drake (1979) called "silicate clast." It will be demonstrated that these clasts are BO chondrule-like in texture, but use the term host silicate to avoid confusion with the other Bencubbin chondritic components. The use of this term is justifiable in that these clasts make up over 99% of the silicate portion of the breccia. Also, for reasons outlined below, we use the term "dark xenolith" for the clast originally described as a carbonaceous chondrite by Lovering (1962).

3.3.1 Textures

The host silicates are angular to subrounded clasts which vary in size and are up to 1 cm or larger across. Some clasts also occur in groups of millimeter- to submillimeter-sized angular fragments intermixed with metal. Many have BO textures (Figs. 3.3.1) consisting of a single grouplet or multiple grouplets of parallel, elongate, optically continuous olivine. Each grouplet can be considered a single crystal of linked parallel growth, or chain olivine, using the terminology for olivine morphology of Donaldson (1976). In some cases grouplets of bars are oriented differently and may cross each other (intergrown crystals).

Olivine bars are remarkably long and in some cases extend the entire length of a cm-sized host silicate fragment, giving many of them a greater length/breadth ratio than that observed in the mm-sized ordinary and carbonaceous chondrite BO chondrules. These are the largest BO-textured silicates of which we are aware. In between the olivine bars is a brownish, feldspathic, glassy material (Fig. 3.3.1a) which contains fine needles of low-Ca pyroxene. The pyroxene crystals are submicron-sized and beyond the quantitative

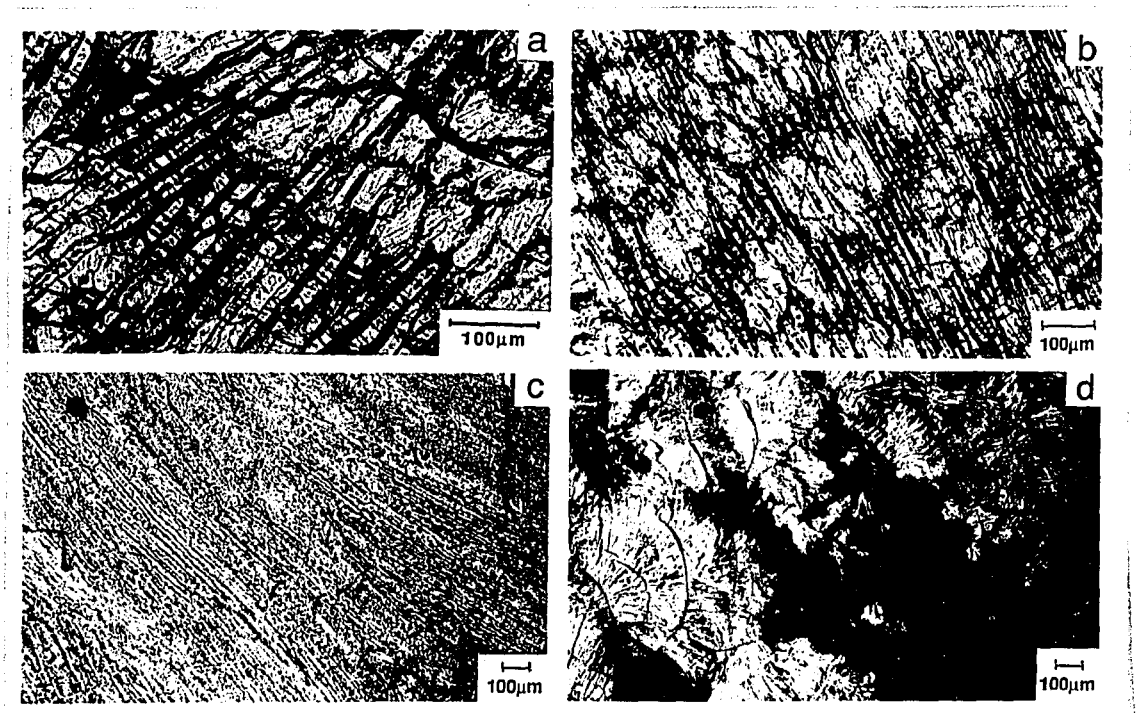

Fig. 3.3.1. Plane light photomicrographs of barred olivine (BO)-textured host silicate clasts in Bencubbin. Textures range from coarse barred, average bar width=20µm (1a,b) to fine barred, average bar width=3µm, to feathery microcrystalline (1d). In between olivine bars is a glassy feldspathic material, as shown in 1a. Coarse BO-textured clasts also exhibit large (up to 400µm) pyroxene crystals (1a,b). These large pyroxene grains are abundant (47 vol.%) and contain inclusions of disjointed olivine bars (1b). The pyroxene grows at the expense of olivine. Note that the SE corner of the feathery microcrystalline-textured clast contains an area of microfine barred olivine. All of the textures shown have chondrule equivalents.

analytical capabilities of the electron microprobe, but an EDS spectrum indicates they are highly magnesian, similar to the larger pyroxene.

Low-Ca pyroxene (both monoclinic and orthorhombic varieties) also occurs as large (mm-sized) crystals which fill the interstices of the bars (Fig. 3.3.1a, b). Olivine bars appear pinched at pyroxene contacts (Fig. 3.3.1a,b) and some pyroxene contains lensoidal inclusions of disjointed olivine bars (Fig. 3.3.1b). These observations are similar to those described in BO chondrules (Nagahara, 1983; Weisberg, 1986; Weisberg, 1987) and suggest that pyroxene grew by reaction of earlier crystallized olivine with the melt.

Although the host silicate clasts are characterized as being BO-textured, the textures vary considerably as do those in BO chondrules (Weisberg, 1987). Host silicate clast textures represent a continuum from coarsely barred (average bar width = 20μm; Fig. 3.3.1a), to finely barred (average bar width=3μm; Fig. 3.3.1c), to feathery microcrystalline (Fig. 3.3.1d). The coarse and fine BO-textured clasts have analogues in ordinary chondrites (Weisberg, 1987). Chondrule equivalents with feathery microcrystalline textures are generally called cryptocrystalline. Like BO chondrules, the textures of the host silicate clasts also resemble the range of spinifex-textured olivine that occurs in the upper layers of komatiite lava flows from the Archean Greenstone Belt (Arndt et al., 1977).

3.3.2 Modes and Mineral Compositions

Modally, the BO-textured host silicates fall within the range of compositions of BO chondrules in ordinary and carbonaceous chondrites, but at the pyroxene-rich end of the spectrum (Table 3.3.1). Both low-Ca and high-Ca pyroxene are present, but low-Ca pyroxene dominates. Mineral compositions are uniform both within and between individual host silicate fragments, and representative analyses are presented in Table 3.3.2. Olivine ($Fo_{96.5}$) and low-Ca pyroxene ($Wo_{0.8}En_{96.9}$) are highly magnesian. Olivine

Table 3.3.1. Modes (vol.%) of barred olivine-textured Bencubbin host silicates compared with barred olivine-textured chondrules.

	Bencubbin Host Silicates	Ordinary Chondrites*	Carbonaceous Chondrites**
Olivine	40	10-91	33-78
Pyroxene	47	0-58	0-48
Feldspar	13	6-47	6-40
No. Clasts/ Chondrules	2	120	32

* Weisberg (1987), ** Weisberg (1986)
Feldspar - includes feldspathic glass

Table 3.3.2. Representative analyses (wt.%) of silicate minerals in barred olivine-textured host silicates in Bencubbin.

	Olivine		Low-Ca Pyroxene	High-Ca Pyroxene	Feldspathic Glass
SiO_2	41.9		58.1	48.7	54.6
TiO_2	0.02		0.12	1.18	0.44
Al_2O_3	0.02		0.67	9.3	24.1
Cr_2O_3	0.55		0.73	1.97	0.21
FeO	3.5		1.66	1.20	1.33
MnO	0.18		0.11	0.12	0.11
MgO	54.4		38.6	18.2	4.7
CaO	0.21		0.42	20.0	14.6
Na_2O	nd		nd	nd	0.14
K_2O	na		na	na	nd
Fo	96.5	En	96.9	54.7	
Fa	3.5	Fs	2.3	2.0	
		Wo	0.8	43.3	

nd = not detected, na = not analyzed

Table 3.3.3. Comparison of silicate and FeNi metal compositions in Bencubbin host silicates, ordinary chondrite clast and dark xenolith and, Renazzo Type I chondrules and ALH85085.

	Bencubbin Host		Renazzo Type I Chondrules	ALH 85085		Bencubbin OC Clast	dark xenolith
Olivine							
Fo	97		97-99.6	90-99.5		69-99.2	62-76
Low-Ca Pyroxene							
En	97		97-98	95-99		73-97	72.2
FeNi		Si-bearing			Si-bearing		
Ni	5.3-7.5	5.8	5.2-14.0	4.5-25.0	6.0-7.7	2.1-26.2	5.9-33.2
Co	0.25-0.35	0.35	0.14-0.54	0.11-0.40	0.26-0.31	0.20-1.1	0.28-1.6
Cr	0.07-0.33	0.10	0.07-0.89	bd-0.50	bd-0.96	bd-1.0	bd-0.34
P	0.16-0.35	0.50	0.06-0.63	bd-0.48	0.07-0.92	bd-0.51	bd-0.46
Si	bd	2.3	bd	bd	3.3-7.5	bd	bd

OC-Ordinary Chondrite, CC-Carbonaceous Chondrite

bd - below detection

contains high Cr_2O_3 (0.55%) and CaO (0.21%), and interstitial feldspathic glass is highly calcic (14.6% CaO) and low in alkalis (0.14% Na_2O; K_2O below detection).

The Mg-rich compositions of the olivine and pyroxene categorizes the host silicates as analogous to Type I chondrules. For comparison, Table 3.3.3 shows the endmember compositions of the mafic silicates in the cores of chondrules in the CR chondrites (mainly Type I) and the major components of the ALH85085 chondrite (Grossman et al., 1988; Scott, 1988; Weisberg et al., 1988a). All of these have similar highly magnesian compositions. The major feldspathic component in the CR and ALH85085 chondrites is highly calcic and low in alkalis (Grossman et al., 1988; Scott, ,1988; Weisberg et al., 1988a), which is also similar to the Bencubbin host silicates.

3.3.3 Bulk Compositions

The average bulk composition of the host silicates in Bencubbin is shown in Table 3.3.4, and is found to be comparable to that of Simpson and Murray (1932), and to Bencubbin sample "B" of Kallemeyn et al. (1978); it is also comparable to that of similar material in the Weatherford meteorite (Mason and Nelen, 1968). Minor differences in FeO/MgO may, in part, reflect differences in analytical methods and the possible inefficiency of magnetic separation of metal from silicate. The lower FeO/MgO of our data, that of Mason and Nelen (1968), and sample B of Kallemeyn et al. (1978) is more compatible with the mineral compositions of the mafic silicates (Table 3.3.2) than is that of Simpson and Murray (1932).

The bulk composition of the Bencubbin host silicates is an average of nine clasts of varying textures (from coarsely barred to microcrystalline). From the standard deviations (Table 3.3.4), it can be seen that the nine clasts are essentially identical in composition, regardless of texture. These clasts are strikingly similar to the average of Type I CR chondrules and to average ALH85085 chondrules.

Table 3.3.4. Average bulk compositions (wt.%) of Bencubbin and Weatherford host silicate clasts and chondrules in Renazzo and ALH85085.

	1 Bencubbin Host Silicate	(S.D.)	2 Bencubbin Host Silicate	3 Weatherford Host Silicate	4 Renazzo Chondrules	5 ALH85085 Chondrules
SiO_2	50.7	(0.60)	48.1	50.3	48.5	53.5
TiO_2	0.18	(0.01)	0.19	0.20	0.13	0.15
Al_2O_3	4.8	(0.37)	4.2	3.9	4.5	3.4
Cr_2O_3	0.62	(0.10)	0.38	0.68	0.72	0.64
FeO	3.2	(0.38)	8.2	4.9	4.1	1.1
MnO	0.28	(0.04)	0.60	0.29	0.42	0.23
MgO	36.8	(0.61)	35.5	36.1	39.7	38.5
CaO	3.4	(0.23)	2.7	3.0	1.96	2.5
Na_2O	0.09	(0.02)	0.10	0.62	0.05	0.03
K2O	0.01	(0.0)	nd	0.07	0.01	0.05

1. Average and standard deviations (S.D.) of broad beam analyses of 9 host silicate clasts.
2. From Simpson and Murray (1932).
3. From Mason and Nelen (1968).
4. Average of 15 type I chondrules in Renazzo.
5. From Weisberg et al., 1988a.

nd - not detected

3.3.4 FeNi Metal

Bencubbin metal occurs in two different textural settings (Newsom and Drake, 1979). Most grains occur as large clasts up to 6 mm in diameter, and other metal occurs interstitially as submicron- to micron-sized "droplets" intermixed with silicate material. Ramdohr (1973) refered to the latter as a "spontaneous fusion" (impact melt) texture and suggested that it is the binding agent of the Bencubbin breccia.

Bencubbin host metal is compositionally very similar to that found in CR chondrules, and to metal in ALH85085 (Weisberg et al., 1988a; Table 3.3.3). However, Ni contents above 8% are not found in the Bencubbin host metal, whereas metal in the CR chondrules and in ALH85085 has as much as 25% Ni (Weisberg et al., 1988a; Table 3.3.3). A few Si-bearing metal grains (~2% Si) were found in Bencubbin (Newsom and Drake, 1979) and some also occur in ALH85085 (up to 12.5% Si) (Weisberg et al., 1988a and Kimura and El Goresy, 1989; Table 3.3.3). Low levels of Si (~0.07%) have also been reported in the Renazzo CR chondrite metal (Wood, 1967), but detectable Si in Renazzo metal was not found in this study. Surprisingly, compositions of the metal in the Bencubbin ordinary chondrite and dark xenolith clasts are also essentially the same as those of metal in the Bencubbin host, the CR chondrites and the ALH85085 chondrite (Table 3.3.3; Fig. 3.3.2). Thus, it appears that metal in the Bencubbin chondritic clasts is directly related to the host FeNi metal.

Plots of Ni and Co in the host metal are positively correlated and exhibit a trend-line with a slope that is similar to the calculated condensation path of the solar abundances (Newsom and Drake, 1979). This Ni vs. Co trend is also found in ALH85085 and CR chondrite metal (Weisberg et al., 1988a), and the FeNi metal in the Bencubbin ordinary chondrite clast and dark xenolith (Fig. 3.3.2). This primitive trend is distinctly different from that found in ordinary chondrites, including the most unequlibrated chondrites

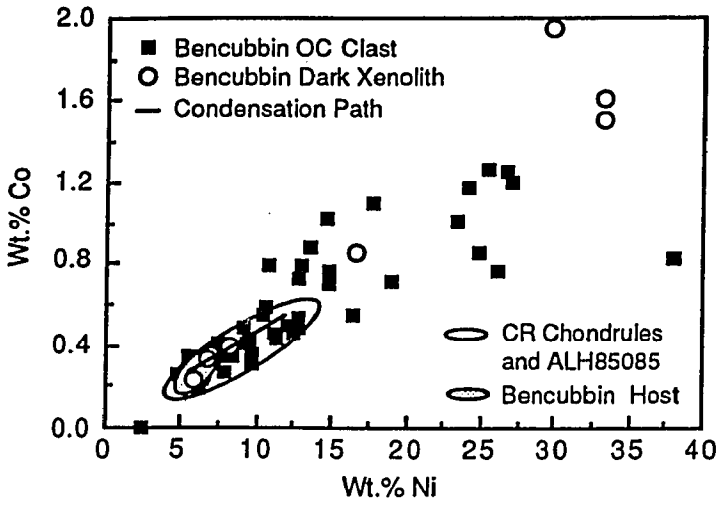

Fig. 3.3.2. Plot of Ni vs. Co for FeNi metal in Bencubbin host silicates, the ordinary chondrite (OC) clast and dark xenolith, CR chondrites, and ALH85085. The Ni vs. Co trends in these meteorites are similar and overlap with the calculated condensation path of solar abundances of Grossman and Olsen (1974) (shown by the solid line).

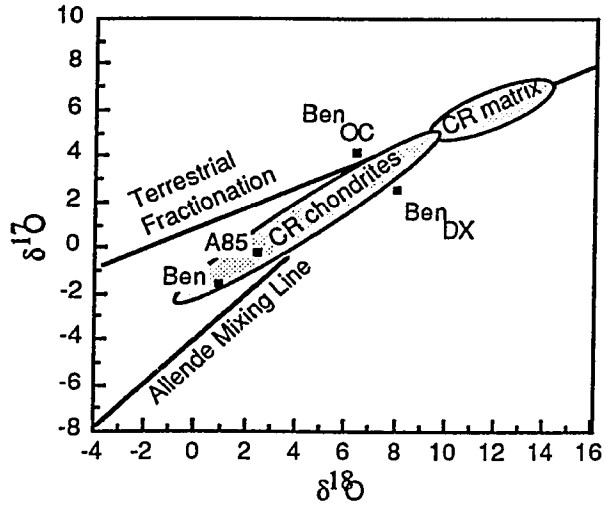

Figure 3.3.3. Oxygen three-isotope diagram in which data for the Bencubbin host silicates (Ben), dark xenolith (Ben_{DX}), and ordinary chondritic clast (Ben_{OC}) are plotted (Clayton and Mayeda, 1978), along with ALH85085 (A85) and the CR chondrite loop (Clayton and Mayeda, 1977; Clayton and Mayeda, 1989; Weisberg et al., 1989). The loop envelops the CR chondrites and chondrules. Bencubbin host silicate clasts plot within the CR chondrite loop at the ^{16}O-rich end, near anhydrous high density separates from Renazzo (Clayton and Mayeda, 1977). The terrestrial mass fractionation line (Earth-Moon) and the Allende (CV3) mixing line are also shown.

(Afiattalab and Wasson, 1980). Metal in carbonaceous chondrites, other then that in CR chondrites, is also compositionally different (McSween, 1977).

Ni and P in the host metal are negatively correlated and also follow a calculated condensation path (Newsom and Drake, 1979). Metal in the CR and ALH85085 chondrites exhibit a similar trend, with some scatter in the data. The Bencubbin ordinary chondrite clast and dark xenolith do not show a similar P trend. Metal compositions in the Bencubbin host, ordinary chondrite clast and dark xenolith do not show clear Cr trends, but this may be due to partitioning of this element into sulfide (Newsom and Drake, 1979).

3.3.5 Ordinary Chondrite and Dark Xenolith Clasts

Lovering (1962) originally described an ordinary chondrite and a "carbonaceous chondrite" clast in the Bencubbin meteorite and oxygen isotopic data appear to concur with their classification into these two groups (Clayton and Mayeda, 1978; Fig. 3.3.3). However, these clasts have some unusual aspects. The ordinary chondrite clast has metal compositions that differ from those of other ordinary chondrites, as noted above. The carbonaceous chondrite clast is a dark xenolith which differs petrologically from that of any carbonaceous chondrite, and also contains metal with the same composition as the host metal clasts.

The ordinary chondrite clast consists of densely packed, well defined chondrules of all textural types, many of which contain feldspathic glass and are surrounded by opaque matrix (Fig. 3.3.4). Olivine compositions range from Fo_{69-99} and low-Ca pyroxene is $Wo_{0.5-1}$, En_{73-97} (Table 3); Fo_{84} is the most common olivine composition. Some olivine has normal zoning. Mineral compositions vary both within and between chondrules and fragments. This clast was described as being type 4±1 by Kallemeyn et al. (1978) and as type 3 by Hutchison (1986). The occurrence of black matrix, abundant feldspathic glass and the large range of olivine compositions indicate a type 3 classification, probably less

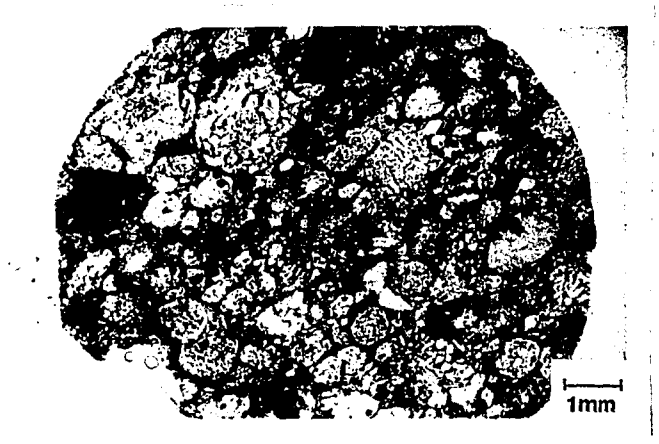

Fig. 3.3.4. Plane light photomicrograph of the ordinary chondrite clast in Bencubbin. Note the large abundance of densely packed chondrules of all textural types, typical of ordinary chondrites.

than 3.5. Based on whole clast Mg/Si, Ca/Si, Al/Si and Zn/Si ratios, and on siderophile element abundances, Kallemeyn et al. (1978) classified the clast as LL ordinary chondrite. The oxygen isotopic composition of the clast (Clayton and Mayeda, 1978) indicates that it is close to that of the Semarkona chondrite (LL3.0) (Grossman et al., 1987). From petrologic considerations Hutchison (1986) concluded that it may be related to silicates in IIE irons or Suwahib Buwah rather than to ordinary chondrites. The data do not support these classifications. The mean olivine composition is too high for classification as an LL chondrite. Since it is a type 3 ordinary chondrite it is inherently difficult to classify as H, L or LL, and this is a problem for many type 3 chondrites. The clast is considered to be a type 3 ordinary chondrite.

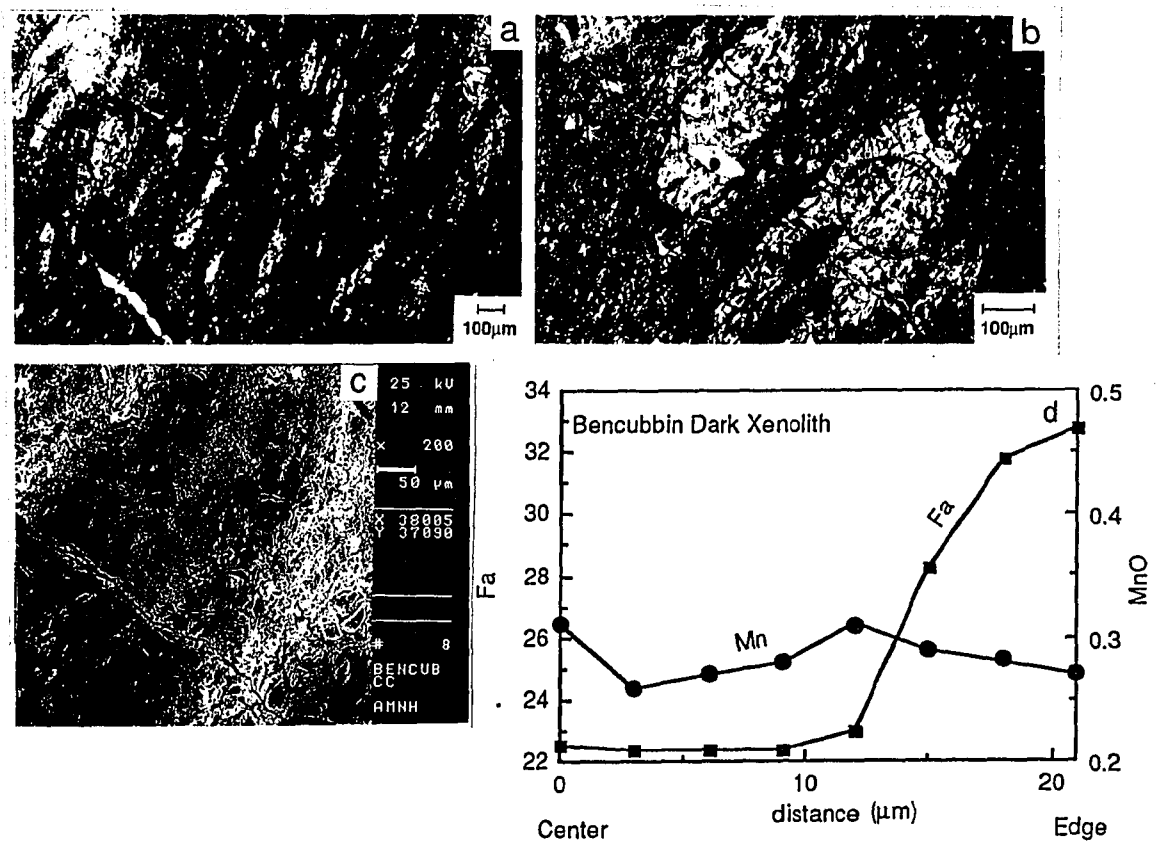

Fig. 3.3.5. Photomicrograph of the dark xenolith in Bencubbin (5a). This clast consists of olivine-rich elongate lenses which are in parallel alignment. The enlargement (5b) shows one of these objects which consists of olivine crystals in a pyroxene-feldspar mesostasis. All of the objects in this clast are texturally similar. The backscattered electron image (5c) shows that the olivine is zoned. The dark centers of grains are up to Fo_{76} and the lighter edges are Fo_{62}. a zoning profile (5d) taken from the center to edge of a representative olivine grain in the dark xenolith. Note that FeO increases and MnO remains constant.

The dark xenolith contains highly elongated olivine-rich lenses which are lineated and surrounded by a darker finer-grained opaque matrix (Fig. 3.3.5a). These lenses have been described as highly deformed chondrules (Lovering, 1962; Hutchison, 1986; Barber, 1987), but there is no evidence to support this hypothesis. These objects experienced deformation or a compaction event responsible for their elongation and alignment. However, similar deformation is absent in other Bencubbin components indicating that the clast was deformed prior to incorporation into the breccia.

The chondrule-like lenses in this clast consist of olivine crystals in a glassy to cryptocrystalline pyroxene and feldspar mesostasis (Fig. 3.3.5b). A backscattered electron

Table 3.3.5. Bulk compositions (wt.%) of the Bencubbin dark xenolith and its components.

	1	2	3	4
SiO_2	40.7	41.4	41.3	38.2
TiO_2	0.13	0.16	0.17	0.16
Al_2O_3	2.35	2.59	2.98	3.4
Cr_2O_3	0.69	0.61	0.63	0.48
FeO	23.0	23.2	22.6	21.7
MnO	0.25	0.41	0.43	0.31
MgO	31.1	28.8	28.4	33.5
CaO	1.02	2.16	2.76	1.14
Na_2O	0.47	0.45	0.50	0.48
K_2O	0.07	0.06	0.07	0.13
P_2O_5	0.15	0.17	0.20	0.39
FeS	0.69	6.9	7.4	9.4
FeNi	0.14	2.2	2.5	1.83
Fe/(Fe+Mg)	0.49	0.51	0.51	0.46

1. Elongate objects in the "carbonaceous" chondrite clast (broad beam analyses).
2. Dark matrix-like areas in the clast (broad beam analyses).
3. Whole clast (broad beam analyses).
4. Whole clast (Easton and Lovering, 1963).

These lenses or augen are unusual in that each lens is texturally identical to all the others, whereas chondrules would be expected to differ. Broad beam electron microprobe analyses of three of these lenses show that they are essentially identical in composition. In addition, the lenses are compositionally similar to the dark matrix surrounding them, but have a much lower metal and sulfide component (Table 3.3.5). The dark matrix is similar in composition to the whole clast (Table 3.3.5) because dark matrix is the dominant component (~80%). Therefore, the dark xenolith consists essentially of only one component with varying amounts of metal and sulfide and may not be a carbonaceous chondrite clast as previously thought, but may represent a single chondrite component such as a matrix lump or dark inclusion. Further work and better sampling is needed on both chondrite clasts in order to better characterize them and determine their relationship to the host silicate clasts and metal.

3.4 Carlisle Lakes-Type Chondrites

3.4.1 General Petrography

A general petrographic description of the Carlisle Lakes, ALH85151, and Y75302 chondrites (Carlisle Lakes-type chondrites) was given by Rubin and Kallemeyn (1989). These meteorites may be classified as type 3 chondrites. They contain well-defined chondrules of various textural types, and lithic and mineral fragments surrounded by a finer-grained, translucent matrix. The translucent matrix is similar to that in the type $\geq$3.5 chondrites. Although most olivine is homogeneous at Fa_{38}, there is some heterogeneity. These characteristics are consistent with the classification of ALH85151 and Carlisle Lakes as type 3.6 and 3.7 chondrites, respectively, as indicated by thermoluminesence data (Sears et al., 1990).

The diameters of chondrules in the Carlisle Lakes-type chondrites range from 100 to 3000μm and average about 450μm, making them similar in size to ordinary chondrite chondrules (Rubin and Kallemeyn, 1989). Chondrules in CM, CO and EH chondrites are much smaller and those in CV chondrites are larger (Rubin, 1989; Rubin and Wasson, 1986; Rubin and Grossman, 1987; Grossman et al., 1988). The chondrule textural types in the Carlisle Lakes-type chondrites include porphyritic, granular, barred, and radial. Porphyritic types are the most abundant, and their relative abundances are approximately similar to those in the ordinary chondrites.

Olivine in most chondrules is homogeneous and, based on chemical composition, is in equilibrium with the matrix olivine and in many cases is associated with homogeneous diopside. Olivine in some chondrules and most of the low-Ca pyroxene is heterogeneous. The zoning in these phases is discussed in detail below.

The translucent matrix is texturally similar to that in type>3.5 ordinary chondrites, but its abundance (35 vol.%) exceeds that of the ordinary chondrites (10-15%) (Rubin and Kallemeyn, 1989). Mineral and lithic fragments are distributed throughout the matrix and most have olivine and pyroxene in equilibrium with the chondrules and matrix. However, rare grains are zoned, having zoning patterns similar to those found in some of the chondrules.

Two types of sulfide occur in Carlisle Lakes-type chondrites: pyrrhotite and pentlandite. Metallic FeNi is absent in Carlisle Lakes and awaruite (64 wt.% Ni) is the major metal phase in ALH85151, occurring in trace amounts. Awaruite grains are found in the matrix, but most is in one unusual, large (2.5mm) angular fragment. Rubin and Kallemeyn (1989) observed rare kamacite and martensite and an unusual Co-rich (37 wt.% Co) metal in the PTS of ALH85151 they studied.

Table 3.4.1. Modal abundances (vol.%) of H, L, and LL chondrites compared with the ALH85151 (A85), Carlisle Lakes (CL), and Y75302 (Y75) chondrites.

	H	L	LL	A85	CL	Y75
Olivine	40.2	50.2	60.5	72.2	71.2	77.7
Low-Ca Pyx	28.7	24.6	16.7	6.8	2.5	3.8
Ca-Pyx	5.1	4.8	4.7	6.6	5.6	3.2
Feld/Glass	12.5	11.6	11.4	7.2	13.6	9.4
Chromite	0.4	0.3	0.3	1.2	0.9	0.5
Phosphate	0.7	0.7	0.7	0.6	0.2	0.2
Troilite	4.0	3.7	3.7	x	x	x
Pyrrh/Pent	x	x	x	4.9	6.0	5.2
Kamacite	7.3	3.1	0.7	x	x	x
Taenite	1.1	1.0	1.3	x	x	x
Awaruite	x	x	x	trace	x	x
%Fa+	19	25	31	38	38	38
No. points				2000	1000	1528
Area (mm^2)				96.1	117.3	64

H, L, LL chondrite data from Van Schmus (1969)
+-average mol.% fayalite, x-not detected
Feld/Glass-feldspathic glass, Pyrrh/Pent-pyrrhotite and pentlandite

Table 3.4.2. Modal abundances (vol.%) of chondrules analyzed for oxygen isotopes.

Texture	A85-1 PO	A85-2 PO	A85-4 BO	CL-1 POP
Olivine	69.8	71.4	67.9	45.1
Low-Ca Pyx	x	x	0.7	41.4
Ca-Pyx	2.1	2.7	23.6	7.9
Feld/Glass	19.3	17.2	7.8	5.4
Chromite	0.5	2.1	x	0.2
Phosphate	x	x	x	x
Pyrrh/Pent	8.3	6.6	x	x
Awaruite	x	x	x	x
%Fa+	38	38	38	17/38
No. points	100	150	150	200
Area (mm^2)	0.12	0.85	0.32	5.18
Diameter (mm)	0.38	1.04	0.64	2.57

PO-porphyritic olivine, POP- porphyritic olivine/ pyroxene, BO-barred olivine
+-average mol.% fayalite, x-not detected
Feld/Glass-feldspathic glass
Pyrrh/Pent-pyrrhotite and pentlandite

3.4.2 Modal Abundances

Whole chondrite modal data for Carlisle Lakes-type chondrites are reported in Table 3.4.1. They differ somewhat from those presented by Rubin and Kallemeyn (1989) in having more olivine and less pyroxene. These differences may be the result of studying different thin sections, but more likely may be the result of differences in the methods used to determine the modal abundances. However, our modal data on ALH85151, Carlisle Lakes, and Y75302 were determined independently by two different authors of this study and there is good agreement. In either case, both studies show that olivine is by far the most abundant phase, pyroxene abundance is low, and FeNi metal is essentially absent, making up <0.1% in ALH85151.

Also shown in Table 3.4.1 are the approximate mineral abundances of equilibrated H, L, and LL chondrites (Van Schmus, 1969). From H to LL, the abundance of olivine increases, and that of low Ca-pyroxene and FeNi decrease. These data suggest that the Carlisle Lakes-type chondrites may be an extension of the H to LL chondrite trend, because they have more olivine, less pyroxene and essentially no FeNi metal.

Modal abundances of individual chondrules span a wide range from olivine- to pyroxene-rich varieties, as do those in other type 3 chondrites. Many, such as A85-4 (Table 3.4.2), consist of olivine, Ca-pyroxene and a feldspathic component, with little or no low-Ca pyroxene. This is quite unusual in comparison to ordinary chondrite chondrules in which the dominant pyroxene is nearly always low-Ca. As a result, the abundance of Ca-pyroxene equals or exceeds low-Ca pyroxene in the whole chondrite (Table 3.4.1). Although this is unusual for ordinary chondrites, note that the low-Ca pyroxene abundance substantially decreases in the sequence of H to LL chondrites, but the abundance of Ca-pyroxene changes only slightly (Table 3.4.1). Thus, the ratio of low-Ca pyroxene to Ca-pyroxene decreases from H to LL and the Carlisle Lakes-type chondrites are an extension of this trend.

3.4.3 Mineral Zoning

Most of the olivine in the Carlisle Lakes-type chondrites is equilibrated at or near Fa_{38} and is commonly associated with Ca-pyroxene (Wo_{45}, Fs_9), which is also equilibrated. Zoning in olivine and low-Ca pyroxene in chondrules and mineral and lithic fragments is rare, but the zoned minerals appear to be an important integral part of these meteorites because: (1) Cores of some of the zoned olivines are compositionally the same as the equilibrated matrix olivine (Fa_{38}). (2) Chondrules having zoned pyroxene contain olivine which is compositionally homogeneous and equilibrated with the matrix olivine. (3) The zoning occurs in all three Carlisle Lakes-type chondrites. (4) Rim compositions of zoned olivines are generally consistent at about Fa_{45} suggesting that all of these grains experienced a similar event. The occurrence of the zoned phases in these chondrites, which are mainly equilibrated, may be important in determining their equilibration and/or pre-lithification histories. Therefore, the chemical compositions of the zoned phases in the Carlisle Lakes-type chondrites, and profiles across their zoning trends are presented to better understand the petrogenesis of this meteorite grouplet.

The zoning patterns may be divided into three types - patchy olivine, oscillatory olivine, and pathcy zoned pyroxene. Examples of each type are shown in backscattered electron images (BSE) in Fig. 3.4.1, and their mineral compositions are shown in Figs. 3.4.2 and 3.4.3, and Tables 3.4.3-3.4.7.

Patchy Zoned Olivine: Olivine with this type of zoning occurs as fragments (Fig. 3.4.1a) and as crystals inside chondrules (Fig. 3.4.1c). The zoning is patchy in the sense that it is not concentric about a single core, as would be expected from igneous zoning or grain boundary diffusion with a surrounding medium, but is instead irregular or patchy and is related to fractures in some cases. This type of zoning appears to be the result of post-chondrule or fragment formation. One example is olivine fragment A85-44 (Fig. 3.4.1a), associated with high-Ca pyroxene and Na-rich feldspathic material. Profile A across the olivine fragment (Table 3.4.3, Fig. 3.4.2a) is taken from the center of the forsteritic portion

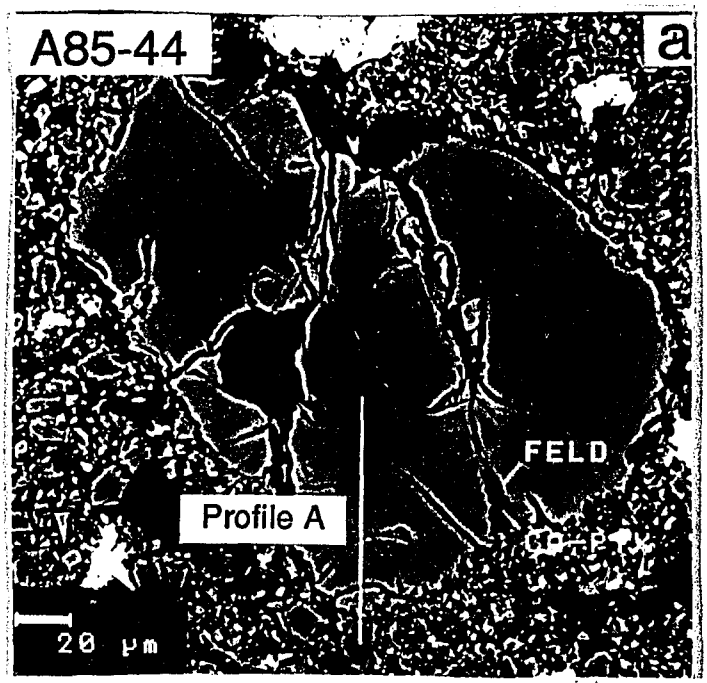

Fig. 1. Backscattered electron images of zoned chondrules and mineral fragments in the Carlisle Lakes-type chondrites: (a) A85-44 is an olivine crystal in ALH85151 which shows pathcy zoned olivine. The solid line shows profile A, taken from the forsteritic core to the fayalitic rim and into the matrix olivine. An enlargement of the fayalitic rim (b) shows a layer of pore space and Ca- and Cr-rich inclusions. (c) A85-13 is a chondrule from ALH85151 with a large central olivine with patchy zoning. The fayalitic rim in this olivine also contains the pore spaces and Ca- and Cr-rich inclusions. Note that zoning is absent in the upper portion of the olivine. (d) A85-14 is a chondrule from ALH85151 which has a large central olivine which exhibits oscillatory zoning. Some of the smaller olivine in this chondrule have similar zoning. In the large crystal the zoning follows the outline of fractures. Also note that the forsteritic layer (dark) fills fine fractures in the large crystal. (e) CL-10 is a chondrule in Carlisle Lakes which has pathcy zoned pyroxene. Olivine occurs as inclusions and as fracture fillings. (f) A85-20 is a chondrule from ALH85151 which has zoning in pyroxene parallel to twin lamellae. The olivine occurs in four textural settings: as large phenocrysts, inclusions in pyroxene, veins in pyroxene, and rims on pyroxene. (g) An enlargement of the chondrule A85-20 shows the lamellar-type zoning and olivine fracture-filling and rimming of the pyroxene.


b
2 µm

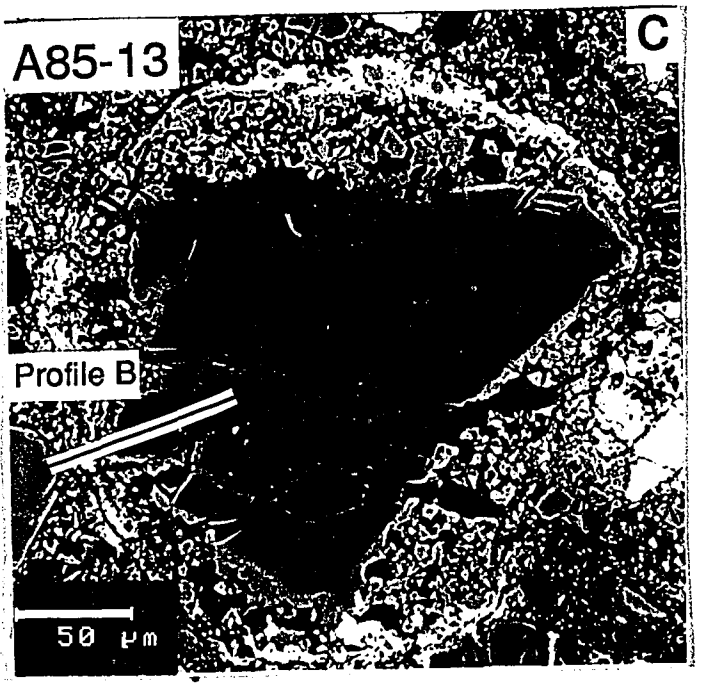
A85-13
C
Profile B
50 µm

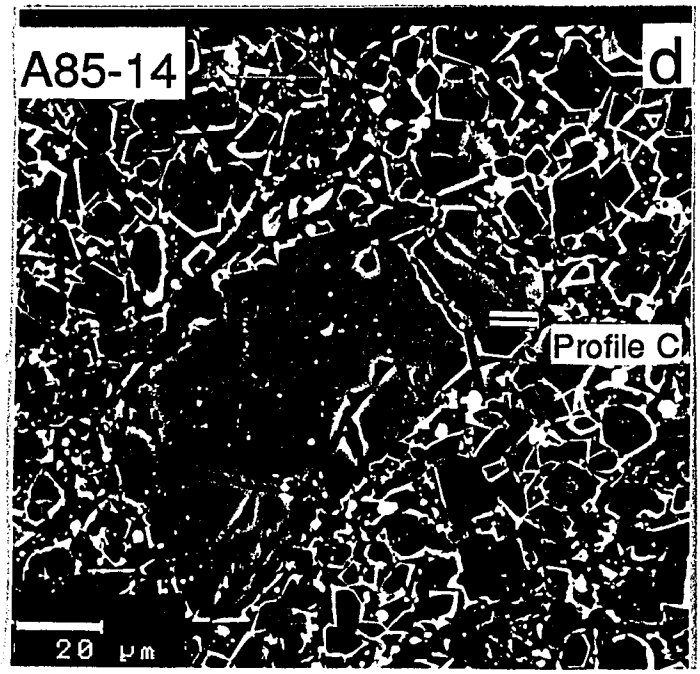
A85-14
d
Profile C
20 µm

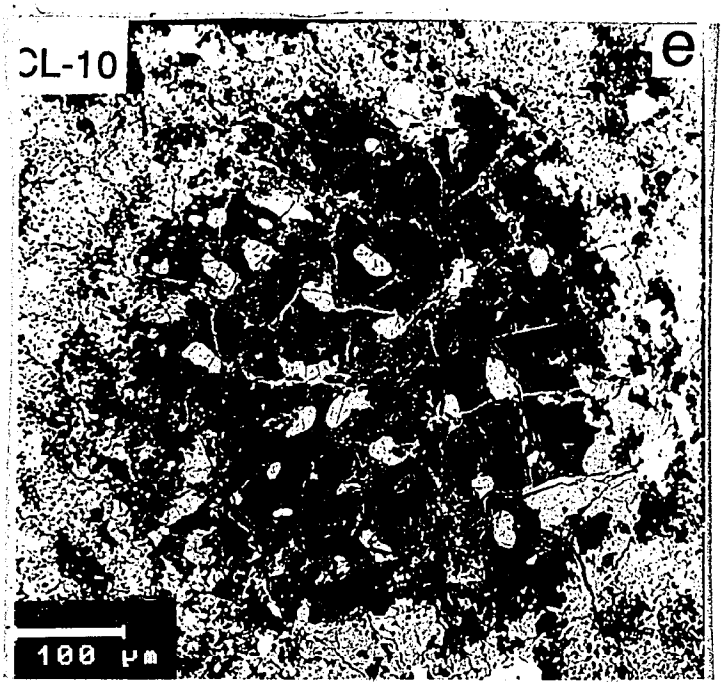
CL-10
e
100 µm

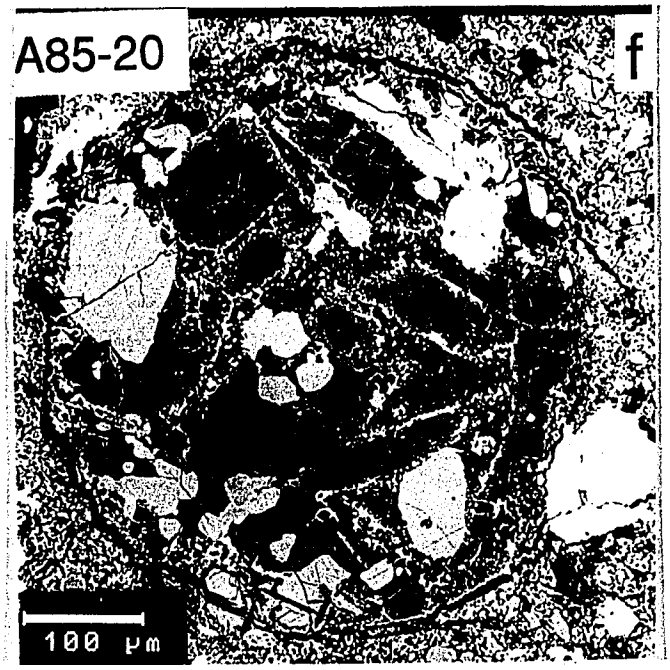
A85-20
f
100 µm

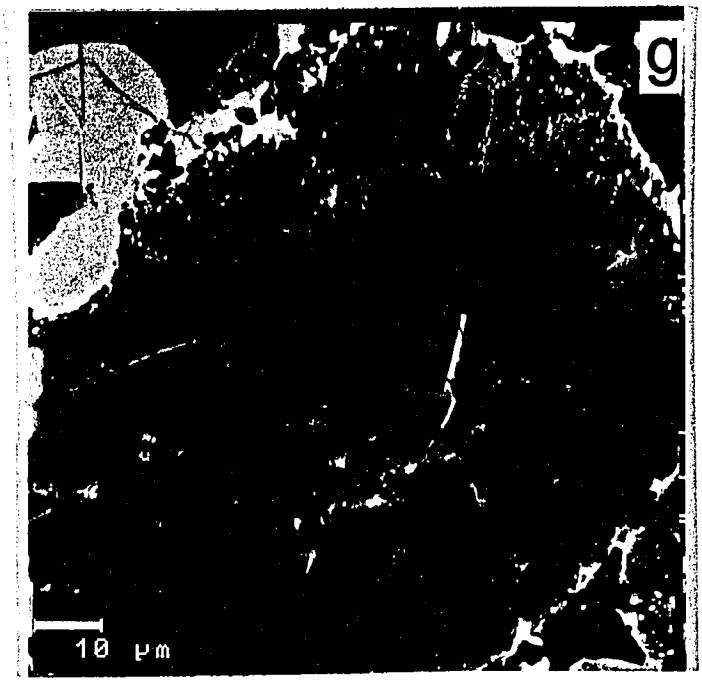
g
10 µm

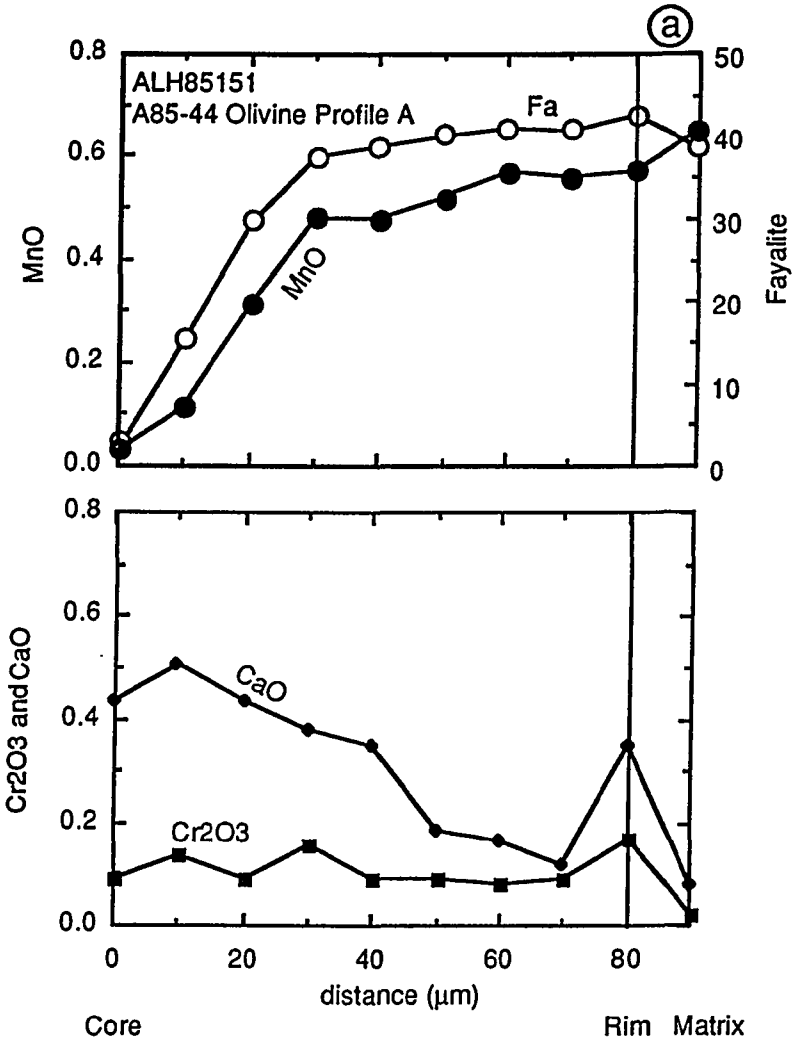

Figure 3.4.2. Zoning profiles of olivine in ALH85151, with mol.% Fa, weight % MnO, CaO and Cr2O3 taken from the forsteritic cores to the fayalitic rims and into the matrix olivine: (a) In the olivine crystal in A85-44, the boundary between the core and the rim is sharp with respect to Fa and MnO. CaO shows a general trend of decreasing from core to rim, and Cr2O3 remains constant until the rim, at which point they both show a sharp increase. Adjacent matrix olivine has a lower Fa content, but greater MnO then the rim. (b) In A85-13, MnO decreases as Fa content increases near the rim. As in the previous example, Cr2O3 increases sharply at the rim. (c) A85-14 olivine exhibits oscillatory zoning. Cr2O3 shows a sharp increase at the rim.

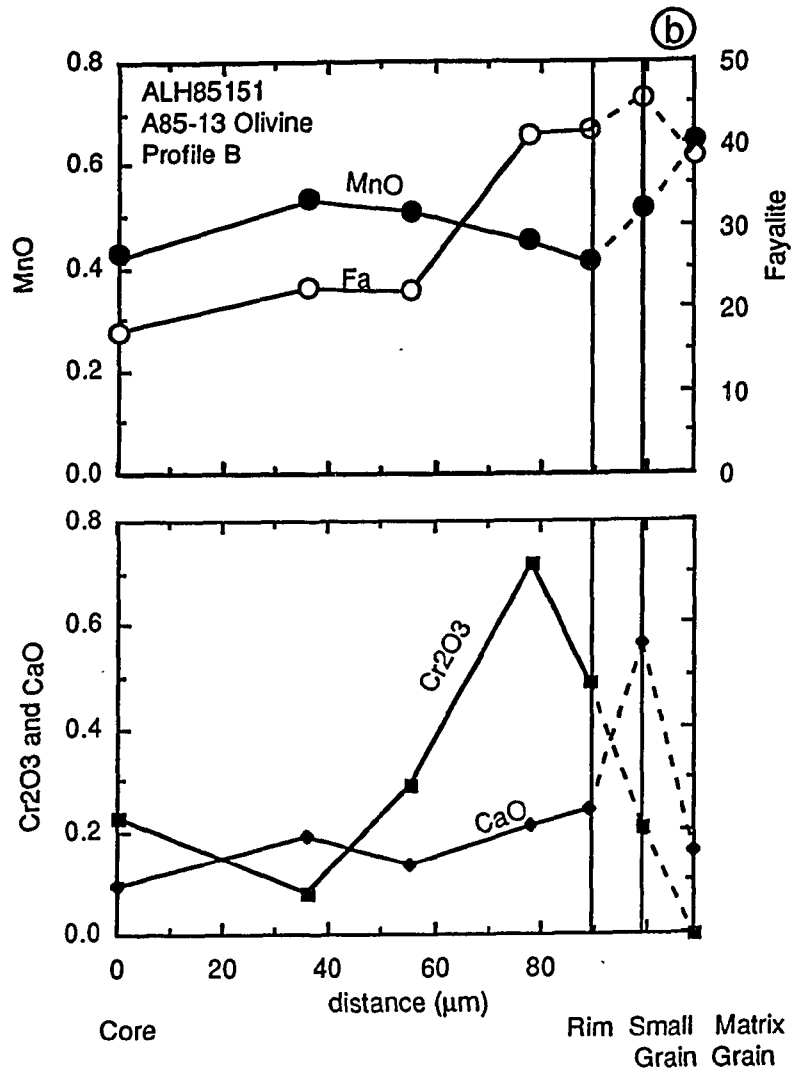
(b)
ALH85151
A85-13 Olivine
Profile B
MnO
Fa
MnO
Fayalite
Cr2O3
CaO
Cr2O3 and CaO
distance (μm)
Core
Rim
Small Grain
Matrix Grain

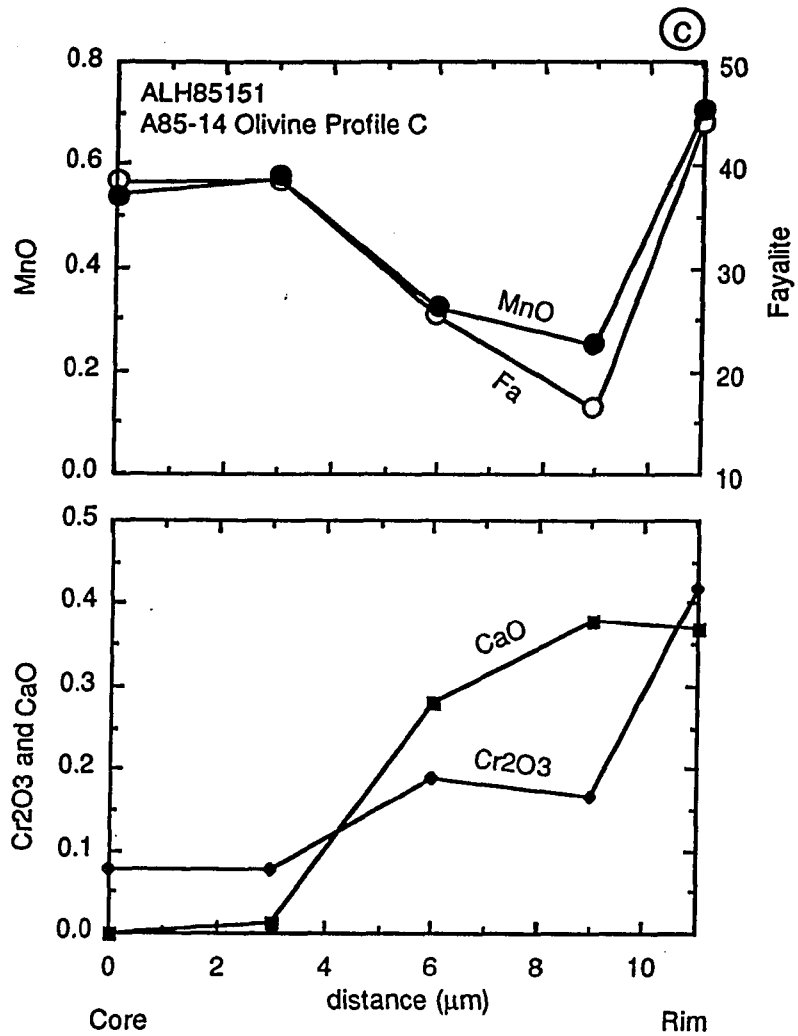
C
ALH85151
A85-14 Olivine Profile C
MnO
Fa
MnO
Fayalite
CaO
Cr2O3
Cr2O3 and CaO
distance (μm)
Core
Rim

Table 3.4.3. Chemical compositional (wt.%) profile A of olivine fragment A85-44 in the ALH8515 chondrite.

Distance (μm)	Center 0	10	20	30	40	50	60	70	Edge 80	Matrix 90
SiO_2	42.1	40.0	38.1	36.9	36.8	36.6	36.4	36.2	36.0	37.2
TiO_2	0.07	0.07	0.07	0.07	0.07	0.08	0.08	0.07	0.06	0.04
Al_2O_3	bd	bd	bd	0.11	0.11	0.42	0.15	0.25	0.23	bd
Cr_2O_3	0.09	0.14	0.09	0.16	0.09	0.09	0.08	0.09	0.17	0.02
FeO	2.3	14.5	26.2	32.4	33.3	34.4	35.1	35.0	35.6	33.6
MnO	0.04	0.11	0.31	0.48	0.48	0.52	0.57	0.56	0.57	0.64
MgO	54.3	45.0	34.8	30.1	29.04	28.7	28.1	28.6	26.9	30.0
CaO	0.44	0.51	0.44	0.38	0.35	0.19	0.17	0.12	0.35	0.08
Total	99.3	100.3	100.0	100.6	100.2	101.0	100.7	100.9	99.9	101.6
%Fa	2.3	15.3	29.7	37.6	38.9	40.2	41.2	40.7	42.6	38.6

bd-below detection

Table 3.4.4. Chemical compositional (wt.%) profile B of olivine in chondrule A85-13 in the ALH85151 chondrite.

Distance (μm)	Center 0	36	55	80	Edge 89	Small grain	Matrix
SiO_2	38.1	37.7	37.8	34.3	34.7	35.7	37.6
TiO_2	bd	bd	bd	bd	bd	0.04	0.03
Al_2O_3	bd	bd	bd	bd	bd	0.20	bd
Cr_2O_3	0.23	0.08	0.29	0.72	0.49	0.21	0.07
FeO	16.0	20.6	20.5	34.4	35.0	37.7	32.8
MnO	0.42	0.53	0.51	0.45	0.41	0.51	0.63
MgO	43.2	40.4	40.7	27.6	27.7	25.5	29.4
CaO	0.09	0.19	0.13	0.21	0.24	0.56	0.13
Total	98.0	99.5	99.9	97.7	98.5	100.4	100.7
%Fa	17.2	22.2	22.0	41.1	41.5	45.4	38.5

bd-below detection

(Fa_2) of the olivine to the fayalite-enriched rim (Fa_{43}). The olivine zoning is concentric about three "islands" (cores) of forsterite which are bounded sharply by the fayalite-rich rim. The core is separated by fractures and fayalite-enrichment occurs on these fractures as well as on the rim, giving the appearance of three cores. The rim is about 50μm thick and is zoned from Fa_{30-43}; MnO increases with FeO , while CaO decreases and Cr_2O_3 remains essentially constant along the profile. At the outermost edge and most fayalitic portion of the grain the CaO and Cr_2O_3 contents show a sharp increase. These spikes are the result of fine inclusions near the edge of the grain (Fig. 3.4.1b) which appear to be part of a discontinuous layer within the most fayalitic portion of the grain. These submicrometer-sized grains are beyond the resolution of a 1-2μm-sized electron probe beam. Qualitative data indicate that these are probably Ca-pyroxene and a chromite-like phase(s). This layer is also dotted with pore spaces. The adjacent matrix olivine is more magnesian (Fa_{38}) than the rim of the crystal, indicating that the Fe-enrichment of the rim could not be the result of thermal diffusion with the matrix olivine. The matrix olivine also has a higher MnO concentration than that of the fayalitic rim (Table 3.4.3, Fig. 3.4.2a), which also suggests a lack of parent body thermal diffusion.

A85-13 (Fig. 3.4.1c) is a chondrule in ALH85151 which consists of a large (~200μm) olivine crystal with patchy zoning, surrounded by finer-grained olivine crystals (~6μm) which are compositionally similar to the fayalitic rim of the large olivine. This chondrule contains a glassy feldspathic mesostasis between the olivine crystals. Profile B (Fig. 3.4.2b, Table 3.4.4) is taken across a section of the large olivine. The large zoned olivine is an angular grain with a composition of Fa_{18} which on some outer surfaces steeply jumps to a rim composition of Fa_{42}. This rim is much thinner (about 8μm) than that observed in olivine fragment A85-44 (Fig. 3.4.1a). The zoning is not restricted to the grain edges, but also occurs in the interior along preexisting fractures. Note that the outer surfaces are unevenly zoned and zoning is absent on some surfaces. MnO increases with FeO in the forsteritic zones, and in contrast with olivine fragment F44 (Fig. 3.4.2a), MnO

decreases with increasing FeO in the fayalitic zones. This suggests that the fayalitic enrichment of the rim of the olivine in A85-13 may be the result of oxidation of FeNi metal and/or sulfide. Cr_2O_3 increases sharply in the fayalitic zones, as in A85-44 and this is again attributed to fine Ca-pyroxene and chromite which form a thin layer within the fayalite-enriched rim. Small olivine grains surrounding the large crystal are homogeneous in composition, at Fa_{45}, and are similar in composition to the outermost rim of the large olivine crystal. The chondrule is surrounded by a rim of sulfide, and beyond this rim is typical olivine-rich matrix, equilibrated at Fa_{38}. As in olivine A85-44, the adjacent matrix olivine is more magnesian and has higher MnO than the fayalitic rim.

The zoning patterns of olivine A85-44 and in chondrule A85-13 are similar in that they are patchy and contain a porous-Ca-pyroxene-chromite-rich layer within the outermost rim. In addition, the outermost rims are similar in composition at about Fa_{45}. However, they differ in that the rim in olivine A85-44 is much thicker (Fig. 3.4.1a) than in A85-13 (Fig. 3.4.1c), and FeO and MnO have a positive correlation in the rim of A85-44 (Fig. 3.4.2a) and not in A85-13 (Fig. 3.4.2b). Thus, these chondrules were exposed to generally similar environments with similar oxidation states, but prior to chondrite accretion.

Pathcy zoned olivine has been described in the Allende (CV3) chondrite by Peck and Wood (1987), Hua et al., (1988), and Weinbruch et al. (1990). They showed olivine grains having fayalitic zones along grain surfaces and fractures, relatively sharp boundaries between forsteritic cores and fayalitic rims, and pore spaces and inclusions within the fayalitic zones. All these features are similar to those in the patchy zoned olivine in the Carlisle Lakes-type chondrites. Weinbruch et al. (1990) found that in many cases both FeO and MnO increase along the core-rim compositional profiles (as in A85-44, Fig. 3.4.2a) and in other cases FeO increases and MnO remains constant (as in A85-13, Fig. 3.4.2b). The inclusions that occur within the fayalitic rims of Allende olivine, however, are enriched in Cr and Al. We observed enrichments of Cr and Ca in A85-44 and -13.

Table 3.4.5. Chemical compositional (wt.%) profile C of olivine in chondrule A85-14 in the ALH85151 chondrite.

	Center				Edge
Distance (μm)	0	3	6	9	11
SiO_2	36.1	36.0	37.6	39.5	37.7
TiO_2	0.16	0.17	0.03	bd	0.05
Al_2O_3	bd	bd	bd	bd	0.45
Cr_2O_3	bd	0.14	0.28	0.38	0.37
FeO	32.5	32.5	22.4	15.2	36.5
MnO	0.54	0.57	0.32	0.25	0.70
MgO	29.3	29.2	37.7	44.0	25.8
CaO	0.06	0.08	0.19	0.17	0.42
Total	98.7	98.7	98.5	99.5	102.0
%Fa	38.4	38.5	25.4	16.3	44.2

bd-below detection

Similar types of zoning have not been found in ordinary chondrites. However, the studies of zoning in ordinary chondrites have concentrated on specific chondrules types, such as type II (Jones, 1990) and Type IA (Jones and Scott, 1989; McCoy et al., 1989) chondrules.

Oscillatory Zoned Olivine: In this type of zoning, the composition of the olivine oscillates from an Fe-rich core to a more Mg-rich layer, and back to an Fe-rich rim. Chondrule A85-14 in ALH85151 (Fig. 3.4.1d) consists of a large central olivine surrounded by smaller olivine crystals. Between the smaller olivine grains is a glassy feldspathic mesostasis. All of the olivine in this chondrule exhibits oscillatory zoning, with respect to FeO and MgO. Profile C (Table ,3.4.5, Fig. 3.4.2c) is taken along a portion of the large central olivine. The core of the large olivine is Fa_{38} and is rimmed by a thin (2-3μm) layer of magnesian olivine ($Fa_{\leq 16}$), followed by a thinner (1μm) layer of $Fa_{\geq 44}$. The magnesian layer and the outermost layer are too thin to allow completely accurate measurements with a 1-2μm

Table 3.4.6. Chemical compositions (wt.%) of zoned low-Ca pyroxene in ALH85151 (A85) and Carlisle Lakes (CL) chondrules.

	CL-1		CL-10		A85-2	
	Core	Rim	Core	Rim	Core	Rim
SiO_2	57.2	55.0	55.8	54.5	58.5	54.5
TiO_2	0.03	bd	0.05	0.11	bd	0.04
Al_2O_3	0.35	0.43	0.44	0.54	0.13	0.32
Cr_2O_3	0.47	0.38	0.57	0.44	0.32	0.49
FeO	8.8	15.6	12.4	18.3	6.6	18.1
MnO	0.22	0.33	0.20	0.43	0.33	0.26
MgO	32.7	28.1	29.2	25.6	34.9	24.9
CaO	0.97	0.90	0.67	0.91	0.21	0.30
Total	100.7	100.7	99.3	100.8	101.0	98.9
%Wo	1.8	1.7	1.3	1.7	0.4	0.6
Fs	12.9	23.3	19.0	28.1	9.6	28.7

bd-below detection

Table 3.4.7. Chemical compositions (wt.%) of olivine in chondrules having zoned low-Ca pyroxene in the ALH85151 (A85) and Carlisle Lakes chondrites (CL).

	A85-20					CL-1	
	1	1	2	3	4	2	5
	core	rim					
SiO_2	36.0	35.7	36.2	36.2	35.1	40.1	36.0
TiO_2	bd	0.06	0.04	0.08	0.07	bd	bd
Al_2O_3	bd	bd	bd	bd	bd	bd	bd
Cr_2O_3	0.08	0.62	0.19	0.57	0.66	0.28	0.13
FeO	33.5	34.5	30.4	33.5	33.5	15.6	33.8
MnO	0.41	0.49	0.42	0.46	0.44	0.29	0.49
MgO	29.1	29.6	31.5	29.0	2.82	43.0	30.3
CaO	0.09	0.10	0.10	0.28	0.22	0.21	0.23
Total	99.2	101.1	98.9	100.1	98.2	99.5	101.0
%Fa	39.2	40.0	35.1	39.4	40.0	16.9	38.5

bd-below detection.
1-large phenocryst.
2-enclosed by pyroxene.
3-vein in pyroxene.
4-rim on pyroxene.
5-small grain on outer edge of chondrule.

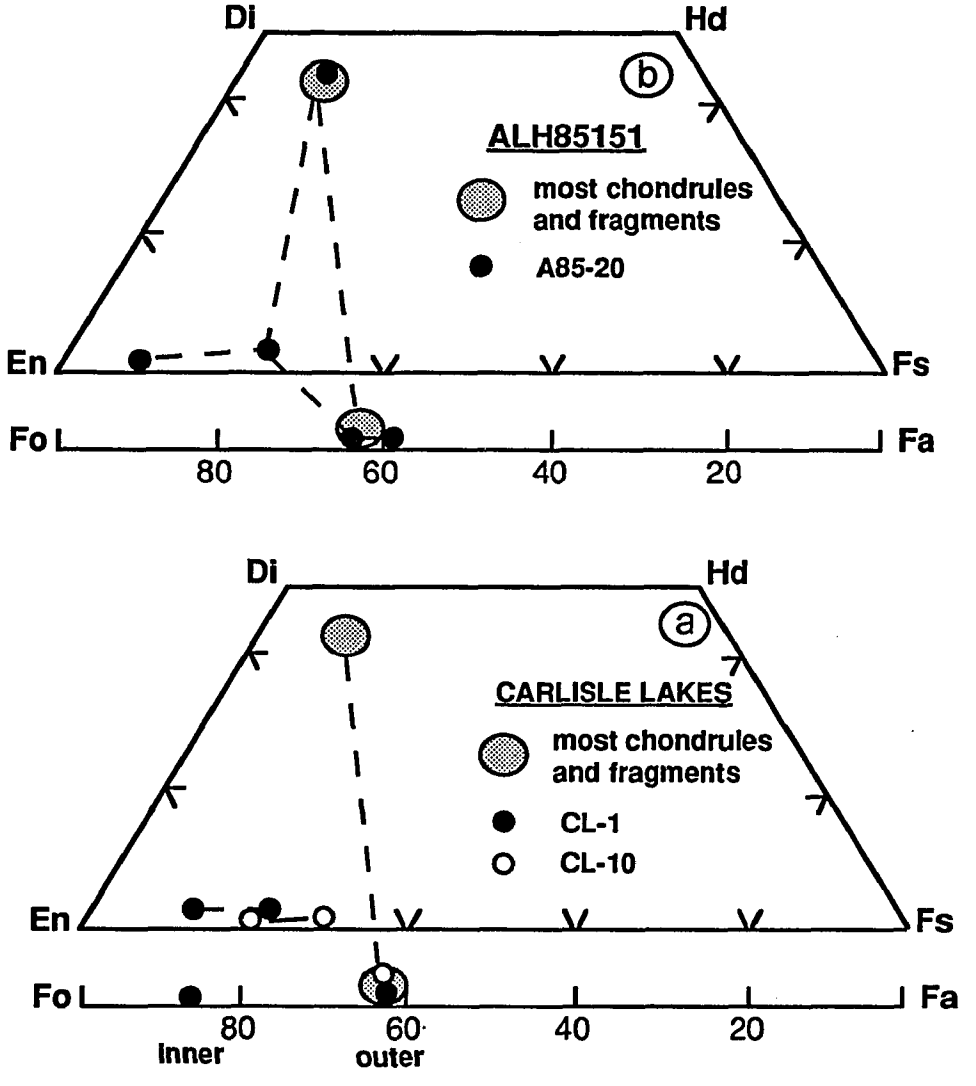

Fig. 3.4.3. Pyroxene quadrilateral showing the compositions of zoned pyroxene and coexisting olivine from (a) the CL-1 and CL-10 chondrules in Carlisle Lakes and (b) the A85-20 chondrule in ALH85151, in relation to olivine and pyroxene from most chondrules and fragments and the matrices of these meteorites.

electron beam; if anything, the differences between them may be even greater. MnO follows FeO, CaO increases as FeO decreases, and Cr_2O_3 increases sharply at the very edge of the fayalitic rim.

The Mg-rich olivine layer follows hairline fractures throughout the large olivine crystal (Fig. 3.4.1d) suggesting that the forsteritic layer is not the result of crystallization from a melt droplet. It is also unlikely that this type of zoning originated in the parent body since it is oscillatory and this would be difficult to explain by thermal metamorphism. The composition of the outer rim (Fa_{44}) of the large crystal is similar to that of the rims on other zoned olivine in the chondrite, suggesting that this chondrule was exposed to an oxidizing environment similar to the others.

Patchy Zoned Pyroxene: All of the previous examples of zoning have been found only in ALH85151 and Y75302. Pathcy zoned pyroxene was found only in Carlisle Lakes and ALH85151. In chondrules and mineral fragments with this type of zoning, the pyroxene grains are zoned in irregular patches (Fig. 3.4.1e), or the zoning is parallel to twin lamellae (Fig. 3.4.1f, g). Two types of olivine, associated with the pyroxene, are present in some cases. More forsteritic olivine may be concentrated in the core of the chondrules, or occurs as inclusions in the pyroxene, whereas more fayalitic olivine is located closer to the rim of the chondrule and occurs as veins in the pyroxene and/or rims on it (Fig. 3.4.1e, f, 3).

CL-10, in Carlisle Lakes (Fig. 3.4.1e), is an example of a chondrule in which the pyroxene has irregular patchy zoning. The pyroxene compositions are $Wo_{1.3}$ and 1.7, $Fs_{19 \text{ and } 28}$ (Fig. 3a, Table 3.4.6), respectively. Olivine in this chondrule is near-homogeneous at Fa38 (Fig.3.4.3a).

A85-20 (Fig. 3.4.1f) is an example of a chondrule in ALH85151 which has pyroxene with lamellar zoning, with compositions of $Wo_{0.4 \text{ and } 0.6}$, $Fs_{10 \text{ and } 29}$ (Table 3.4.6, Fig. 3.4.3b). Olivine occurs in four textural settings in this chondrule: (1) as large phenocrysts, partially enclosed by pyroxene, (2) poikilitically enclosed within pyroxene, (3) as veins in pyroxene, and (4) rimming pyroxene. Compositions of each type of

olivine are presented in Table 3.4.7. The veins and rims of olivine necessarily post-date the pyroxene, and the olivine inclusions crystallized prior to the pyroxene. The poikilitic olivine is more magnesian (Fa_{35}) than the olivine in the other textural settings (Fa_{40}). The olivine filling veins and rimming pyroxene has higher Cr_2O_3 (0.6wt.%) than the poikilitic olivine (0.2%). The large olivine phenocrysts show an increase in Cr_2O_3 from 0.1% in the core to 0.6% at the rim. Ca-pyroxene and a feldspathic component (8.7% Na_2O, 2.9% CaO) also occur in this chondrule.

The lamellar zoning in pyroxene is similar to that described by Tsuchiyama et al. (1988) in type $\geq$3.5 ordinary chondrites. However, they did not report veins and rims of olivine associated with the pyroxene that they studied. Additionally, they reported homogeneous olivine in all their samples. These are important distinctions between the chondrules with patchy pyroxene in the ordinary chondrites (Tsuchiyama et al., 1988) and those in the Carlisle Lakes-type chondrites. The pyroxene zoning in the Carlisle Lakes-type chondrites and that in the ordinary chondrites may be the result of different processes.

3.4.4 Petrology of the Chondrules Analyzed for Oxygen Isotopes

Chondrules A85-1, -2, and -4 from ALH85151 and CL-1 from Carlisle Lakes were analyzed for oxygen isotopic analysis. A85-1 and -2 are porphyritic olivine (PO) chondrules and A85-4 is a barred olivine (BO) chondrule (Table 3.4.2). All three of these chondrules have homogeneous olivine (Fa_{38}) and pyroxene (Wo_{45}, Fs_{12}) that is compositionally similar to the host chondrite. CL-1 is atypical of other chondrules in the Carlisle Lakes chondrite in that it is relatively large (diameter, 2.5mm) and is rich in low-Ca pyroxene. The pyroxene exhibits patchy pyroxene-type zoning, similar to that in CL-10, having core to rim variations (Table 3.4.6 and Fig. 3.4.3a). In addition, it contains olivine in two types of textural settings, with differing compositions. One type of olivine is enclosed by pyroxene and its composition is Fa_{17}; the other is near the outer edge of the chondrule and is more FeO-rich (Fa_{38}) (Table 3.4.7).

3.4.5 Oxygen Isotopes

Oxygen isotopic data for chondrules and whole chondrites ALH85151, Carlisle Lakes, and Y75302 are presented in Table 3.4.8. On an oxygen 3-isotope diagram (Fig. 3.4.4) these chondrites plot closest to the ordinary chondrites, but at much higher $\Delta^{17}O$ values (2.47-2.91‰). They have the highest $\Delta^{17}O$ values ever reported. Other materials with high $\Delta^{17}O$ include an unusual cristobalite-pyroxene inclusion (CRISPY) in the ALH76003 L6 chondrite ($\Delta^{17}O$=1.9‰, Olsen et al., 1981), magnetite in the Orgueil CI chondrite (1.7‰, Rowe et al., 1989), and feldspathic glass in the Mezo-Madaras chondrite (1.8‰, Mayeda et al., 1989). In addition, the hypothetical composition of the

Table 3.4.8. Oxygen isotopic compositions of ALH85151, Carlisle Lakes and Y75302 whole chondrites and chondrules.

	$\delta^{18}O$	$\delta^{17}O$	$\Delta^{17}O$
Whole Chondrite			
Carlisle Lakes	5.00	5.39	2.79
	5.62	5.71	2.79
	5.41	5.41	2.60
ALH85151	4.49	5.24	2.91
Y75302	4.11	4.61	2.47
Chondrules			
CL-1	5.44	3.51	0.68
A85-1	3.32	4.76	3.03
A85-2	3.47	4.34	2.54
A85-4	4.63	5.24	2.83

Data from Weisberg et al. (1991)

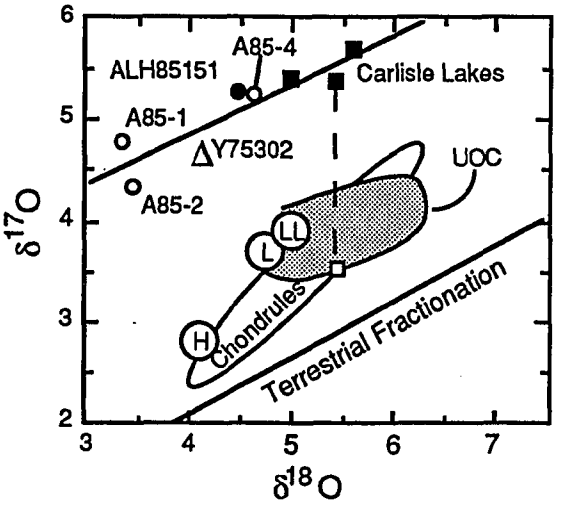

Fig. 3.4.4. Oxygen 3-isotope diagram showing data for whole chondrite ALH85151 (filled circles) and Carlisle Lakes (filled squares), their chondrules (open symbols) and whole chondrite Y75302 (filled triangle) in relation to equilibrated and uequilibrated H, L and LL chondrites and chondrules. The ALH85151 and Carlisle Lakes whole chondrites have higher $\Delta^{17}O$ values than the ordinary chondrites or any other known material in the solar system. The chondrules in ALH85151 and whole chondrites plot on the same mass fractionation line. Chondrule CL-1 from Carlisle Lakes differs in that it plots in the field of ordinary chondrite chondrules.

nebular gas that exchanged oxygen with the Murchison (CM2) chondrite, according to the model of Clayton and Mayeda (1984), has a high $\Delta^{17}O$ of 8.6‰.

The whole chondrites and the ALH85151 chondrules all plot on a mass fractionation line. The chondrule from the Carlisle Lakes chondrite (CL-1), however, does not fall on this mass fractionation line. Instead, it has a relatively low $\Delta^{17}O$ (0.68) and plots within the field of the ordinary chondrites, on the oxygen 3-isotope diagram (Fig. 3.4.4). It is possible that this chondrule is related to the ordinary chondrite chondrules and does not have high $\Delta^{17}O$ like the other Carlilsle Lakes-type chondrites and chondrules because it is atypically large and oxygen diffusion is slower in larger chondrules (Clayton and Mayeda, 1983). Therefore, it may be a relict precursor to the other chondrules.

However, a relationship to the ordinary chondrites can not be drawn from only one datum point. Atypically large chondrules in ordinary chondrites often have atypically low $\Delta^{17}O$ values (R.N. Clayton, unpublished data) and the proximity of CL-1 to the ordinary chondrite chondrules on the oxygen 3-isotope diagram may not be meaningful.

4. DISCUSSION

4.1 CR Chondrites

4.1.1 Classification of the CR Chondrites

The CR chondrites all have a similar set of petrologic and isotopic characteristics that are unique to them and thus, they should be distinguished as a group from other chondrite groups. Some of the general petrologic features of the CR chondrites include: (1) Occurrence of large (up to 3 mm, average=1 mm) multilayered, FeNi metal-rich chondrules that have olivine- and/or pyroxene- rich cores surrounded by olivine-, pyroxene-, serpentine-, FeNi metal, and/or Ca-carbonate-rich layers. (2) Abundant matrix and dark inclusions (DI) that contain non-layered microchondrules (<500 μm) and refractory-rich inclusions. (3) Unique assemblages and compositions of aqueous alteration products that include chlorite-rich chondrule mesostases, serpentine-rich rims on chondrules, and serpentine-rich brown spheres on chondrule margins, in chondrule rims and in the matrix. In addition, Ca-carbonates are compositionally different from those in other chondrite groups and Ca-carbonate rims on chondrules have not been reported in other chondrite groups. (4) FeNi metal having a positive Ni vs. Co trend which overlaps the predicted trend of FeNi condensing from a solar gas. (5) Low abundances of refractory-rich inclusions and AOAs that have Mn-rich and Mn-poor olivine. (6) Matrices that contain magnetite framboids and platelets.

The oxygen isotopic composition of the CR chondrites lie on a unique mixing line defined by their chondrules and whole chondrite compositions (Fig. 3.1.9). Matrix lies at the intersection of the CR mixing line and the terrestrial mass fractionation line, presumably due to mixing with a liquid component having heavier oxygen.

Another chemical property which appears to be a unique characteristic of the CR chondrites is their nitrogen isotopic compositions. Most meteorites have nitrogen isotopic

compositions of $\delta^{15}N$=-90 to 50‰, where $\delta^{15}N$ is the permil deviation of the $^{15}N/^{14}N$ ratio in the sample from that of atmospheric nitrogen, i.e.

$$\delta^{15}N(‰) = \left(\frac{(^{15}N/^{14}N_{sample})}{(^{15}N/^{14}N_{atmosphere})} - 1\right) x\ 1000$$

Renazzo has a $\delta^{15}N$ value up to 190 (Kung and Clayton, 1978; Robert and Epstein, 1981) and the other CR chondrites have similarly heavy nitrogen (Grady et al., 1991). As discussed in section 4.3.4, heavy nitrogen may reflect the presence of a primitive component, in the CR chondrites, which resulted from stellar nucleosynthesis and escaped homogenization in the nebula. Attempts to isolate this component have been unsuccessful.

The only discrepancy in the classification of these meteorites as a group lies in the INAA bulk compositional data of Kallemeyn and Wasson (1981). They analyzed Renazzo and Al Rais and found that they have similar refractory lithophile and siderophile elements, but that Al Rais had much higher volatile lithophile abundances. Based on these data they suggested that Renazzo and Al Rais should not be grouped together. However, it is clear that the petrologic data and oxygen and nitrogen isotopic compositions are overwhelmingly in favor of grouping Al Rais with Renazzo and the other CR chondrites. Differences in volatile element abundances may be a result of the greater abundance of matrix and DI in Al Rais (Table 3.1.2). These components have higher volatiles than chondrules and inclusions.

It is suggested that the seven chondrites be considered members of the same group, designated CR, and that they should be examined further in order to understand the variability in volatile abundances which may be an inherent characteristic of this group. One step toward resolving this problem has already been taken. For a future project, I have separated chondrules and matrix from Renazzo, Al Rais, MAC87320, and EET87770 in order to obtain INAA bulk chemical compositions of individual components in the CR chondrites. These will also be compared to their oxygen isotopic compositions. In

following sections, the relationship of other ungrouped meteorites (ALH85085 and Bencubbin) to the CR chondrites will be discussed.

4.1.2 Petrologic Evidence for a Condensation Origin for the Refractory-Rich Inclusions

Of the five types of refractory-rich inclusions in the CR chondrites, only the calcium-aluminum-rich chondrules (CAC) are spherical, having a shape consistent with crystallization from a melt droplet, analogous to the common olivine-pyroxene-rich chondrules. All the other inclusions have irregular shapes and aggregational textures and their sequence of phases are consistent with those of phases predicted to condense from a gas of solar composition (Grossman, 1972). The compact type A (CTA) inclusion has a Wark-Lovering rim sequence which can also be explained by condensation events in the nebula (Wark and Lovering, 1977). The sequence of minerals in the fluffy type A (FTA) inclusion is similar to that of FTA inclusions in Allende (MacPherson and Grossman, 1984), and is consistent with the predicted order of condensation from a solar gas in the temperature range (1600-1400 K) at 10^{-6} atm.

The spinel-pyroxene aggregate (Sp-Pyx-Agg) is similar to Sp-Pyx-Agg in CM chondrites (MacPherson et al., 1983). They are aggregates of spinel nodules rimmed by diopside, the spinel contains inclusions of perovskite and a fine-grained matrix-like material fills the space between the nodules. MacPherson et al. (1983) studied similar inclusions in CM chondrites and pointed out that these inclusions could not have crystallized from spinel-rich melt droplets. Such spinel-rich melt droplets would be so rich in spinel that the spinel would be the first phase to crystallize and the inclusions would appear as diopside rimmed by spinel, instead the reverse relationship is observed. MacPherson et al. (1983) explained these inclusions by condensation and heterogeneous nucleation of spinel onto preexisting dust, followed by condensation of diopside onto the spinel. These inclusions may have originally existed in the nebula as loosely bound aggregates of spinel-diopside

nodules. Spaces between the nodules were later filled by a lower temperature material, compositionally similar to chondrite matrix.

Of the refractory-rich inclusions in CR chondrites, the amoeboid olivine aggregates (AOA) are the most unusual having two types of olivine (see section 3.1.4, Table 3.1.9, Fig.3.1.7). One type has a blue cathodoluminescence and it is forsterite. The other has a red luminescence and it is forsteritic, but has a higher abundance of Mn. Some of the red (high Mn-olivine) have MnO concentrations that equal or exceed their FeO concentrations. These are compositionally similar to some of the LIME (Low Iron, Manganese-Enriched) olivines that have been found in interplanetary dust particles (IDP) (Klock et al., 1989).

It is difficult to envisage a process that would result in these Mn-rich olivines if they crystallized from a melt. Reduction of chondritic olivine could possibly result in olivine with high MnO/FeO ratios, but there is no evidence of a reduction process, as evidenced by the presence of low-Ni metal, or any of the expected byproducts of reduction of olivine. Reduction reactions (*in situ*) between AOA and the surrounding matrix can be ruled out because the matrix is highly oxidized, containing Fe-rich phyllosilicates and magnetite. The irregular shapes and aggregational appearance of the AOA also suggest that they did not crystallize from a melt. In addition, the occurrence of fassaite with spinel inclusions and spinel-pyroxene nodules in the center of some aggregates (Fig. 3.1.6) suggests that the AOA are related to other refractory-rich inclusions which are also believed to be products of nebular condensation. Therefore, a condensation model for these inclusions is suggested. The fassaite-spinel-rich nodules are early high temperature phases that condensed in the range 1600-1400K, at 10^{-6} atm. At 1450K, forsterite began to condense and aggregated onto these nodules. These aggregates remained in contact with the nebular gas until about 1100K at which temperature Mn_2SiO_4, the tephroite molecule was able to condense in solid solution with forsterite (Wai and Wasson, 1977). Fayalitic olivine forms at much lower temperatures (~500K) via reaction of Fe-metal and forsteritic olivine. The high MnO/FeO

ratios may result because these olivines did not equilibrate with Fe-metal at lower nebular temperatures.

4.1.3 Aqueous alteration of the CR Chondrites

Most chondrite groups exhibit some degree of aqueous alteration. In ordinary chondrites products of aqueous alteration are very minor components within the matrix and have been described in only three meteorites: Semarkona (LL3), Bishunpur (LL3), Tieschitz (H3) and Krymka (L3) (Alexander et al., 1986; Hutchison et al., 1987). Aqueous alteration products have been identified in the "anhydrous" CV and CO chondrites (Bunch and Chang, 1980; Michel-Levy, 1969; Kurat, 1975; Kerridge, 1964; Cohen et al., 1983; Tomeoka and Buseck, 1982, 1985 and 1990; Keller and Buseck, 1990), but are not as pervasive as they are in the hydrous CM and CI chondrites (e.g., Kerridge, 1976; McSween, 1979; Bunch and Chang, 1980; Tomeoka and Buseck, 1988, Fredrikkson and Kerridge, 1988). In CR chondrites, aqueous alteration is quite extensive as in the CM chondrites, occurring throughout the matrices, on chondrule rims, and even in chondrule interiors. However, as shown in Fig. 3.1.4 the compositions of the phyllosilicates deviate from those in other chondrite groups. Serpentines in CR chondrites are more FeO-rich than those in CI chondrites and more restricted in composition than in CM chondrites; CRs contain an Al-rich chlorite-like phase not found in any of the other chondrite groups. In addition, the Ca-carbonates differ compositionally from those in CM or CI chondrites (Table 3.1.6). The obvious conclusion is that the aqueous alteration products (phyllosilicates, carbonates, and oxides) in CR chondrites formed under a different set of conditions than those in other chondrite groups. These conditions may have included differing temperatures and water/rock ratios. Attempts to quantify these parameters have not been made because of the difficulties in obtaining precise chemical compositions, as a result of the fine grain sizes of the phases, and the unequilibrated nature of the phases. Most of the phyllosilicates are mixtures of more than one phase, too fine to resolve with a

1-2μm electron probe beam and the carbonates are metastable forms, as suggested by their irregular shapes and compositions, and are also too fine for precise microprobe analysis. HRTEM analysis is needed to better understand the nature of these phases.

Three hypotheses are presented as to the origin of the phyllosilicates in CR chondrites: (1) Primary condensation from a solar nebular gas, (2) Alteration of preexisting materials by exchange with H_2O vapor in the solar nebula, and (3) Alteration of preexisting materials in a parent body by H_2O-rock interaction. Petrographic evidence suggests that the phyllosilicates are products of alteration of preexisting materials and thus preclude the first scenario. The evidence includes: (a) Phyllosilicate rims enclose partially altered preexisting pyroxene. (b) Brown serpentine-like microspherules contain relict sulfides and silicates. (c) Some melt droplet-formed chondrules have Al-rich chlorite-like mesostases, suggesting replacement of the glassy feldspathic mesostasis typically found in anhydrous chondrules. (d) The morphologies of magnetite (framboids, platelets, etc.) are typical of that expected if they crystallized from a gel or fluid phase (Kerridge et al., 1979).

It has also been argued that rates of hydration reactions in the nebula at low temperatures are too slow, eliminating the second hypothesis. Armstrong et al. (1982) considered the formation of calcite in the nebula by the reaction:

$$CaO + CO_2 \rightarrow CaCO_3$$

and suggested that CaO would not be a stable phase under nebular conditions and that CO_2 could not be present at any significant pressure. They also considered the formation of $CaCO_3$ at low temperatures from the carbonation of Ca-rich phases, such as in the reaction:

$$Ca_2MgSi_2O_7 + CO_2 \rightarrow CaCO_3 + CaMgSi_2O_6$$

and suggested that the kinetics at such low temperatures and pressures would not allow formation of $CaCO_3$. Thus, they concluded that Ca-carbonate in chondrites does not form in a gaseous nebula, but forms as a result of interaction of CO_2 and H_2O with preexisting minerals in a chondrite parent body.

Phyllosilicates, carbonates, and magnetite in the CR2 chondrites thus appear to be the result of hydration reactions on the CR parent body (hypothesis 3). The serpentine rims that surround chondrules are probably alteration products of the fine grained olivine-rich rims observed on some anhydrous chondrules. The Al-rich chlorites that occur in chondrule cores are replacement products of the feldspathic glassy mesostases that are observed in anhydrous chondrule cores with olivine and/or pyroxene contributing Mg and Fe metal and/or sulfides contributing Fe. An idealized hydration reaction that could result in chlorite and Ca-carbonate is:

$$\underset{\text{(Anorthite)}}{2\cdot CaSi_2Al_2O_8} + \underset{\text{(Forsterite)}}{2\cdot Mg_2SiO_4} + 6\cdot Fe + 14\cdot H_2O + CO_2 \text{ -------}>$$

$$\underset{\text{(Chlorite)}}{[(Fe,Mg)_{10}Al_2]\,(Si_6Al_2)O_{20}} + (OH)_{16} + CaCO_3 + 6\cdot H_2$$

In some cases, the Ca-carbonate nucleated on the outer surfaces of the chondrule forming a rim.

From petrographic observation it appears that aqueous alteration predated the final lithification of the CR2 chondrites. The chondrule in Fig. 3.1.3 is broken and the Ca-carbonate only surrounds the original curved surface and not the angular, broken edge, suggesting that the Ca-carbonate rim predated chondrule breakage and lithification of the host chondrite. It is thus concluded that if the Ca-carbonate formed as a result of aqueous

alteration of preexisting phases in the CR parent body, it was prior to lithification of the host chondrite.

Further evidence of prelithification aqueous alteration is observed in Fig. 3.1.3a which shows two chondrules linked by a bridge of chlorite which is compositionally similar to that found in the cores, and the chondrules occur as a single unit surrounded by concentric phyllosilicate-rich and sulfide-rich layers. It is clear that these two chondrules were altered as a single unit, and that they are found adjacent to chondrules that experienced little or no alteration. Although aqueous alteration can be a highly selective process, it is most likely that these chondrules were first altered, as a unit, and later incorporated into the host chondrite. Additionally, dark inclusions within the same thin section of Renazzo appear to be texturally and compositionally similar, yet some contain anhydrous chondrules and in others the chondrules have been totally altered to serpentine-like phases. The degree of aqueous alteration that a particular DI exhibits does not cross its sharp angular boundary.

It is therefore concluded that aqueous alteration occurred prior to lithification of the host chondrite either in preexisting lithified units that were later brecciated via impacts and eventually relithified, or in poorly consolidated masses which were later lithified. The CR chondrite parent bodies experienced maximum temperatures of 150°C during aqueous alteration according to Zolensky (1991), based on the phyllosilicate assemblage of the matrix. A possible source of liquid water for aqueous alteration could be from melting of ice via heat generated by decay of short-lived radionuclides (DuFrense and Anders, 1962) or from residual heat from condensation (Larimer and Anders, 1967).

Differences in degree of aqueous alteration can be observed among the six CR chondrites studied. Of all the CR chondrites, Al Rais appears to have the highest degree of aqueous alteration. It is more hydrated than Renazzo, as evidenced by the higher abundance of H_2O in its chemical composition (Table 3.1.10). Al Rais contains the highest abundance of DI and matrix components and the fine-grained and porous character of these components make them more susceptible to the chemical interaction with water-

rich fluids. Some of its chondrules have been almost totally serpentinized, containing only relicts of anhydrous phases. Many chondrules have a mesostasis that has been replaced by chlorite-like phases. Renazzo is somewhat less hydrated than Al Rais, but still has some chondrules that have been totally serpentinized and many chondrule cores have chlorite-like phases. The other CR chondrites are much less altered showing some of the products of aqueous alteration, but the alteration products are less common than in Al Rais and Renazzo, and anhydrous chondrule cores are more common.

The degree of aqueous alteration is grossly correlated with the oxygen isotopic compositions of the chondrules and whole chondrites too. The compositions of chondrules and whole rock Al Rais are displaced to the northeast (higher water/rock ratios) on the CR mixing line relative to those of Renazzo; the matrix and DI compositions are also further northeast on the terrestrial fractionation line. Renazzo whole chondrite is further up the mixing line relative to the other CR chondrites. The positions of the CR chondrites on the mixing line are not simply the result of differing chondrule/matrix ratios. This is demonstrated by Y793495, which has a high abundance of matrix and DI, and it plots close to EET87770 which has a low abundance of matrix. Therefore, it is most likely that the water is the carrier of the heavy oxygen. For Murchison (CM2), Clayton and Mayeda (1984) suggested the mixing of solids with a hypothetical liquid component having relatively heavy oxygen ($\delta^{17}O$=30.3, $\delta^{18}O$=20.2).

4.2 ALH85085

4.2.1 Classification of ALH85085

ALH85085 is a unique chondrite. Unique features include the small size of its chondrules, high FeNi metal content, deficiency in sulfide, lack of matrix between chondrules and fragments and the occurrence of matrix as lithic clasts or lumps. Based on the whole rock Fe/Si, Mg/Si, Ni/Si, S/Si and Na/Si ratios, ALH85085 does not fit closely

into any group (Table 3.2.4) However, its Al/Si, Ca/Si and Mg/Si ratios closely approach the CR chondrite group (Fig. 3.2.6).

Nevertheless, this unusual meteorite shares characteristics with O and E as well as C chondrites. The abundance of Mg-rich enstatite, cryptocrystalline, and radial pyroxene chondrules and fragments, in association with subordinate Mg-rich olivine, is similar to that in EH3 chondrites. In addition, E chondrites have the highest abundance of FeNi metal relative to other chondrite groups, as does ALH85085. The reduced nature of ALH85085 as indicated by its magnesian silicates, high Fe/Ni metal content, and phases such as osbornite, indicates a similarity to E chondrites. However, differences are numerous also. EH3 chondrites contain less olivine than ALH85085 and are typically rich in sulfide (Table 3.2.1) and contain a wide variety of unusual sulfides such as niningerite, alabandite, oldhamite, djerfisherite, etc. (Keil, 1968). Additionally, FeNi metal in E chondrites is Si-bearing (Keil, 1968) and only three metal grains in ALH85085 were found to contain Si.

The occurrence of CAIs (Grossman et al., 1988) is suggestive of a close association with C chondrites. The Al/Si and Ca/Si ratios are also C chondritic, and although the Mg/Si ratio is somewhat greater than in any of the other chondritic groups, carbonaceous chondrites are at the higher end of the spectrum (Fig. 3.2.6). Like ALH85085, carbonaceous chondrites are also known to contain magnetite (McSween, 1977), although it may rarely be present in other chondrite groups.

ALH85085 most closely resembles the CR group of chondrites and the Bencubbin chondritic metal-silicate assemblage. CR chondrites have comparably low sulfide abundance and are the most metal-rich relative to other C chondrites (McSween, 1977). They contain up to 8 vol.% FeNi metal and have as little as 1.5 vol.% sulfide. The matrix lumps in ALH85085 are compositionally similar to CM and CR chondrites (Fig. 3.2.3). Metal compositions in CR chondrites and ALH85085 overlap (Fig. 3.2.5).

Association with the Bencubbin-Weatherford group is also a possibility. Metal in ALH85085 overlaps with that in Bencubbin as shown in Fig. 5, and the oxidation as well as volatile depletion state of the silicates is also similar to that in ALH85085. Bencubbin major silicates consist mainly of one chondritic component (barred olivine), and the majority of the silicates in ALH85085 are also made up of one chondritic component (cryptocrystalline). Both of these indicate high temperatures (above the liquidus) and complete melting (Nagahara, 1983; Hewins, 1988).

Clearly there are also major differences between CR chondrites, Bencubbin, and ALH85085. For example, CR chondrites have large and often layered chondrules rimmed by hydrous glassy material and phyllosilicates. Bencubbin has mainly barred olivine-textured clasts. Nevertheless, from a petrologic point of view ALH85085 has some strong similarities to CR chondrites and Bencubbin, and may belong to a new group which relates these groups.

4.2.2 Occurrence of matrix lumps

The occurrence of opaque chondrite matrix as sharply bound lumps has been observed in other meteorites (Scott et al., 1984; Prinz et al., 1987). With regard to major element composition, the matrix lumps in ALH85085 appear to be most similar to CR and CM chondrite matrices (Fig. 3.2.3). These lumps may be hydrous, although there is no direct evidence of this as yet (Scott, 1988; Grossman et al., 1988). Grossman et al. (1988) suggested that these lumps may be C1 materials. This was based on their observation of magnetite morphology, i.e., framboidal, spheroidal and platelet forms. However, framboids and platelets occur in CR matrices as well.

The large percentage of angular fragments and the low abundance of whole chondrules suggest that ALH85085 accreted in a high-energy environment. This environment might have contained a relatively higher density of particles moving at relatively faster speeds, increasing the possibility of collisions. It is surprising that fragile,

friable matrix material could survive under such conditions. One possibility is that the clasts may have arrived late. Their wide distribution throughout the two thin sections studied indicates that they were thoroughly mixed with other components just prior to cementation of the chondrite. Earlier incorporation would have resulted in a greater degree of breakup. The end result would have been a uniformly dispersed powder surrounding chondrules and fragments, much like that in typical type 3 chondrites.

If matrix lumps were late arrivals it should be noted that they still fall within the same small size range as the chondrules and other fragments. This indicates that the matrix lumps experienced the same size-sorting process as did the other components. If size sorting occurred in the nebula (as discussed below) then matrix lumps coexisted with the chondrules in the nebula at the time of aggregation.

4.2.3 Size sorting of ALH85085 components

Ranges of chondrule sizes within any single chondrite or chondrite group generally are restricted. Chondrules in ordinary and CV chondrites are usually coarser (90-2800μm) than those in CM-CO chondrites (55-800μm) and grain size frequency distributions are similar for all components (i.e., chondrules, mineral fragments, lithic fragments) in the same chondrite (King and King, 1978, 1979). From these data, King and King (1978, 1979) suggested that chondrites may have been size sorted. Within the ordinary chondrites, LL chondrules are larger than those in H and L chondrites.

Limited size ranges are also observed in the components of other chondritic material. Clasts of type 3 chondrites which were originally thought to be graphite-magnetite assemblages were described to have small chondrules ranging from 100 to 500μm (Scott et al., 1981). Chondrules in a clast in the Piancaldoli LL3 chondrite are 0.2-64 μm in diameter (Rubin et al., 1982).

The mechanisms which have been proposed to explain size distributions in chondrites are all variations of aerodynamic sorting in the nebula. Whipple (1971, 1972)

and Dodd (1976) suggested that as a planetesimal moves through a mixture of gas and dust, aerodynamic drag will result in exclusion of smaller particles and inclusion of larger ones. Such aerodynamic accretion of planetesimals depends on the size and velocity of the planetesimal and the viscosity of the gas through which it travels. Whipple (1971, 1972) and Dodd (1976) explored the Stokes and Epstein drag laws and derived equations to predict the size of the smallest particle which may accrete to a growing planetesimal.

For Stokes drag law

$$v_I=0.36Z\pi S/s^2\rho_s$$

where v_I is the velocity of a planetesimal of radius S, π is the viscosity of the gas, and ρ_s is the density of the smallest particle of radius s that can accrete to the planetesimal.

For Epstein drag law

$$v_I=0.11v\rho S/s\rho_s$$

where v is the mean molecular velocity of the gas, ρ is the density of the gas, and all other variables are the same as in Stokes drag.

According to Whipple (1971, 1972) Stokes drag applies only to a gas with a density greater than that predicted for the solar nebula and that aerodynamic accretion of chondrites obey the Epstein drag law. Dodd (1976) tested both of these laws by applying size and density data from the ordinary chondrites. He found that most ordinary chondrites appear to have accreted in an Epstein regime, but that some H chondrites may have accumulated under conditions transitional to a Stokes regime. Therefore, aerodynamic drag appears to be a suitable mechanism for explaining size distributions of chondrules and other components in chondrites.

Based on his observation that compound chondrules are similar in size, Rubin et al. (1982) suggested that pre-existing dustballs were size sorted prior to chondrule

formation and planetesimal accretion. Since the sizes of chondrules and lithic fragments in ALH85085 are very similar, and the majority of lithic fragments are similar in texture and composition to the chondrules, it is likely that the lithic fragments represent broken chondrules. Likewise, many mineral fragments in ALH85085 are as large or larger than the chondrules. Assuming that mineral fragments must have been much larger than chondrules observed in ALH85085. Thus, it seems likely that chondrules and other components were sized sorted after chondrule formation, and subsequent breakup, of larger chondrules.

The following sequence of events for the history of ALH85085 components is proposed. Chondrules of variable sizes and compositions formed in the nebula. Large olivine fragments in ALH85085 are generally richer in FeO than olivine in the chondrules, and therefore, the larger chondrules from which these fragments are derived must have formed at a different time or location in the nebula where conditions were more oxidizing. Solidified chondrules were broken up, probably as a result of collisions, and chondrules and fragments began to accumulate onto a parent body. Sorting by aerodynamic drag probably occurred at this time. The matrix lumps must have been added to this region close to the end of the breakup period.

4.2.4 Evidence for a possible condensation origin for ALH85085 metal

Equilibrium condensation calculations have been performed by Grossman and Olsen (1974) and Wai and Wasson (1977). These models predict the compositional trends that condensing metal will follow. Grossman and Olsen (1974) showed that the metal in CM2 chondrites followed this calculated path.

In the Co vs. Ni diagram (Fig. 3.2.4), the solid line is a condensation path calculated by Grossman and Olsen (1974), based on cosmic Fe, Ni and Co abundances of Cameron (1973). As illustrated in the diagram, the data for Bencubbin metal follows the calculated path. In fact, Bencubbin metal follows the condensation path even closer than

CM chondrites. As temperature decreases the Ni content of the condensing metal also decreases until the cosmic Ni/Fe ratio is reached. The data presented for CR chondrites show that CR metal also follows this trend, but the CR trend line has a slightly different slope. However, Grossman and Olsen (1974) rejected Renazzo metal as a product of equilibrium condensation because of the low values of CR in the metal.

ALH85085 metal is similar to the metal in Bencubbin and CR chondrites, and metal from all three overlap on the Ni-Co diagram (Fig. 3.2.5). Based on these data alone, it is suggested that ALH85085 metal compositions may also be the result of condensation trends in the nebula. In all three cases (ALH85085, Bencubbin and CR chondrites), Ni and Co fall below the cosmic Ni/Fe and Co/Ni ratios. Grossman and Olsen (1974) observed the same problem in CM metal and suggested a disequilibrium condensation in which early formed (high Ni and Co) metal is removed from the system. In this nebular fractionation process, Ni and Co concentrations below the limiting values can be achieved.

Newsom and Drake (1979) also showed that the P-Ni trend in Bencubbin is similar to the P-Ni condensation path of Wai et al. (1977). In general, ALH85085 is similar to Bencubbin in this regard. However, there is some scatter in the data. With regard to Cr, concentrations in ALH85085 are low, as are those in Bencubbin and CR chondrites. However, Grossman and Olsen (1974) showed wide thermodynamic uncertainty in their Cr data.

On the Ni vs. Co diagram, the Si-bearing metal grains (solid squares) follow the same trend as other metal in ALH85085 (Fig. 3.2.5), However, one grain has more P and the other has more Cr than the other metal in ALH85085. (Table 3.2.4). Calculations of Saxena and Benimoff (1977) showed that an FeNi liquid containing Si in solution could condense from a gas of nebular composition, but higher pressure (1.5 atm) is required to condense a liquid containing 2.5 wt.% Si and , in general, higher pressures are needed to condense more Si. One ALH85085 metal grain contains up to 7.5 wt.% Si (Table 3.2.4). It is possible that Si-bearing metal may have condensed at nebular pressures (10^{-3} to 10^{-4})

if the nebula gas was fractionated (Newsom and Drake, 1979). The Si-bearing metal, therefore, may have condensed along with the other metal in ALH85085, but may have resulted from local fluctuations during condensation.

4.2.5 Chondritic vs. non-chondritic origin for ALH85085

Wasson (1988) points out that ALH85085 may not be chondritic in the sense that it may not be a direct product of the solar nebula. The reasons he gives for doubting its nebular origin include: (1) the high Fe/Si ratio (1.6 X CI); (2) the low S/Si ratio (0.03 X CI); (3) the low alkali (Na and K) content; (4) the small chondrule sizes and their rarity; (5) the uniformity of the metal sizes and its even distribution and irregular shapes. He suggested that these features are best explained by impact processes on the surface of a chondritic parent body, and he draws analogies to Bencubbin . Kallemeyn et al. (1978) proposed that Bencubbin major silicates were impact generated on a carbonaceous chondrite planetesimal. However, it is demonstrated below that the Bencubbin silicates are not impact generated, but are more likely chondritic.

The high Fe/Si ratio is obviously a reflection of the high abundance of metal, and no known chondrites contains as much. However, high metal abundance is not reason enough to distinguish chondritic from nonchondritic. The size distribution of the metal in ALH85085 may also reflect size sorting; metal grains do not exceed the other components in this chondrite with respect to size. The even distribution of the metal may be a reflection of efficient mixing processes. Other components, such as matrix lumps and chondrules, also appear to be even distributed. Wasson (1988) also suggests that the other components, such as other chondrule types, CAI fragments, and matrix lumps, may be survivors of the impact-vaporization event. However, the majority of these components are all similar in size to the chondrules. It is unlikely that impact would randomly create chondrule-like spheres which fall within the same size range as the survivors of the event.

Assuming that chondrules form by melting of clumps of dust particles in the nebula, as summarized by Taylor et al. (1983), and that some of these were heated to temperatures above the liquidus (Hewins, 1988), it is possible that some may have been heated enough to result in vaporization and volatile loss (Na, K, and S), and thus impact on a planetary surface is not required. Heating to high temperatures in ALH85085 is evident by the presence of the cryptocrystalline textures of the chondrules. Hewins (1988) determined that cryptocrystalline chondrules require relatively high initial temperatures. Since chondrules with small sizes are also present in other chondritic meteorites (e.g., Piancaldoli), this also indicates that impact is not essential. The majority of lithic fragments in ALH85085 are similar in texture and composition to the chondrules, indicating that larger broken chondrules were present, and the rarity of chondrules may only reflect a high degree of chondrule breakage. If so, chondrules may have been as abundant as in most chondrites, prior to aggregation of ALH85085. Impact is not an efficient chondrule forming process (Taylor et al., 1983) and on this basis it is not favored for the origin of chondrules in ALH85085.

4.3 Bencubbin

4.3.1 Barred Olivine Character of the Bencubbin Host Silicates

As evidenced by the textural, modal and bulk compositional data presented, the host silicate clasts in Bencubbin are equivalent to Type I barred olivine chondrules. The textural term barred olivine is usually reserved for fluid droplet chondrules, but angular fragments having this texture are commonly found in chondrites. Similar olivine morphologies have been observed in terrestrial rocks such as some of those in the Rhum pluton, and in spinifex rocks (Donaldson, 1974; Arndt et al., 1977). In addition, Roedder and Weiblen (1977) observed a barred olivine spherule in a lunar spinel troctolite; they suggested that the spherule is the result of an impact-generated melt globule which solidified in flight. In the

following discussion, two possible origins for the BO-textured host silicate clasts are examined: (1) they are nebular-formed chondrule-like materials, and (2) they are impact-generated melt rocks.

The Bencubbin host silicate clasts are chondritic, as shown by the bulk compositional data of Kallemeyn et al. (1978). These authors showed that the host silicate clasts have chondritic proportions of lithophile elements which are inconsistent with igneous differentiation. The oxygen isotopic composition (Fig. 3) of the Bencubbin host silicates (Clayton and Mayeda, 1978) plot on the CR chondrite mixing line, close to chondrules from Renazzo (Clayton and Mayeda, 1977; Clayton et al., 1984; Clayton and Mayeda, 1989; Weisberg et al., 1989).

Kallemeyn et al. (1978) speculated that the host silicates were produced by impact melting of chondritic material and the resulting magma was injected into the breccia. There is no evidence of flow in the host silicates, or any other textural evidence of impact melt phenomena within these clasts. Newsom and Drake (1979) presented textural evidence which suggests that the host silicates were solid clasts when incorporated into the Bencubbin metal-silicate breccia. This includes the angular shapes of the clasts and intrusion of the breccia cementing agent into the silicate clasts. In addition, injection of molten silicate would result in a rapid density separation from the host metal clasts. Also, the high degree of uniformity of composition of each host silicate clast, in spite of their textural differences, is unlikely to result from an impact melt.

However, it is possible that the host silicate clasts represent broken fragments from a large, homogeneous impact melt pool or flow. The best documented example of similar-textured materials produced by lava flows are observed in komatiites. These are ultramafic, layered lava flows which characteristically contain well-developed spinifex-textured rocks in the middle and upper parts of the flow (Arndt et al., 1977). It is conceivable that an impact event on a chondrite parent body could yield a compositionally homogeneous komatiite-like lava flow and mimic the conditions necessary to form spinifex texture. Host

silicates with feathery microcrystalline and coarse barred olivine textures could represent upper and lower layers, respectively, of such flows. This scenario is unlikely. The uppermost layers of komatiites are typically chilled zones which contain skeletal crystals of olivine in a glassy mesostasis and the lower layers are generally granular in texture. Clasts with these textures are not known in Bencubbin. Also, komatiites are compositionally zoned and this is to be expected in any layered lava flow. Bencubbin host silicates are texturally diverse, but compositionally near-identical. Further, the host silicate compositions indicate an unusual precursor that must have been BO chondrule-like originally. Thus, it seems unnecessarily complicated to remelt BO chondrule-like material in order to reproduce a BO chondrule-like texture. Most BO-like material observed in chondritic meteorites is considered chondritic and is presumed to have formed in the solar nebula, and there is no compelling reason to interpret these clasts in any other way. In summary, I recognize the possibility that the host silicates could be angular fragments from an impact-produced lava flow, but find a nebular origin more reasonable.

Clearly, Bencubbin is an impact-assembled breccia. This is evident from the angularity of its clasts and the glassy matrix which acts as the cementing agent of the breccia (Ramdohr, 1973; Newsom and Drake, 1979). However, this impact event post-dated the formation of the host silicate clasts, as demonstrated by ^{40}Ar-^{39}Ar ages of 3.7 to 4.0 Ga for the glassy matrix and 4.5 Ga for the BO-textured clasts (Kelly and Turner, 1987).

In spite of the evidence that the host silicate clasts in Bencubbin are BO chondrule-like materials, they differ from average BO chondrules (Weisberg, 1987) in some respects. Bencubbin clasts are much larger, are irregular in shape (because they are broken clasts), and lack olivine shells. In addition, they are not associated with other chondritic components (i.e., other chondrule types, matrix material, etc.). Further, the host silicate clasts constitute approximately 40% of the Bencubbin metal-silicate breccia (Simpson and Murray, 1932), and BO chondrules are generally minor (3-4%) components in chondrites

(Gooding and Keil, 1981). However, a droplet-shaped, 5cm chondrule was observed in the Gunlock (L3) chondrite (Prinz et al., 1988), a 4.5 cm, angular chondrule fragment was found in the Parnallee chondrite (Binns, 1967), and BO-textured material (one cm or larger in width) with irregular shapes are sometimes found in chondrites (Weisberg et al., 1988b). Many barred olivine chondrules are irregular in shape and do not have continuous shells of olivine (Weisberg, 1987). If the host silicate clasts were found scattered in a carbonaceous chondrite, they would be regarded as extremely large, broken BO chondrules and would not be considered unusual, except for their abundance.

The host silicate clasts probably formed in the solar nebula under similar conditions to those which have been proposed for BO chondrules (Weisberg, 1987). Taylor et al. (1983) give a comprehensive review of the arguments in favor of chondrule formation in a nebular setting. Conditions of formation include melting of preexisting materials (Grossman et al., 1979; Gooding et al., 1980; Lux et al., 1981; Wood, 1981; Grossman and Wasson, 1981, 1982, 1983) to temperatures at or above the liquidus to produce melts of very few nuclei (Tsuchiyama et al., 1980; Tsuchiyama and Nagahara, 1981; Radomsky et al., 1986), followed by crystallization at rates varying from 10° to 1000°C/hr (Radomsky et al., 1986). Host silicate clasts which exhibit feathery microcrystalline textures undoubtedly cooled at faster rates than those of finely barred clasts and therefore cooled at rates even faster than 1000°C/hr.

One possibility for the large size of the Bencubbin silicate clasts may be that they are due to melt droplet coalescence. Compound chondrules are those which are attached, with one indenting the other, and are believed to be formed by collisions of chondrules in space, while they are still in the plastic state (Gooding and Keil, 1981). In most cases these chondrule pairs have the same composition and texture (McSween, 1977; Gooding and Keil, 1981) suggesting a high density of specific chondrule types in local nebular regions. If these chondrules were still molten when they collided, coalescence into larger melt bodies is possible. Alternatively, high dust:gas ratios and/or higher electrostatic

attraction between particles in the solar nebula may also result in unusually large chondrules. However, all these suggestions are speculative.

4.3.2 Condensation Origin for the FeNi Metal.

Newsom and Drake (1979) presented convincing evidence for a condensation origin for the Bencubbin host FeNi metal. Their strongest argument was that the Ni vs. Co trends of the FeNi metal completely overlapped the calculated condensation paths of Grossman and Olsen (1974). Their calculations predicted that as condensation proceeds, Ni and Co concentrations in the condensing FeNi will decrease until a lower limit (cosmic Ni/Fe) is reached. Weisberg et al. (1988a) showed that FeNi in CR chondrites and the ALH85085 chondrite is compositionally similar to that in Bencubbin and exhibits the same Ni vs. Co trend (Fig. 3.3.2). Thus, they suggested a condensation origin for the FeNi in all three meteorite groups.

The FeNi metal in the ordinary chondrite clast and dark xenolith (see section 3.3.5) is compositionally similar to that in the Bencubbin host metal, the CR chondrites, and the ALH85085 chondrite and can also be interpreted as representing primitive condensed materials. Therefore, the chondrite clasts as well as the host all contain this common primitive metal component. Since Bencubbin host metal has a lower Ni/Fe ratio than metal in the clasts, and the Ni/Fe ratio of condensing FeNi metal decreases with decreasing temperature, the host metal may have condensed at a much lower temperature than that in the clasts. In addition, ALH85085 and CR chondrite FeNi metal may have also condensed at a higher temperature than Bencubbin host metal.

However, there are some problems with the interpretation of this FeNi metal as a nebular condensation product. In all three cases, the FeNi exceeds the theoretical lower (cosmic) limit of Ni/Fe. This situation is possible if non-equilibrium conditions, such as

the removal of early condensed metal from the system (Grossman and Olsen, 1974), are assumed. An additional problem is that the Ni vs. P trends of the ordinary chondrite clast and dark xenolith do not follow the condensation curve as does Bencubbin host metal (Newsom and Drake, 1979) and the CR and ALH85085 chondrites. However, this may be due to movement of P into other phases.

Another problem is that the condensation path is derived via calculations in which ideal conditions are assumed, and the similarity may be fortuitous. Palme and Wlotzka (1976) stress the lack of knowledge concerning activity coefficients of siderophile elements in alloys, and their calculations show that early condensed Ni-rich metal may have high Ni/Co ratios (up to 60) relative to the chondritic ratio (20). It is possible that the Ni-rich metal grains in Bencubbin as well as ALH85085 and CR chondrites are the result of modification by later events in which Fe was depleted, but the Ni/Co ratio was essentially maintained. These events may include nebular oxidation and sulfidation at lower temperatures and may also account for the larger amount of scatter in the Ni-Co trend of the high-Ni metal (Fig. 3.3.2).

Other explanations for the Ni-Co metal trend may include fractional crystallization and shock heating. However, P is anticorrelated with Ni in both Bencubbin metal clasts (Newsom and Drake, 1979) and in ALH85085 metal (Scott, 1988), and in any melting event a positive correlation would be expected between these elements since they are both partitioned into the liquid phase.

The high Si content found in a few of the metal grains in the Bencubbin and ALH85085 meteorites is also not a predicted consequence of equilibrium condensation from a nebular gas. Condensation of Si-rich metal is possible at higher pressure (1.5 atm; Saxena and Benimoff, 1977), or at lower pressures (10^{-3} to 10^{-4} atm) if the solar gas has a fractionated C/O ratio (Newsom and Drake, 1979). Kimura and El Goresy (1989) showed that the Si-bearing metal in ALH85085 is associated with highly reduced phases, such as alabandite and osbornite, common to enstatite chondrites, but this is a minor component

and it is possible that it is the result of contamination by impact. However, the minor Si-rich grains in Bencubbin (Newsom and Drake, 1979) and in ALH85085 (Weisberg, 1988a) exhibit the same chemical trends as the major metal components, suggesting that they are related and share a common origin.

It is therefore concluded that the origin of the FeNi metal in the Bencubbin host, as well as the ordinary chondrite clast and dark xenolith, and the CR and ALH85085 chondrites may be the result of non-equilibrium nebular condensation processes and possibly modified by later oxidation and sulfidation events.

4.3.3 The Origin of the Bencubbin Breccia

In the previous sections possible origins for the individual components in Bencubbin were discussed. Two scenarios are now presented for the origin of the entire breccia. One scenario assumes that the Bencubbin components are chondritic, were produced by nebular processes, and were later modified by brecciation and reorganization, with minor impact melting. The other scenario assumes that Bencubbin components were produced by massive impact melting of previously chondritic material of an unspecified type.

Chondritic origin: In this scenario, the BO-textured host silicates formed as free floating molten objects in the solar nebula. The unusually large size of these objects may be due to melt-droplet coalescence and/or high dust:gas ratios, as suggested above. The Bencubbin chondrite may be highly enriched in FeNi metal because its agglomeration took place early in the history of the nebula, prior to major metal-silicate fractionation. Metal-rich chondrites consisting mainly of one chondrule type are already known to exist. A prime example is ALH85085 which consists mainly of one chondrule type (cryptocrystalline) and contains twice the amount of metal found in any other chondrite type. Most investigators argue that its major characteristics are the result of nebular processes (Grossman et al., 1988; Scott, 1988; Weisberg et al., 1988a). In addition, Rubin et al. (1982) described a

chondritic clast, in Piancaldoli (LL3) which consists only of microchondrules of one textural type. These microchondrules are orders of magnitude smaller than most chondrules. Chondrules much larger than typical mm-sized chondrules (macrochondrules) have also been recognized (Binns, 1967; Weisberg et al., 1988a; Prinz et al., 1988). Thus, the existence of a chondrite which is relatively enriched in metal, containing unusually large chondrules which are mainly of one type (barred olivine to cryptocrystalline) is a reasonable possibility.

This proposed BO/metal-rich chondrite was later disaggregated and reassembled by an impact event(s) on a parent body, with relatively minor impact melting. The minor impact melts which were generated bind the silicate and metal clasts together. The impact melt material dated at ~4.0 Ga, based on the ^{40}Ar-^{39}Ar (Kelly and Turner, 1987), was formed ~0.5Gy after the formation of the chondritic components and resulted in a monomict chondrite breccia.

There are some serious arguments against this scenario. One is the interpretation of the host silicates as BO chondrule-like objects because of their large size and lack of rounded surfaces. Another drawback is that the Bencubbin breccia does not contain any of the other components typically associated with chondrites (i.e., porphyritic chondrules, matrix, etc.). In addition, chondrites which resemble the pre-brecciated Bencubbin are not known. Finally, this scenario calls for highly unusual nebular conditions in comparison to other known chondritic meteorite groups.

Impact origin: In this scenario, the BO-textured host silicates resulted from an impact induced lava flow in the regolith of a chondritic parent body of unknown type. This flow crystallized as texturally layered olivine spinifex rocks texturally similar to those in terrestrial komatiites. Post-crystallization fragmentation by further impacts resulted in the mechanical mixing of angular host silicate fragments with the host metal component which was present in the parent body regolith. Concentration of metal in the parent body regolith came about through shock mobilization and separation of metal as proposed for the

formation of the "nonmagmatic" iron meteorites (Wasson, 1985). The anomalously high $\delta^{15}N$ values of Bencubbin (Prombo and Clayton, 1985; Franchi et al., 1986) may be attributed to extensive fractionation as a result of vaporization and recondensation.

Arguments against the Bencubbin host silicates as impact-generated komatiite-like flows were presented above. In addition, komatiite-like flows are not commonly associated with impact events. An impact hypothesis would call for an unusual target material, an unknown chondritic type with the bulk composition of barred olivine chondrules. Furthermore, relicts of this precursor material, or its the regolith, might be expected to occur as xenoliths within the host silicate clasts and these are not found. The argument that metal enrichment in Bencubbin is due to the impact process is not persuasive. This is not found in other impact-brecciated chondrites. In addition, the metal is not homogeneous in composition (as in IAB iron meteorites) but varies from clast to clast in a systematic trend. Wasson (1988) has proposed that the metal-rich ALH85085 chondrite is also impact-produced and is subchondritic rather than chondritic. He suggests the metal (as well as the silicates) are the result of impact melting, vaporization and recondensation. But the presence of calcium-aluminum-rich inclusions (CAI) and chondritic matrix argue against the impact hypothesis for the metal-rich chondrite, as shown by Grossman et al. (1988), Scott (1988) and Weisberg et al. (1988).

Grady and Pillinger (1990) also rejected vaporization and recondensation as a means of enriching the ALH85085 chondrite in ^{15}N since it would require removal of >99.99% of the initial nitrogen reservoir and would imply that the initial N concentration was greater than in any known meteorite. This argument can also be made for the nitrogen anomaly in Bencubbin. As a result, Grady and Pillinger (1990) proposed that the nitrogen isotopic composition of Bencubbin may have been introduced by the impactor. However, I find that this too is unlikely since the impactor would need levels of ^{15}N greater than in any known meteorite in order to result in the $\delta^{15}N$ values of Bencubbin. It is therefore argued that the nitrogen isotopic composition was an inherent part of the Bencubbin pre-brecciation

chondrite and probably could not have survived impact melting, vaporization and recondensation.

Both scenarios have difficulties and the evidence in support of each is inconclusive. However, a brecciated chondritic origin for Bencubbin appears to be more likely. The nebular scenario encounters difficulties because of our limited understanding of nebular processes which are based on limited sampling of primitive chondritic materials. The impact scenario has difficulties because of our limited understanding of all the dimensions of impact processes and lack of good analogues.

4.3.4 Relationship of Bencubbin to CR Chondrites and ALH85085

Since a chondritic origin for the Bencubbin breccia is proposed, its relationship to other chondritic groups should be explored. Below data which suggest that Bencubbin is closely related to CR chondrites (specifically Type I chondrules) and the unique ALH85085 chondrite are discussed. Kallemeyn et al. (1978) showed that when the host silicates are normalized to CM chondrites, low volatility and non-volatile elements scatter about unity suggesting that the host silicates may be related to CI-CM-CO chondrites. The possible relationship of Bencubbin to Renazzo and Al Rais (CR chondrites) was first suggested by Prombo and Clayton (1985), on the basis of nitrogen isotopic data. It was later suggested (Weisberg et al., 1988a) that this relationship extend to include the ALH85085 chondrite.

Clearly, there are many differences between the Bencubbin breccia, CR chondrites and the ALH85085 chondrite. Bencubbin contains about 60% FeNi metal and the remaining silicates are cm-sized BO-textured host silicates. CR chondrites contain mm-sized, mainly porphyritic, chondrules and fragments embedded in an opaque matrix containing hydrous phases. ALH85085 contains sparse microchondrules (most <100μm), and abundant mineral and lithic fragments which are mainly glassy to cryptocrystalline (Grossman et al., 1988; Scott, 1988; Weisberg et al., 1988a). It has also been shown that

ALH85085 contains components from enstatite, ordinary and carbonaceous chondrite reservoirs (Kimura and El Goresy, 1989). However, I compare Bencubbin to the major carbonaceous chondrite components of ALH85085 and not the minor enstatite and ordinary chondrite components. Even when the Bencubbin breccia is compared to the anhydrous Mg-rich silicate components in CR chondrites and the carbonaceous chondritic components in ALH85085, there are still marked differences in petrography, but the nebular histories have strong similarities.

The compositions of the mafic silicates in the Bencubbin host silicate clasts, CR chondrules (Type I) and the ALH85085 silicates are all highly magnesian (Table 3) and have low Fe/Mg bulk ratios, suggesting that all of them formed in a similar highly reducing environment. Concentrations of TiO_2, Al_2O_3 and Cr_2O_3 are also similar, as is the commonality of having low volatiles (Na_2O and K_2O) (Table 4). The enrichments in refractory lithophiles, and depletions in volatiles, indicates that all three meteorite groups experienced similar volatile depletion events, or they all initially accumulated earlier condensed higher temperature components.

Although the abundance of FeNi metal in Bencubbin (60 vol.%) is much greater than that in the CR (up to 10%) or ALH85085 (up to 20%) chondrites (Grossman et al., 1988; Scott, 1988; Weisberg et al., 1988a,89), metal abundance in all three groups is high relative to other chondrites. Additionally, the close compositional similarity between the FeNi metal in the Bencubbin host, the CR chondrites, and the ALH85085 chondrite lend strong support to a genetic link between these three meteorite groups. The Ni vs. Co trend in the metal of these meteorites is not observed in any other chondrite group.

Bencubbin, ALH85085 and CR chondrites all have remarkably high $^{15}N/^{14}N$ ratios ($\delta^{15}N$ values are ~1000, 1500, and 190‰, respectively) (Prombo and Clayton, 1985; Franchi et al., 1986; Keeling et al., 1987; Grady and Pillinger, 1989, 1990). Most meteorites have $\delta^{15}N$ which range from -90 to +50‰. The ^{15}N-rich components in Bencubbin are in the host FeNi metal and silicate, but it is not clear which components are

the carriers of the heavy nitrogen in the other meteorites. However, based on the combustion temperatures of nitrogen, and the solubilities of its host phases, the carrier phases of the heavy nitrogen in Bencubbin may differ from those in ALH85085 and the CR chondrites (Grady and Pillinger, 1990)

Although it is not yet clear as to whether the heavy nitrogen resides in the same components in Bencubbin, ALH85085 or CR chondrites, it is suggested that since the high $\delta^{15}N$ values appear to be nebular effects, all three meteorites may be related to a single ^{15}N-rich reservoir. Alternatively, the anomalously high concentrations of ^{15}N in Bencubbin, ALH85085 and the CR chondrites may also reflect primordial heterogeneity which resulted from stellar nucleosynthesis and these three groups may contain especially primitive, relatively unaltered components which escaped homogenization in the nebula (Franchi et al., 1986; Prombo and Clayton, 1985; Grady and Pillinger, 1989, 1990). In addition, in Bencubbin, the ^{15}N is located in the host silicates as well as in the FeNi metal (Prombo and Clayton, 1985; Grady and Pillinger, 1989), and this is another indication that the BO-textured silicates may be primitive nebular materials and not impact melts.

Oxygen isotopic data also support the proposed relationship. On an oxygen 3-isotope diagram Bencubbin host and the ALH85085 chondrite plot within the field of the CR chondrites, at the ^{16}O-enriched end (Clayton and Mayeda, 1977, 1989; Weisberg et al., 1989) (Fig. 3).

Bencubbin, ALH85085 and the CR chondrites all are highly primitive chondritic meteorites which contain major components that are closely related. They appear to have formed in similar oxygen isotope reservoirs and all contain primitive components enriched in heavy nitrogen. In addition, all three meteorite groups have similar FeNi metal which appears to record a nebular condensation trend. Thus, it is suggested that Bencubbin originally formed in the CR region of the nebula and is part of a chondritic clan which includes the CR chondrites and the unique ALH85085 chondrite. Differences in the

petrographic characteristics of these meteorite types may be due to local heterogenities and/or differences in their time of agglomeration.

4.4 Carlisle Lakes-Type Chondrites

4.4.1 Evidence for Nebular Oxidation

The zoning patterns of the mafic silicates described in this study are not those expected from crystallization of a melt droplet chondrule, and appear to be post-chondrule and fragment formation. Melt droplet crystallization cannot produce zoning along fine fractures or lamellar zoning in pyroxene. Further, the zoning would be expected to be relatively evenly distributed on all exposed surfaces of a crystal and this is not the case for some of the olivine. These crystals appear to be the result of diffusive transfer via a medium which preferentially utilizes existing pathways, such as fractures, fissures, and twin planes.

I explore two scenarios for the origin of the zoning in the Carlisle Lakes-type chondrites: (1) *Parent Body Thermal Metamorphism* . Solid-solid diffusion between the coarse-grained Mg-rich chondrules and the fine-grained Fe-rich matrix on a parent body, and (2) *Nebular Gas Reactions/Condensation.* Solid-gas exchange between Mg-rich chondrules and a nebular gas with a high oxygen fugacity. This may be accompanied by growth (condensation) of new olivine from this gas utilizing existing olivine as nucleation sites.

(1) *Planetary Thermal Metamorphism* . Study of the ordinary chondrites has led to a classification of these meteorites into various petrologic grades. Petrologic types 3-6 represent an increasing degree of textural recrystallization, as well as compositional homogenization of mineral phases (see Van Schmus and Wood, 1967). Thermal metamorphism on an asteroidal body has become widely accepted as the process responsible for the textural and mineralogical variations among the various petrologic grades of ordinary chondrites (e.g., Dodd and Van Schmus, 1967; Dodd, 1969) and the

C4-6 carbonaceous chondrites (Scott and Taylor, 1985). Therefore, the observation of post-crystallization fayalitic rims on olivine in type 3 chondrites leads to the conclusion that ion exchange occurred between the Mg-rich chondrules and the Fe-rich matrix as a result of metamorphic equilibration. In a recent study, McCoy et al. (1989) supported this hypothesis by showing that the major and minor element composition of rims on olivine in unequilibrated LL3 chondrites approached that of an equilibrated LL4 and considered this to be evidence of progressive metamorphism on a parent body asteroid.

Tsuchiyama et al. (1988) studied low-Ca pyroxene in ordinary chondrites and found that zoned pyroxene was common in 3.5<types<4 and rare in type<3.5 and type≥4. They suggested that zoning was the result of thermal metamorphism, and that pyroxene zoning is absent in lower metamorphic grades because of the sluggishness of diffusion in pyroxene and is absent in higher grades because equilibration has gone to completion. Aside from the above mentioned studies, documentation of zoning in ordinary chondrites is sparse in the meteorite literature.

Studies of zoning in carbonaceous chondrites have been restricted mainly to Allende (CV3). Housley and Cirlin (1983) studied Fe-enrichment on grain boundaries and in internal cracks of Mg-rich olivine in Allende and observed intergrowths of clinoenstatite and fayalitic olivine. They concluded that Fe-enrichment is the result of chondrite-matrix-FeNi interaction and is controlled by the reaction :

$$Fe + 1/2O_2 + MgSiO_3 \rightarrow (Fe,Mg)_2SiO_4.$$

They abandoned the possibility of this reaction taking place in a nebular gas since the fayalitic olivine that they observed would only become stable below 500K and, at this temperature, reaction rates are slow and gaseous transport would be limited. Thus, they suggested a model in which these reactions occurred on a small internally heated planetesimal to produce the Fe-rich zones on magnesian chondrule olivine as well as the

Fe-rich matrix olivine. However, their arguments against Fe-enrichment in a nebular environment have been challenged by Palme and Fegley (1990) who demonstrated that fayalite could form at 1200°C if a nebular environment became more oxidizing as a result of higher H_2O/H_2.

Recent studies of zoning in Allende (CV3) olivine have demonstrated that parent body metamorphism is not a viable hypothesis to explain the formation of this zoning (Peck and Wood, 1987; Hua et al., 1988; Weinbruch et al., 1990; Palme and Fegley, 1990). All of these studies point out petrographic features which cannot be explained by parent body processes. For example: (1) Zoning is not uniformly distributed about the outer surfaces of crystals and, in some cases, is absent along broken surfaces. Thus, zoning could not have originated via parent-body metamorphism. (2) The minor elements Cr, Al and Ti are enriched in rims relative to matrix and olivine cores and, therefore profiles are not smooth as would be expected from matrix to olivine diffusion. (3) Diffusion profiles of Fe and Mg of zoned crystals are also not smooth.

For the ferrous zoning of olivine in the chondrules of the Carlisle Lakes-type chondrites, in situ solid-solid matrix-chondrule reactions, as a result of parent-body metamorphism, can be ruled out for similar reasons. If zoning were the result of chondrule-matrix reactions, the fayalitic rims should be compositionally intermediate between the Fe-rich matrix olivine and the Mg-rich olivine cores. Instead, compositions of the olivine rims are more Fe-rich than the host matrix (Fa_{38}) and the core olivine, and are as high as Fa_{45}. McCoy et al. (1991) show that, in ordinary chondrites, the rims of the zoned olivine grains have compositions that approach the equilibrium composition of the whole chondrite, as expected for, in situ, chondrule-matrix metamorphic exchange reactions.

The absence of zoning on broken surfaces of some zoned olivine supplies additional evidence against in situ metamorphic equilibration as the origin of the zoning. An olivine grain embedded in a matrix with which it is equilibrating would be expected to

show approximately even zoning on all surfaces. Some olivine mineral fragments are zoned to Fa_{45} on some surfaces and broken surfaces have compositions equal to that of the core of the grain. These olivines must have been zoned prior to their breakage and incorporation into the host chondrite.

It is possible that the chondrules with rims of Fa_{45} equilibrated with another asteroidal environment prior to incorporation into the host. Scott et al. (1985) observed unequilibrated chondrules and mineral fragments in equilibrated ordinary chondrites and suggested that these "aberrant" grains were incorporated into the host chondrite after it had reached its peak metamorphic temperatures, and the ordinary chondrites may have experienced post-metamorphic lithification. Thus, chondrites may contain components which experienced various metamorphic histories. Since ALH85151 and Y75302 are both breccias this hypothesis should be considered. However, none of the chondrules or fragments studied show any evidence of prior matrix material clinging to their outer surface. It is difficult to believe that a chondrule or fragment could be dislodged entirely free of its prior host chondrite. It is of course possible that these chondrules and fragments were metamorphosed in a loosely bound, poorly sintered matrix and thus could be easily dislodged and free of its prior matrix material

More critical arguments can be made against a parent body metamorphism hypothesis for the zoned olivine and pyroxene in the Carlisle Lakes-type chondrites. Most of the zoned olivines have rims of Fa_{45}, suggesting a uniform process. This would require an unusual parent body in which there were at least two environments, one in which the equilibrated olivine composition was Fa_{38} and another which was considerably more FeO-rich. The occurrences of olivine-filled veins in zoned pyroxene suggests the presence of a fluid. Models of parent body metamorphism usually envisage a dry environment in which liquids were driven off prior to or during metamorphic heating, and there is no direct evidence of water on the Carlisle Lakes-type chondritic parent body. A gaseous fluid is possible in an ordinary chondrite environment, but the absence of olivine-

filled veins in zoned pyroxene in ordinary chondrites (Tsuchiyama et al., 1988) suggests that this is not the operative process.

The observations of Tsuchiyama et al. (1988) indicate that in types 3.5-4.0 ordinary chondrites, pyroxene exhibits strong Fe-Mg zoning, texturally similar to the patchy pyroxene in the Carlisle Lakes-type chondrites, and olivine is homogeneous. In the Carlisle Lakes-type chondrites, heterogeneous olivine coexists with zoned pyroxene. For example, zoning of olivine and pyroxene occurs in the same chondrule in A85-20 in ALH85151 and CL-1 in Carlisle Lakes. This should not occur if it is due to thermal metamorphism, because of differing diffusion rates for olivine and pyroxene.

Oscillatory zoning, as observed in the A85-14 chondrule in ALH85151, cannot be explained by parent body metamorphism since a change of conditions is not conceivable on an asteroidal body. Jones (1990) described oscillatory zoning in olivine in type II chondrules from Semarkona. She suggested that the fayalitic core was the result of supercooling of a molten chondrule and was overgrown by normally zoned olivine. I find this an unlikely scenario for the oscillatory zoning found in ALH85151. The Mg-rich layer not only forms a rim around the fayalitic core, but also infiltrates fine fractures throughout the crystal (fig. 1d). This suggests that the Mg-rich layer as well as the Fe-rich outer rind of this olivine are the result of post crystallization diffusion.

If the oscillatory zoning were the result of parent body metamorphism, this chondrule would have had to experience three different environments. The first would be one in which the forsteritic layer was deposited, either by Fe-Mg exchange or reducing conditions. This would be followed by an environment in which the Fe-rich rim (Fa_{45}) was deposited, either by Fe-Mg exchange or oxidation reactions. Lastly, this chondrule was incorporated into the Carlisle Lakes chondrites in which the matrix is equilibrated at Fa_{38}, the same composition of the cores of the oscillatory zoned olivines. I find this to be an unlikely scenario. A preferable hypothesis would be that the Mg-rich layer of this chondrule is the result of Fe-Mg exchange or reduction in the nebular and the Fe-rich layer

is the result of metamorphic equilibration (parent body) superimposed upon it. In this latter scenario, the similarity in composition of the cores of these olivines to that of the matrix would have to be interpreted as being fortuitous.

In summary, I acknowledge that the zoning in the Carlisle Lakes-type chondrites could be explained by a unique, complex parent body metamorphism model in which the zoned grains may be from less equilibrated local regions of the parent body. The Carlisle Lakes-type chondrites may have been metamorphosed as a poorly consolidated aggregate and subsequently brecciated and reassembled following their metamorphic equilibration. However, the complexities and problems presented by this scenario lead us to explore a nebular hypothesis as an alternative.

(2) Nebular Gas Reactions/Condensation. I now examine a nebular scenario to explain the zoned olivine in the Carlisle Lakes-type chondrites. A model which involves nebular gas-solid exchange, and the condensation of vapors along grain boundaries and in fractures, as described by Peck and Wood (1987), Hua et al. (1988), Weinbruch et al., (1990), and Palme and Fegley (1990) could explain the observed zoning patterns in olivine as well as in pyroxene. Peck and Wood (1987) proposed the exchange of nebular gases with forsteritic olivine followed by condensation of fayalitic olivine to explain the zoning in the Allende CV3 chondrite. Hua et al. (1988) suggested that the fayalitic rims on forsterite crystals in Allende formed by condensation of solar nebular gas. Weinbruch et al. (1990) also suggested that the fayalite rims on Allende olivine formed by condensation of nebular gas and utilized the model of Palme and Fegley (1990) to explain condensation of fayalitic olivine under high oxygen fugacity and temperatures of about 1400K.

For the Carlisle Lakes-type chondrites I propose that hot nebular vapors attacked olivine surfaces and infiltrated into existing fractures of olivine grains with the result that fayalitic olivine condensed from this vapor onto these surfaces. In addition, forsteritic olivine reacted with these vapors and formed fayalitic olivine. In the case of pyroxene, these gases utilized fractures and twin planes to enter the grains and react with enstatitic

pyroxene to produce ferrosilitic pyroxene, resulting in the lamellar-type zoning. In addition to these vapor-solid reactions, surfaces of the existing olivine and pyroxene may have acted as nucleation sites for new olivine to condense from these nebular vapors.

In most of the zoned olivine studied, MnO increases with an increase in FeO in the zoned crystals. This is an expected consequence of olivine condensing from a nebular gas with a relatively higher oxygen fugacity (Weinbruch et al., 1990). In one of the chondrules (A85-13), in ALH85151, the zoned olivine shows a decrease in MnO as FeO increases along the rim (Fig. 2b). Weinbruch et al. (1990) found this to be the case in some of the zoned olivine in Allende. They suggested that this is the result of oxidation of existing metal or sulfide. This particular chondrule in ALH85151 is rimmed by sulfide which also occurs as spheres and fracture fillings in the olivine. Thus, oxidation of preexisting metal and/or sulfide may explain the zoning pattern in this chondrule.

Oscillatory zoning (Fig. 1d and 2c) is difficult to explain in any scenario. The Fa value of the olivine rim in this chondrule and the increase in Cr_2O_3 at the rim also suggest that the rim equilibrated with a similar environment to that in which the olivine rims on the other zoned olivine in ALH85151 formed. I can only speculate that there were local heterogeneities in the H_2O/H_2 ratio within this nebular environment which resulted in the deposition of a forsteritic layer onto the fayalitic olivine. This chondrule was later exposed to a higher oxygen fugacity at which point fayalitic olivine again began to condense.

I recognize that there are problems in applying a nebular model, such as that presented by Palme and Fegley (1990), to explain the zoned olivine and pyroxene in the Carlisle Lakes-type chondrites. For example: there may be a problem of volatile loss at high temperatures in the nebula, the exact mechanism for producing oxidizing conditions in the nebula is not known, and there may be problems with the kinetics of Fe-Mg exchange in the nebula. However, there are now many examples of chondritic materials having characteristics that are believed to be the result of oxidizing conditions in the nebula. As mentioned above, the ferrous zoning on Allende olivine has been considered to be the result

of Fe-Mg exchange and condensation of fayalitic olivine in an oxidizing nebula (Peck and Wood, 1987; Hua et al., 1988; Weinbruch et al., 1990). In addition, Mo and W depletions in metal from Ca-Al-rich inclusions in carbonaceous chondrites have been attributed to condensation of refractory-rich metal from an oxidized nebular gas (Fegley and Palme, 1984; 1985). Also, the FeO contents in CAI have been attributed to condensation under oxidizing conditions (Kornacki and Wood, 1985).

In summary, it is recognized that there are many problems associated with the nebular hypothesis. However, there is growing support for nebular reactions taking place at relatively high oxygen fugacities and high temperatures, and this provides a more favorable way to explain all the features of the zoned minerals in the Carlisle Lakes-type chondrites. FeO zoning in olivine and pyroxene may have formed by Fe-Mg exchange reactions between chondrules and a hot oxidizing nebular gas. Some zoning developed by oxidation of preexisting metal and sulfide. Olivine on grain edges and along fractures may be the result of condensation of new olivine under oxidizing conditions in the nebula.

4.4.2 Formation of the Cr-Rich Zones

The high Cr-rich spots in the outer fayalitic layers of the zoned olivine appear to be chromite which crystallized into pore spaces. These chromites may have formed by: (1) melt droplet crystallization, such as described in Semarkona type II chondrules (Jones, 1990), (2) diffusional processes, as described in the fayalitic rims on Allende olivine (Weinbruch et al., 1990), or (3) condensation from a nebular gas with greater than solar oxygen fugacity (Weinbruch et al., 1990). I again rule out crystallization from a melt droplet because these chromites are never euhedral, as are those typically observed in type II chondrules which are considered to be of igneous origin. Type II chondrules also contain euhedral olivine in the mesostasis and none are found in the ALH85151 chondrule mesostasis. Additionally, since the fayalitic rims which surround these chromites do not

appear to be the result of crystallization from a melt droplet, it is unlikely that the chromites are.

I find it difficult to distinguish between diffusional processes and nebular vapor condensation for the origin of these chromites. However, I suggest that the Ca-rich phase (Ca pyroxene), associated with the chromite appears to be the result of diffusional processes. Some of the olivine zoning profiles show a depletion in Ca from core to rim (e.g., Fig. 2a). Thus, the chromites may have also formed by diffusion of Cr from the core of the olivine to the fayalitic rim, and chromite may have exsolved from the olivine when the appropriate oxidation conditions and temperatures were reached.

4.4.3 Relationship to Ordinary Chondrites

The petrologic characteristics of the Carlisle Lakes-type chondrites are most similar to those of the ordinary chondrites, except for being more oxidized, and their oxygen isotopic compositions differ. Rubin and Kallemeyn (1989) point out that the chondrule sizes, distribution of chondrule types, and the occurrence of recrystallized matrix in these meteorites parallels those of the ordinary chondrites. They also note that lithophile elements are within the ordinary chondrite range and siderophile element abundances are intermediate between H and L chondrites. Gold is the only element which is not OC-like being anomalously low.

The equilibrated ordinary chondrites represent a sequence of increasing degree of oxidation from H to L to LL, as determined by their mineralogy. From H to LL, the modal abundances of olivine increases, and those of pyroxene and FeNi metal decrease. FeO content in the silicate phases increases, as do Ni and Co contents of the FeNi metal. In comparison with the LL chondrites, the Carlisle Lakes-type chondrites are more oxidized, contain more olivine, less pyroxene and have essentially no FeNi metal. Olivine in this group is more fayalitic (Fa_{38}), the major metal, when present, is awaruite (64% Ni, 2% Co), and the sulfides are pyrrhotite and pentlandite. Rubin and Kallemeyn (1989) rejected

the possibility that these meteorites are highly oxidized ordinary chondrites because some of their chemical characteristics do not follow the H-L-LL sequence. Siderophile elements are not lower than in LL chondrites, and their oxygen isotopic compositions have higher $\Delta^{17}O$ values and thus, do not fall on the same trend line as the equilibrated ordinary chondrites.

I propose that the Carlisle Lakes-type chondrites formed from an H or L chondrite-like precursor, but oxygen isotopically distinct. Their siderophile abundances suggest that the parental material may have experienced the same degree of metal/silicate fractionation as the H or L chondrites. As a result of oxidation the siderophiles must have been redistributed and transferred to the sulfides. The oxygen isotope data suggest that the chondrules from ALH85151 formed from a different population than those from the ordinary chondrites. The large chondrule (CL-1) from Carlisle Lakes may be a relict of a type 3 ordinary chondrite precursor in that its oxygen isotopic composition falls within the field of the ordinary chondrites. However, this argument for a link to the ordinary chondrites is weak because CL-1 represents only one datum point and this chondrule is atypical in other respects. The high matrix abundance of the Carlisle Lakes-type chondrites is uncharacteristic of ordinary chondrites, but this may be an overestimate. If these meteorites experienced extended comminution in a regolith, their chondrules may eventually have come to superficially resemble fine-grained chondrite matrix material. The latter hypothesis is supported by the brecciated appearance of ALH85151 and Y75302 and can be tested further by measurement of solar noble gas abundances.

The Carlisle Lakes-type chondrites are unusual in that the matrix is recrystallized and most of the olivine is equilibrated at Fa_{38}, and yet some olivine grains in chondrules and fragments are zoned to Fa_{45}. The occurrence of these zoned grains in a host that is mainly equilibrated suggests that the equilibration of the Carlisle Lakes-type chondrites must have occurred prior to final lithification. In addition, some of the zoned crystals have cores that are in equilibrium with the host matrix. If, as I suggest, the zoning is the result

of processes in an oxidizing nebula, equilibration of the host may have also been a nebular event.

5. CONCLUSIONS

Petrologic and geochemical properties of several ungrouped chondrites have been examined in order to determine the relationship of these meteorites to existing chondrite groups and if their unusual characteristics are the results of nebular or planetesimal processes. The conclusions of this study are numbered below:

1. New Types of Chondrites.

a. Renazzo, Al Rais, MAC87320, Y790112, Y793495, and EET87770 have a similar set of petrologic and chemical characteristics that are unique to these chondrites and they should be classified as a new chondrite group-the CR group. Preliminary study of the El Djuof meteorite suggests that it is the seventh member of the CR group. The CR group represents a new location in the solar nebula (having a set of conditions unique to that location) and they all accreted onto the same (CR) parent body. These meteorites are breccias and differences in their bulk chemical compositions (i.e., volatile lithophiles) may be explained by differences in their matrix/chondrule ratios and sampling problems.

b. ALH85085 is a chondrite having a unique set of characteristics. Its characteristics can be interpreted as a result of nebular processes and thus this meteorite is considered to be a primitive chondrite. However, since there is only one of these chondrites at present, it is better left as an unclassified chondrite. Based on the composition of its FeNi metal and oxygen isotopic composition it is closely related to the CR chondrites, either in time or location in the nebula. This relationship is further supported by nitrogen isotopic data reported by Grady and Pillinger (1989, 90).

c. The Bencubbin metal-silicate breccia is one of the most perplexing meteorites, and has previously been relegated to that of an anomalous sample. The discovery of unusually high $^{15}N/^{14}N$ ratios in components of the host silicate and metal portions (Prombo and Clayton, 1985; Franchi et al., 1986; Keeling and Marti, 1987) has raised the level of its importance, and indicates that it contains primitive nebular or prenebular components which are preserved. The metal and silicates also have unusual petrologic and chemical characteristics. Bencubbin appears to be chondritic, in spite of its non-chondritic petrographic characteristics. The host silicates are barred olivine chondrule-like material and the host metal is most likely the product of nebular condensation, as originally suggested by Newsom and Drake (1979).

Based on the nitrogen and oxygen isotopic data, Prombo and Clayton (1985) suggested that Bencubbin may be related to Renazzo, and it is suggested that the unique ALH85085 chondrite may also be part of this relationship. Although these meteorites have many grossly different petrographic features, their major silicate and metal components have highly similar chemical and isotopic characteristics which suggest they may be related.

d. The Carlisle Lakes-type chondrites (Carlisle Lakes, ALH85151, and Y79302) should be classified as a new chondrite grouplet. Carlisle Lakes-type chondrites may be related to ordinary chondrites and formed originally from an ordinary chondrite-like precursor, but are oxygen isotopically distinct.

2. Primitive (Nebular) Processes.

a. Many properties of the CR chondrites can be attributed to primary nebular processes. The FeNi metal in the CR group (as well as that in ALH85085 and

Bencubbin) records a relict, primitive nebular condensation trend. Many of the refractory-rich inclusions may be primary nebular condensates or their altered products.

b. The narrow range in size of the components in ALH85085 is indicative of size-sorting processes, in the nebula, possibly as a result of aerodynamic drag during parent body accretion. This may also explain why chondrules in each chondrite group have a size range characteristic of that group.

c. The occurrence of matrix lumps (DI) in ALH85085 and in CR chondrites suggests that some matrix was originally partly to completely lithified material that may have been later disaggregated to form the ("matrix") material interstitial to chondrules. However, this does not preclude the fact that some matrix also coated chondrules while still in the nebular, prior to or during formation of the parent body.

d. Zoning of olivine in some of the chondrules and fragments in these chondrites cannot be the result of crystallization from a melt droplet and thermal metamorphism on a parent body is also an unlikely mechanism. Zoning may be the result of Fe-Mg exchange between the forsteritic olivine cores and hot nebular vapors. This was accompanied by condensation of fayalitic olivine from the hot nebular gas onto the outer surfaces and internal fractures of preexisting forsteritic olivine. The fayalitic olivine may have condensed from the nebular gas at temperatures in the range of 1400K, if the gas had an H_2O/H_2 ratio greater than solar.

Most of the zoned olivine grains in the Carlisle Lakes-type chondrites have a positive correlation of Fa vs. MnO, but some have a negative correlation. The latter may have resulted from oxidation of preexisting FeNi and/or Fe-sulfide upon contact with an oxidizing nebular gas.

Zoning in pyroxene in the Carlisle Lakes-type chondrites may be the result of solid-gas exchange in the same oxidizing nebular environment. Nebular vapors utilized preexisting fractures and twin planes to infiltrate pyroxene crystals, producing lamellar-type zoning.

e. Two oxidation events are recorded in the Carlisle Lakes-type chondrites. One major event is that in which most of the chondrule and matrix olivine grains were equilibrated at Fa_{38}. The other event was more oxidizing and resulted in zoned olivine and pyroxene, with olivine rims having compositions up to Fa_{45}. This latter event may be representative of local heterogeneities of H_2O/H_2 in this region of the nebula.

3. Secondary (Parent Body) Processes.

a. Some of the properties of the CR chondrites can be attributed to planetesimal processes. Brecciation and aqueous alteration probably occurred in a planetesimal regolith. Petrographic evidence strongly suggests that aqueous alteration occurred prior to lithification of the CR chondrites.

b. The Bencubbin chondrite was brecciated and experienced minor impact melting following its formation and the present Bencubbin may be considered a monomict chondrite breccia.

6. REFERENCES

Afiattalab F. and Wasson J.T. (1980) Composition of the metal phases in ordinary chondrites: implications regarding classification and metamorphism. Geochim. Cosmochim. Acta 44, 431-446.

Armstrong J.T., Meeker G.P., Huneke, and Wasserburg G.J. (1982) The Blue Angel: I. The mineralogy and petrogenesis of a hibonite inclusion from the Murchison meteorite. Geochim. Cosmochim. Acta 46, 575-595.

Arndt N.T., Naldrett A.J. and Pyke D.R. (1977) Komatiite and iron-rich tholeiitic lavas of Munro Township, Northeast Ontario. J. Petrol. 18, 319-369.

Barber D.J. (1987) An ATEM investigation of a "carbonaceous chondrite" clast in the Bencubbin stony-iron breccia. Meteoritics 22, 321-322.

Binns, R.A. (1967) An exceptionally large chondrules in the parnallee meteorite. Min. Mag. 36, 319-324.

Binns R.A. and Pooley G.D. (1979) Carlisle Lakes (a): A unique oxidized chondrite (abstract). Meteoritics 14, 349-350.

Bischoff A. and Keil K. (1984) Al-rich objects in ordinary chondrites: related origin of carbonaceous and ordinary chondrites and their constituents. Geochim. Cosmochim. Acta 48, 693-709.

Bunch T.E. and Chang S. (1980) Carbonaceous chondrites-II: Carbonaceous chondrite (CM) phyllosilicates and light element geochemistry as indicators of parentbody processes and surface conditions. Geochim. Cosmochim. Acta 44, 1543-1577.

Cameron A.G.W. (1973) Abundances of the elements in the solar system. Space Sci. Rev. 15, 121-146.

Christophe Michel-Levy M. (1969) Etude mineralogique de la chondrite CIII de Lance. In: Meteorite Research (ed. P. Millman), pp 492-499. Springer-Verlag, New York.

Clayton R.N. and Mayeda T.K. (1963) The use of bromine pentafluoride in the extraction of oxygen from oxides and silicates for isotopic analysis. Geochim. Cosmochim. Acta 27, 43-52.

Clayton R.N. and Mayeda T.K. (1977) Anomalous anomalies in carbonaceous chondrites. Lunar Planet. Sci. VIII, 193-194.

Clayton R.N. and Mayeda T.K. (1978) Multiple parent bodies of polymict brecciated meteorites. Geochim. Cosmochim. Acta 41, 1777-1790.

Clayton R.N. and Mayeda T.K. (1983) Oxygen isotopes in eucrites, shergotites, nakhlites, and chassignites. Earth Planet. Sci. Lett. 62, 1-6.

Clayton R.N., Onuma N., Ikeda Y., Mayeda T.K., Hutcheon I.D., Olsen E.J., and Molini-Velsko C. (1983) Oxygen isotopic compositions of chondrules in Allende and ordinary chodrites. In: Chondrules and Their Origins (ed. E.A. King), pp37-43. Lunar and Planetary Institute, Houston, Texas.

Clayton R.N., Mayeda T.K. and Yanai K. (1984) Oxygen isotopes in Yamato meteorites. NIPR Symp. Antarct. Met. 9, 40-1 - 40-2.

Clayton R.N. and Mayeda T.K. (1984) The oxygen isotope record in Murchison and other carbonaceous chondrites. Earth Planet. Sci. Lett. 67, 151-161.

Clayton R.N. and Mayeda T.K. (1989) Oxygen isotope classification of carbonaceous chondrites (abstract). Lunar Planet. Sci. XX, 169-170.

Cohen R.E., Kornacki A.S. and Wood J.A. (1983) Mineralogy and petrology of chondrules and inclusions in the Mokoia CV3 chondrite. Geochim. Cosmochim. Acta 47, 1739-1757.

Colby J.W. (1968) Quantitative microprobe analysis of thin insulating films. Advan. X-Ray Anal. 11, 287-305.

Davis A.M., Grossman L. and Ganapathy R. (1977) Yes, Kakangari is a unique chondrite. Nature 265, 230-232

Delaney J.S., Takeda H. and Prinz M. (1983) Modal studies of Yamato and Allan Hills polymict eucrites. Mem. Natl. Inst. Polar Res., Spec. Issue No. 30, 206-223.

Donaldson C.H. (1974) Olivine crystal types in harrisitic rocks of the Rhum pluton and Archean Spinifex rocks. Geol. Soc. Am. Bull. 85, 1721-1726.

Donaldson C.H. (1976) An experimental investigation of olivine morphology. Contrib. Min. Petrol. 57, 187-213.

Dodd R.T. (1969) Metamorphism of the ordinary chondrites; A review. Geochim. Cosmochim. Acta 33, 161-203.

Dodd (R.T. (1976) Accretion of the ordinary chondrites. Earth Planet. Sci. Lett. 30, 281-230.

Dodd R.T., VanSchmus W.R. and Koffman D.M. (1967) A survey of the unequilibrated ordinary chondrites. Geochim. Cosmochim. Acta 31, 921-951.

DuFrense E.R. and Anders E. (1962) On the chemical evolution of carbonaceous chondrites. Geochim. Cosmochim. Acta 26, 1085-1114.

Franchi I.A., Wright I.P. and Pillinger C.T. (1986) Heavy nitrogen in Bencubbin - a light-element isotopic anomaly in a stony-iron meteorite. Nature 323, 138-140.

Fredriksson K. and Kerridge J.F. (1988) Carbonates and sulfates in CI chondrites: Formation by aqueous activity on the parent body. Meteoritics 23, 35-44.

Fredriksson K., Mason B., Beauchamp R. and Kurat G. (1981) Carbonates and magnetites in the Renazzo chondrites (abstract). Meteoritics 16, 316.

Gooding J.L., Keil K., Fukuoka T. and Schmitt R.A. (1980) Elemental abundances in chondrules from unequilibrated chondrites: Evidence for chondrule origin by melting of pre-existing materials. Earth Planet. Sci. Lett. 50, 1171-1180.

Gooding J.L. and Keil K. (1981) Relative abundances of chondrule primary textural types in ordinary chondrites and their bearing on conditions of chondrule formation. Meteoritics 16, 17-42.

Gooding J.L. (1983) Survey of chondrule\ average properties in H-, L- and LL-group chondrites: are chondrules the same in all unequilibrated ordinary chondrites? In: Chondrules and Their Origins (ed. E.A. King), pp61-87, Lunar and Planetary Institute, Houston, Texas.

Grady M.M. and Pillinger C.T. (1989) Nitrogen and carbon in ALH85085 - Links with Bencubbin? Lunar Planet. Sci. 20, 351-352.

Grady M.M. and Pillinger C.T. (1990) ALH85085: nitrogen isotope analysis of a highly unusual primitive chondrite. Earth Planet. Sci. Lett. 97, 29-40.

Grady M.M., Ash R.D., and Pillinger C.T. (1991) EET87770: A light element stable isotope study of a new Renazzo-like carbonaceous chondrite (abstract). Lunar and Planet. Sci. Conf. XXII, 471-472. Lunar and Planetary Institute, Houston.

Graham A.L. and Hutchison R. (1974) Is Kakangari a unique chondrite? Nature 251, 128-129.

Graham A.L., Easton A.J., and Hutchison R. (1977) Forsterite chondrites-the meteorites Kakangari, Mount Morris (Wisconsin), Pontlyfni and Winona. Mineral. Mag. 41, 201-210.

Graham A.L., Bevan A.W.R., and Hutchison R. (1985) Catalogue of Meteorites, Fourth Edition. University of Arizona Press, Tucson, AZ. 460pp.

Grossman L. (1972) Condesation in the primitive solar nebula. Geochim. Cosmochim. Acta 36, 597-619.

Grossman L. (1975) Petrography and mineral chemistry of Ca-rich inclusions in the Allende meteorite. Geochim. Cosmochim. Acta 39,433-454.

Grossman L. and Olsen E. (1974) Origin of the high temperature fraction of C2 chondrites. Geochim. Cosmochim. Acta 38, 173-187.

Grossman L., Olsen E. and Lattimer J.M. (1979) Silicon in carbonaceous chondrite metal: Relic of high-temperature condensation. Science 206, 449-451.

Grossman J.N. and Wasson J.T. (1981) The refractory components in Semarkona chondrules and the fractionation of refractory elements during the formation of ordinary chondrites. Meteoritics 16, 321-322.

Grossman J.N. and Wasson J.T. (1982) Evidence for primitive nebular components in chondrules from the Chainpur chondrite. Geochim. Cosmochim. Acta 46, 1081-1099.

Grossman J.N. and Wasson J.T. (1983) Refractory precursor components of Semarkona chondrules and the fractionation of refractory elements among chondrites. Geochim. Cosmochim. Acta 47, 759-771.

Grossman J.N., Clayton R.N. and Mayeda T.K. (1987) Oxygen isotopes in the matrix of the Semarkona (LL3.0) chondrite. Meteoritics 22, 395-396.

Grossman J.N., Rubin A.E. and MacPherson G.J. (1988) ALH85085: a unique volatile-poor carbonaceous chondrite with possible implications for nebular fractionation processes. Earth Planet. Sci. Lett. 91, 33-54.

Grossman J. N., Rubin A.E., Nagahara H., and King E.A. (1988) Properties of chondrules. In: Meteorites and the Early Solar System (eds. J.F. Kerridge and M.S. Matthews), pp619-659. University of Arizona Press, Tucson.

Hewins R.H. (1988) Experimental studies of chondrules. Meteorites and the Early Solar System (eds. J.F. Kerridge and M.S. Matthews), pp 660-679. University of Arizona Press, Tucson, Ariz.

Housley R.M. and Cirlin E.H. (1983) On the alteration of Allende chondrules and the formation of matrix. In: Chondrules and Their Origins (ed. E.A. King), pp145-161. Lunar and Planetary Institute, Houston, Texas.

Hua X., Adam J., Palme H., and El Goresy A. (1988) Fayalite-rich rims, veins, and halos around and in forsteritic olivines in CAIs and chondrules in carbonaceous chondrites: Types, compositional profiles and constraints of their formation. Geochim. Cosmochim. Acta 52, 1389-1408.

Huss G.R., Keil K., and Taylor G.J. (1981) The matrices of unequilibrated ordinary chondrites; Implications for the origin and history of chondrites. Geochim. Cosmochim. Acta 45, 33-51.

Hutchison R. (1986) New data on the Bencubbin polymict stony-iron breccia. Lunar Planet. Sci. XVII, 374-375.

Johnson C.A. and Prinz M. (1991) Chromite and olivine in type II chondrules in carbonaceous and ordinary chondrites: Implications for thermal histories and group differences. Geochim. Cosmochim. Acta 55, 893-904.

Jones R.H. (1990) Petrology and mineralogy of Type II, FeO-rich chondrules in Semarkona (LL3.0): Origin by closed system fractional crystallization with evidence for supercooling. Geochim. Cosmochim. Acta 54, 1785-1802.

Jones R.H. and Scott E.R.D. (1989) Petrology of Type IA chondrules in the Semarkona (LL3.0) chondrite. Proc. 19th Lunar Planet. Sci. Conf., pp. 523-536.

Kallemeyn G., Boynton W.V., Willis J. and Wasson J.T. (1978) Formation of the Bencubbin polymict meteorite breccia. Geochim. Cosmochim. Acta 42, 507-515.

Kallemeyn G.W. and Wasson J.T. (1981) The compositional classification of chondrites-I. The carbonaceous chondrite groups. Geochim. Cosmochim. Acta 45, 1217-1230.

Kallemeyn G.W. and Wasson J.T. (1982) The compositional classification of chondrites: III. Ungrouped carbonaceous chondrites. Geochim. Cosmochim. Acta 46, 2217-2228.

Keeling D.L. and Marti K. (1987) Nitrogen anomalies in Weatherford metal clasts, Meteoritics 22, 426-427.

Keil K. (1968) Mineralogical and chemical relationships among enstatite chondrites. J. Geophys. Res. 73, 6945-6976.

Keller L.P. and Buseck P.R. (1990) Aqueous alteration products in CV3 and CO3 carbonaceous chondrite meteorites: Phyllosilicates (abstract). Lunar Planet. Sci. XVI, 619-620.

Kelly S. and Turner G. (1987) Laser probe ^{40}Ar-^{39}Ar investigation of the polymict breccia Bencubbin. Meteoritics 22, 427.

Kerridge J.F. (1964) Low temperature minerals from the fine grained matrix of some carbonaceous chondrites. Ann. N.Y. Acad. Sci. 119, 41-53.

Kerridge J.F. (1976) Major element composition in phyllosilicates in the Orgeuil carbonaceous chondrite. Earth Planet. Sci. Lett. 29, 341-348.

Kerridge J.F., MacKay, and Boynton W.V. (1979) Magnetite in CI carbonaceous meteorites: origin by aqueous activity on a planetesimal surface. Science 205, 395-397.

Kimura M. and El Goresy A. (1989) Discovery of E-chondrite assemblages, SiC, and silica-bearing objects in ALH85085: Link between E- and C-chondrite. Meteoritics 24, 286.

King T.V.V. and King E.A. (1978) Grain size and petrography of C2 and C3 carbonaceous chondrites. Meteoritics 13, 47-72.

King T.V.V. and King E.A. (1979) Size frequency distributions of fluid drop chondrules in ordinary chondrites. meteoritics 14, 91-96.

Klock W., Thomas K.L., McKay D.S., and Palme H. (1989) Unusual olivine and pyroxene composition in interplanetary dust and unequilibrated ordinary chondrites. Nature 339, 126-128.

Kung C.C. and Clayton R.N. (1978) Nitrogen abundances and isotopic compositions in stony meteorites. Earth and Planet. Sci. Lett. 38, 421-435.

Larimer J.W. and Anders E. (1975) Chemical fractionation in meteorites-II. Abundance patterns and their interpretation. Geochim. Cosmochim. Acta 31, 1239-1270.

Larimer J.W. (1967) Chemical fractionation in meteorites, I. Condensation of the elements. Geochim. Cosmochim. Acta 31, 1215-.

Lovering J.F. (1962) The evolution of the meteorites - evidence for the co-existence of chondritic, achondritic and iron meteorites in a typical parent meteorite body. In Researches on Meteorites (ed. C.B. Moore), pp179-197. Wiley.

Lux G., Keil K. and Taylor G.J. (1981) Chondrules in H3 chondrites: textures, compositions and origins. Geochim. Cosmochim. Acta 45, 675-685.

MacPherson G.J. and Grossman L. (1984) "Fluffy" Type A Ca-Al-rich inclusions in the Allende meteorite. Geochim. Cosmochim. Acta 48, 29-46.

MacPherson G.J., Bar-Matthews M., Tanaka, T., Olsen, E., and Grossman L. (1983) Refractory inclusions in the Murchison meteorite. Geochim. Cosmochim. Acta 47, 823-839.

Mason B. (1963) The chemical composition of olivine-bronzite and olivine-hypersthene chondrites. Am. Mus. Novit. 2223, 38.

Mason B. (1987) ALH85085. Ant. Met. News. 10, 19.

Mason B. (1987) ALH85151. Ant. Met. News. 10, 21.

Mason B. (1989) MAC 87320. Ant. Met. News. 12, 1.

Mason B. (1989) EET87770. Ant. Met. News. 12, 3.

Mason B. and Nelen J. (1968) The Weatherford meteorite. Geochim. Cosmochim. Acta 32, 661-664.

Mason B. and Wiik H.B. (1962) The Renazzo meteorite. Amer. Mus. Novit. 2106, 11pp.

Mason B. and Wiik H.B. (1966) The composition of Bath, Frankfort, Kakangari, Rose City, and Tadjera meteorites. Amer. Mus. Novit. 2272, 24pp.

Mayeda T.K., Clayton R.N. and Sodonis A. (1989) Internal oxygen isotope variations in two uequilibrated chondrites (abstract). Meteoritics 24, 300.

McCall G.J.H. (1968) The Bencubbin meteorite: Further details, including microscopic character of the host material and two chondrite enclaves. Mineral Mag. 36, 726-739.

McCoy T.J., Scott E.R.D., Jones R.H. and Keil K. (1989) Homogenization of chondrule silicates in ordinary chondrites: constraints on asteroidal metamorphism (abstract). Lunar and Planet. Sci. Conf. XX, 654-655. Lunar and Planetary Institute, Houston.

McSween H.Y. (1977a) Petrographic variations among carbonaceous chondrites of the Vigarano type. Geochim. Cosmochim. Acta 41, 1777-1790.

McSween H.Y. (1977b) Carbonaceous chondrites of the Ornans type: a metamorphic sequence. Geochim. Cosmochim. Acta 41, 477-491.

McSween H.Y. (1977c) Chemical and petrographic constraints on the origin of chondrules and inclusions in carbonaceous chondrites. Geochim. Cosmochim. Acta 41, 1843-1860.

McSween H.Y. (1979) Are carbonaceous chondrites primitive or processed? Rev. Geophys. Space Phys. 17, 1059-1078.

McSween H.Y. and Richardson S.M. (1977) The composition of carbonaceous chondrite matrix. Geochim. Cosmochim. Acta 41, 1145-1161.

Nagahara H. (1983) Texture of chondrules. Mem. Natl. Inst. Polar Res., Spec. Issue No. 30, 61-83. National Institute of Polar Research, Tokyo.

Nehru C.E., Prinz, M., Weisberg, M.K. and Delaney J.S. (1984) Parsa: An unequilibrated enstatite chondrite (UEC) with an aubrite-like impact melt clast. Lunar Planet Sci. Conf. XV, 597-598.

Nehru C.E., Weisberg M.K., and Prinz P. (1986) Chondrules in the Kakangari chondrite (abstract). Meteoritics 21, 468.

Newsom H.E. and Drake M.J. (1979) The origin of metal clasts in the Bencubbin meteoritic breccia. Geochim. Cosmochim.Acta 43, 689-707.

Olsen E.J., Mayeda T.K. and Clayton R.N. (1981) Cristobalite-pyroxene in an L6 chondrite: implications for metamorphism. Earth Planet. Sci. Lett. 56, 82-88.

Palme H. and Wlotzka F. (1976) A metal particle from a Ca, Al-rich inclusion from the Allende meteorite, and the condensation of refractory siderophile elements. Earth Planet. Sci. Lett. 33, 45-60.

Palme H. and Fegley B., JR. (1990) High temperature condensation of iron-rich olivine in the solar nebula. Earth Planet. Sci. Lett., in press.

Peck J.A. and Wood J.A. (1987) The origin of ferrous zoning in Allende chondrule olivines. Geochim. Cosmochim. Acta 51, 1503-1510.

Prinz M., Nehru C.E., Delaney J.S., Harlow, G.E. and Bedell R.L. (1984) Modal studies of mesosiderites and related achondrites, including the new mesosiderite ALHA 77219. Proc. 11th Lunar Planet. Sci. Conf., pp. 1055-1077.

Prinz M., Weisberg M.K., Nehru C.E. and Delaney J.S. (1987) Black inclusions of carbonaceous chondritic matrix in polymict ureilites (abstract). Meteoritics 22, 482-483.

Prinz M., Weisberg M.K. and Nehru C.E. (1988) Gunlock, a new type 3 ordinary chondrite with a golfball-sized chondrule. Meteoritics 23, 297.

Prombo C.A. and Clayton R.N. (1985) A striking nitrogen isotope anomaly in the Bencubbin and Weatherford meteorites. Science 230, 935-937.

Radomsky P.M., Turrin R.P. and Hewins R.H. (1986) Dynamic crystallization experiments on a pyroxene-olivine chondrule composition. Lunar Planet. Sci. XVII, 687-688.

Rambaldi E.R., Sears D.W. and Wasson J.T. (1980) Si-rich Fe-Ni grains in highly unequilibrated chondrites. Nature 287, 817-820.

Ramdohr P. (1973) The Opaque Minerals in Stony Meteorites. Elsevier.

Robert F. and Epstein S. (1982) The concentration and isotopic composition of hydrogen, carbon and nitrogen in carbonaceous meteorites. Geochim. Cosmochim. Acta 46, 81-95.

Roeder E. and Weiblen P.W. (1977) Barred olivine "chondrules" in lunar spinel troctolite 62295. Proc. Lunar Sci. Conf. 8th, 2641-2654.

Rowe W., Clayton R.N. and Mayeda T.K. (1989) Oxygen isotopes in separated components of CI and CM chondrites (abstract). Meteoritics 24, 321.

Rubin A.E. (1989) Size-frequency-distributions of chondrules in CO3 chondrites. Meteoritics 24, 179-189.

Rubin A.E., Scott E.R.D. and Keil, K. (1982) Microchondrule-bearing clast in the Piancaldoli LL3 meteorite: a new kind of type 3 chondrite and its relevance to the history of chondrules. Geochim. Cosmochim. Acta 46, 1763-1776.

Rubin A.E. and Wasson J.T. (1986) Chondrules in the Murray CM2 meteorite and compositional differences between CM-CO and ordinary chondrite chondrules. Geochim. Cosmochim. Acta 50, 307-315.

Rubin A.E. and Grossman J.N. (1987) Size-frequency-distributions of EH3 chondrules. Meteoritics 22, 237-251.

Rubin A.E. and Kallemeyn G.W. (1989) Carlisle Lakes and Allan Hills 85151: Members of a new chondrite grouplet. Geochim. Cosmochim. Acta 53, 3035-3044.

Rubin A.E., Fegley B. and Brett R. (1988) Oxidation state in chondrites. In: Meteorites and the Early Solar System (eds J.F. Kerridge and M.S. Matthews), pp488-511. University of Arizona Press, Tucson, Arizona.

Saxena S.K. and Benimoff A. (1977) Formation of Fe-Ni-S planetary cores. Nature 270, 333-334.

Scott E.R.D. (1988) A new kind of primitive chondrite, Allan Hills 85085. Earth Planet. Sci. Lett. 91, 1-18.

Scott E.R.D., Rubin A.E., Taylor G.J. and Keil K. (1981) New kind of type 3 chondrite with a graphite-magnetite matrix. Earth Planet. Sci. Lett. 56, 19-31.

Scott E.R.D., Rubin A.E., Taylor G.J. and Keil K. (1984) Matrix in type 3 ordinary chondrites-occurence, heterogeneity and relationship with chondrules. Geochim Cosmochim. Acte 48, 1741-1757.

Scott E.R.D. and Taylor G.J. (1985) Petrology of types 4-6 carbonaceous chondrites. Proc.15th Lunar Planet. Sci. Conf., C699-C709.

Scott E.R.D., Lusby D. and Keil K. (1985) Ubiquitous brecciation after metamorphism in equilibrated ordinary chondrites. Proc. 16th Lunar Planet. Sci. Conf., D137-D148.

Sears D.W.G., Hasan F.A., Batchelor J.D. and Jie L. (1990) Chemical and physical studies of type 3 chondrites - XI: Metamorphism, pairing, and brecciaition of type 3 ordinary chondrites. Proc. 21st Lunar Planet. Sci. Conf., in press.

Simon S.B. and Haggerty S.E. (1979) Petrography and olivine mineral chemistry of chondrules and inclusions in the Allende meteorite. Proc. 10th Lunar Planet. Sci. Conf., 871-883.

Simpson E.S. and Murray D.G. (1932) A new siderolite from Bencubbin, Western Australia. Mineral Mag. 23, 33-37.

Stolper E. (1982) Crystallization sequences of Ca-Al-rich inclusions from Allende: an experimental study. Geochim. Cosmochim. Acta 46, 2159-2180.

Taylor G.J., Scott E.R.D. and Keil K. (1983) Cosmic setting for chondrule formation. In: Chondrules and Their Origins (ed. E.A. King), pp262-278, Lunar and Planetary Institute, Houston, Texas.

Tomeoka K. and Buseck P.R. (1982) Intergrown mica and monmorillonite in the Allende carbonaceous chondrite. Nature 299, 326-327.

Tomeoka K. and Buseck P.R. (1986) Mineralogical evidence for hydration and oxidation of Fe-rich olivine in the Mokoia CV3 meteorite matrix (abstract). Meteoritics 21, 526.

Tomeoka K. and Buseck P.R. (1988) Matrix mineralogy of the Orgueil CI carbonaceous chondrite. Geochim. Cosmochim. Acta 52, 1627-1640.

Tomeoka K. and Buseck P.R. (1990) Phyllosilicates in the Mokoia CV carbonaceous chondrite: Evidence for aqeous alteration in an oxidizing environment. Geochim. Cosmochim. Acta 54, 1745-1754.

Tsuchiyama A. (1985) Partial melting kinetics of plagioclase-diopside pairs. Contrib. Mineral. Petrol. 91, 12-23.

Tsuchiyama A., Nagahara H. and Kushiro I. (1980) Experimental reproduction of textures of chondrules. Earth Planet. Sci. Lett. 48, 155-165.

Tsuchiyama A. and Nagahara H. (1981) Effects of precooling thermal history and cooling rate on the texture of chodrules; a preliminary report. Mem. Nat. Inst. Polar Res. Spec. Issue 20, 175-192.

Tsuchiyama A., Fujita, T. and Morimoto N. (1988) Fe-Mg heterogeneity in the low-Ca pyroxene during metamorphism of the ordinary chondrites. Proc. NIPR Symp. Antarc. Meteorites 1, 173-184.

Van Schmus W.R. (1969) Mineralogy, petrology, and classification of types 3 and 4 carbonaceous chondrites. In Meteorite Research (ed. P. Millman), pp480-491. Reidel.

Van Schmus W.R. and Hayes J.M. (1974) Chemical and petrological correlations among carbonaceous chondrites. Geochim. Cosmochim. Acta 38, 47-64.

Van Schmus W.R. and Wood J.A. (1967) A chemical-petrologic classification for the chondritic meteorites. Geochim Cosmochim. Acta 31, 747-765.

Wai C.M. and Wasson J.T. (1977) Nebular condensation of moderately volatile elements and their abundances in ordinary chondrites. Earth Planet. Sci. Lett. 36, 1-13.

Wai C.M., Wasson J.T., Willis J. and Kracher A. (1978) Nebular condensation of moderately volatile elements and their abundances in iron metoerites, and the

quantization of Fe and Ga abundances (absract). Lunar Planet. Sci. Conf. IX, 1193-1195.

Wark D.A. and Lovering J.F. (1977) Marker events in the early solar system: Evidence from rims on Ca-Al-rich inclusions in carbonaceous chondrites. Proc. 8th Lunar Planet. Sci. Conf., 95-112.

Wasson J.T. (1974) Meteorites: Classification and Properties. Springer. 316pp.

Wasson J.T. (1985) Meteorites: Their Record of Early Solar System History. W.H. Freeman and Co., New York, N.Y., 267pp.

Wasson J.T. (1988) A non-nebular origin for the Allan Hills 85085 subchondritic meteorite. Lunar Planet. Sci. XIX, 1240.

Weinbruch S., Palme H., Muller W.F. and El Goresy A. (1990) FeO-rich rims and veins in Allende forsterite: Evidence for high temperature condensation at oxidizing conditions. Meteoritics 25, 115-125.

Weisberg M.K. (1986) Barred olivine chondrules in carbonaceous chondrites. Meteoritics 21, 535-536.

Weisberg M.K. (1987) Barred olivine chondrules in ordinary chondrites. Proc. Lunar Planet.Sci. Conf. 17th, Journ. Geophys. Res. 92, E663-E678.

Weisberg M.K., Prinz M. and Nehru C.E. (1988a) Petrology of ALH85085: a chondrite with unique characteristics. Earth Planet. Sci. Lett. 91, 19-32.

Weisberg M.K., Prinz M. and Nehru C.E. (1988b) Macrochondrules in ordinary chondrites: Constraints on chondrule forming processes. Meteoritics 23, 309-310.

Weisberg M.K., Prinz M., Clayton R.N. and Mayeda T.K. (1989) The Renazzo-type CR chondrites. Meteoritics 24, 339.

Weisberg M.K., Prinz M., Nehru C.E., Clayton R.N. and Mayeda T.K. (1989) ALH85151 and Carlisle Lake 001: members of a new chondrite group (abstract). Lunar Planet. Sci. 20, 1191-1192. Lunar and Planetary Institute, Houston.

Whipple F. (1971) Accumulation of chondrules on asteroids. In Physical Studies of Minor Planets (ed. T. Gehrels), pp251-265, NASA Spec. Publ. SP-267 .

Whipple F. (1972) On certain aerodynamic proceeses for asteroids and comets. In From Plasma to Planet , Nobel Symposium 21 (ed. A. Elvins), pp211-230, Wiley-Interscience, New York, NY.

Wiik H.B. (1956) The chemical composition of some stony meteorites. Geochim. Cosmochim. Acta 9, 279-289.

Wood J.A. (1967) Chondrites: their metallic minerals, thermal histories, and parent planets. Icarus 6, 1-49.

Wood J.A. (1981) The intersteller dust as a precursor of Ca, Al-rich inclusions in carbonaceous chondrites. Earth Planet. Sci. Lett. 56, 32-44.

Yanai K., Kojima H. and Matsumoto Y. (1985) A new type chondrite? Yamato-75302 consists mostly of very high iron olivine (abstract). Meteoritics 20, 791.

Yanai K. and Kojima H. (1987) Photographic Catalog of the Antarctic Meteorites. National Institute of Polar Research, Tokyo, Japan, 298pp.

Zanda B., Bourot-Denise M., and Perron C. (1991) Cr, P and Si in the metal of Renazzo (abstract). Lunar Planet. Sci. 22, 1543-1544. Lunar and Planetary Institute, Houston.

Zolensky M.E., Barrett R.A., and Gooding J,L.(1989) Matrix and rim compositions compared for 13 carbonceous chondrite meteorites and clasts (abstract). Lunar Planet. Sci. 20, 1249-1250. Lunar and Planetary Institute, Houston.

Zolensky M.E. (1991) Mineralogy and matrix composition of "CR" chondrites Renazzo and EET8770, and ungrouped chondrites Essebi and MAC 87300 (abstract). Meteoritics, in press.